Impact of water matrix on the removal of micropollutants by advanced oxidation technologies

PLEASE CITE THE PUBLISHED VERSION

https://doi.org/10.1016/j.cej.2019.01.080

PUBLISHER

© Elsevier

VERSION

AM (Accepted Manuscript)

PUBLISHER STATEMENT

This paper was accepted for publication in the journal Chemical Engineering Journal and the definitive published version is available at https://doi.org/10.1016/j.cej.2019.01.080.

REPOSITORY RECORD

Ribeiro, Ana R. Lado, Nuno F.F. Moreira, Gianluca Li-Puma, and Adrian M.T. Silva. 2019. “Impact of Water Matrix on the Removal of Micropollutants by Advanced Oxidation Technologies”. figshare. https://hdl.handle.net/2134/37018.

Impact of water matrix on the removal of micropollutants by advanced oxidation technologies

Ana R. Ribeiro[1,*], Nuno F.F. Moreira[1], Gianluca Li Puma[2,*], Adrián M.T. Silva[1]

[1]Laboratory of Separation and Reaction Engineering - Laboratory of Catalysis and Materials (LSRE-LCM), Faculdade de Engenharia, Universidade do Porto, Rua Dr. Roberto Frias s/n, 4200-465 Porto, Portugal

[2]Environmental Nanocatalysis & Photoreaction Engineering, Department of Chemical Engineering, Loughborough University, Loughborough, United Kingdom

*Corresponding authors: ritalado@fe.up.pt (A.R. Ribeiro), G.Lipuma@lboro.ac.uk (G. Li Puma)

Abstract

Micropollutants (MPs) in the aquatic compartments originate from many sources and particularly from the effluents of urban wastewater treatment plants (UWWTPs). Advanced oxidation technologies (AOTs) usually applied after biological processes, have recently emerged as effective tertiary treatments for the removal of MPs, but the oxidation rates of the single compounds may be largely affected by the constituent species of the water matrix. These species include dissolved organic matter and inorganic species (e.g., carbonate, bicarbonate, nitrite, sulphate, chloride). This review analyses the impact of such substances on common AOTs including photolysis, UV/H_2O_2, Fenton, photocatalysis, and ozone-based processes. The degradation efficiency of single MPs by AOTs results from the combined impact of the water matrix constituents, which can have neutral, inhibiting or promoting effect, depending on the process and the mechanism by which these water components react. Organic species can be either inhibitors (by light attenuation; scavenging effects; or adsorption to catalyst) or promoters (by originating reactive oxygen species (ROS) which enhance indirect photolysis; or by regenerating the catalyst). Inorganic species can also be either inhibitors (by scavenging effects; formation of radicals less active than hydroxyl radicals; iron complexation; adsorption to catalyst or decrease of its effective surface area) or promoters (e.g., nitrate ions by formation of ROS; iron ions as additional source of catalyst). The available data reviewed here is limited and the role and mechanisms of individual water components are still not completely understood. Further studies are needed to elucidate the wide spectrum of reactions occurring in complex wastewaters and to increase the adoption of AOTs in UWWTPs.

Keywords: Advanced oxidation processes; Chemical oxidation technologies; Contaminants of emerging concern; Matrix effect; Micropollutants; Wastewater constituent.

Contents

1. Introduction

Micropollutants (MPs) are natural or anthropogenic substances occurring in the aquatic environment at low concentrations, usually between ng L^{-1} and μg L^{-1} levels. MPs comprise a vast array of substances, namely pesticides, industrial compounds, pharmaceuticals, personal care products, steroid hormones, drugs of abuse and others [1]. Many of them are considered contaminants of emerging concern (CECs), a term currently used in the framework of environmental sciences for: (i) compounds recently known (e.g., new synthetic substances); (ii) hazardous compounds recently identified as such despite the previous knowledge about their occurrence in the environment (e.g., estrogens); and (iii) previously unknown compounds present in the environment, which have only been detected due to advances in analytical methods and instrumentation [2].

The anthropogenic sources of MPs are numerous and include domestic, hospital and industrial wastewater, agriculture runoff, livestock and aquaculture [2]. The treated effluents released by urban wastewater treatment plants (UWWTPs) are consensually recognised as a significant origin of MPs, since UWWTPs using conventional physicochemical and biological treatments are not designed to fully eliminate organic compounds occurring at trace concentrations [1-3]. MPs in domestic and hospital wastewater reach UWWTPs after metabolism and excretion as parent compounds and/or metabolites, although the release by direct discharge of unused or expired drugs may also be a significant contributing factor [3]. MPs in industrial effluents discharged into UWWTPs are generally poorly removed, even when these have been previously treated at industrial level [3]. Therefore, the uninterrupted discharge of MPs and their metabolites into UWWTPs can be considered a continuous source of toxicity which harms the receiving aqueous compartments, such as surface, ground and drinking waters.

Innovative advanced oxidation technologies (AOTs), including chemical oxidation technologies (COTs) and advanced oxidation processes (AOPs), have recently gaining interest as polishing post-treatment methods usually applied after biological processes in water and wastewater treatment. Such processes are designed to enhance the degradation and mineralization of MPs or to transform them into less toxic compounds [1]. In highly toxic water effluents, AOTs can be applied as a pre-treatment, to enhance the biodegradability of the water and reduce its toxicity. The installation of supplementary AOTs after secondary biological treatment has been triggering a huge interest among the water industry, due to the recognized efficiency of such processes for the removal of a wide range of MPs from UWWTPs effluents [1]. The reduction of the release of MPs into the aquatic compartments, therefore, improves the effluent quality and can promote the reuse of reclaimed water.

AOTs are widely studied technologies for the oxidation of organic MPs via reactions with the highly reactive radicals. Hydroxyl radical-mediated AOTs utilize hydroxyl radicals ($HO^{\bullet}$), the most powerful oxidizing species after fluorine, with an $E^0 = 2.80$ V [4]. These unselective radicals might mineralize the parent compounds with no generation of secondary waste, yielding CO_2, H_2O and inorganic ions as final products [1]. AOTs can be classified as chemical, photochemical, electrochemical, sonochemical and hydrochemical processes, depending on the way the $HO^{\bullet}$ are generated, or as homogeneous and heterogeneous processes, depending on the number of phases involved during the transport and reaction of the species. Homogeneous processes include processes that utilize UV, H_2O_2, the Fenton reagent, dissolved O_3, wet oxidation (WO) and wet peroxide oxidation (WPO); whereas heterogeneous AOTs comprise heterogeneous photocatalysis, heterogeneous Fenton-like processes, catalytic and photocatalytic ozonation, catalytic wet oxidation (CWO) and catalytic wet peroxide oxidation (CWPO). UV, UV/H_2O_2 and ozonation processes have been successfully implemented in full-scale UWWTPs to degrade MPs. AOTs not yet applied at full-scale include UV/O_3, UV/O_3/H_2O_2, UV/H_2O_2/Fe (mild photo-Fenton) and other advanced processes such as heterogeneous photocatalysis, heterogeneous photo-Fenton, photocatalytic ozonation, photocatalytic membrane processes, electrochemical oxidation and sonolysis [1]. This review focuses on the treatment of MPs by hydroxyl radical-mediated AOTs and related processes and on the impact of the water matrix components, which is particularly deficient on sulphate and chlorine radical-mediated AOTs. Sulphate radical-mediated AOTs have recently gained a great attention due to the high redox potential of $SO_4^{\bullet-}$, which is comparable with that of $HO^•$ [5]. While $HO^•$ is reported to react with MPs through three competing pathways (addition, hydrogen abstraction, and electron abstraction), $SO_4^{•-}$ reacts preferentially through an electron transfer mechanism. Both radicals can react with inorganic ions (e.g., Cl^- and CO_3^{2-}), generating secondary reactive species ($Cl^•$/$CO_3^{•-}$) with relatively high reactivity with MPs [5]. Conversely, chlorine radical-mediated AOTs (e.g., UV/chlorine) are based on selective oxidants produced by photolysis of chlorine: $Cl^•$ (selective and with higher reactivity than $HO^•$ for certain organic compounds, such as benzoic acid, chlorobenzene, and phenol), $Cl_2^{•-}$ (selective for olefinic compounds and aromatics ring-substituted with hydroxy, methoxy and amino groups) and $ClO^•$ (selective for aromatics possessing methoxy groups), with redox potentials of 2.4, 2.0, and 1.5 − 1.8 V, respectively [6]. The use of AOTs in hybrid processes has been also envisaged through integration with membrane technologies and through the coupling of two or more AOTs. This last strategy can result: (i) typically in a synergistic effect due to the positive interactions among the single processes; (ii) in a cumulative effect caused by the increased generation of reactive oxygen species (ROS); and less commonly (iii) in an antagonistic effect, due to excessive formation of ROS, which may act as self-scavengers [7].

2. AOTs and matrix effects

Overall, the elimination of MPs by AOTs is largely influenced by the quality of the water matrix that needs to be treated, and the effectiveness results from the impact of the dissolved components, which can have neutral, inhibitory or promoting effects. The composition of the water matrix can also have a significant impact on the inactivation of bacteria in water disinfection processes, as shown in the literature [8, 9].

The occurrence of scavengers in the matrix may also hinder the removal of dissolved organic matter (DOM), representing the main fraction of the effluent organic matter (a heterogeneous mixture of recalcitrant organic compounds comprising natural organic matter (NOM), soluble microbial products and trace MPs) present in biologically treated urban wastewater [10]. The composition of DOM depends on the wastewater sources (domestic, industrial, agricultural, etc.), location, the season of the year and the operating conditions (temperature, pH, flow, etc.) [11]. The structural and functional complexity of DOM turns difficult its full characterization, therefore, the DOC is commonly used as a surrogate parameter for its quantification, providing a general assessment and lacking on structural elucidation [10]. Its transformation and the generation of by-products during WWTP processes may change the biological properties and environmental impact of the DOM, but the knowledge about its transformation in the WWTPs is still limited. A recent review on this subject described the characterization of DOM based on its MW distribution, hydrophobicity and optical properties [11]. Several analytical techniques have been used to characterize the chemistry and reactivity of the DOM components, including physicochemical analysis, spectroscopic, chromatographic, and thermal degradation methods, and other fractionation techniques [10]. Wastewater components include a broad range of organic (e.g., NOM composed by humic and fulvic acids, carbohydrates, proteins) and inorganic species (e.g., carbonate, bicarbonate, nitrite, sulphate, chloride), which react with $HO^{\bullet}$, either competing with organic MPs for oxidation [1, 10] or forming the respective radicals with lower oxidation potential [12]. Moreover, some wastewater components are able to favour the efficiency of certain AOTs. Figure 1 summarizes the key factors that contribute to the removal efficiency of MPs by the AOTs discussed in this review, acting as either promoters or as inhibitors.

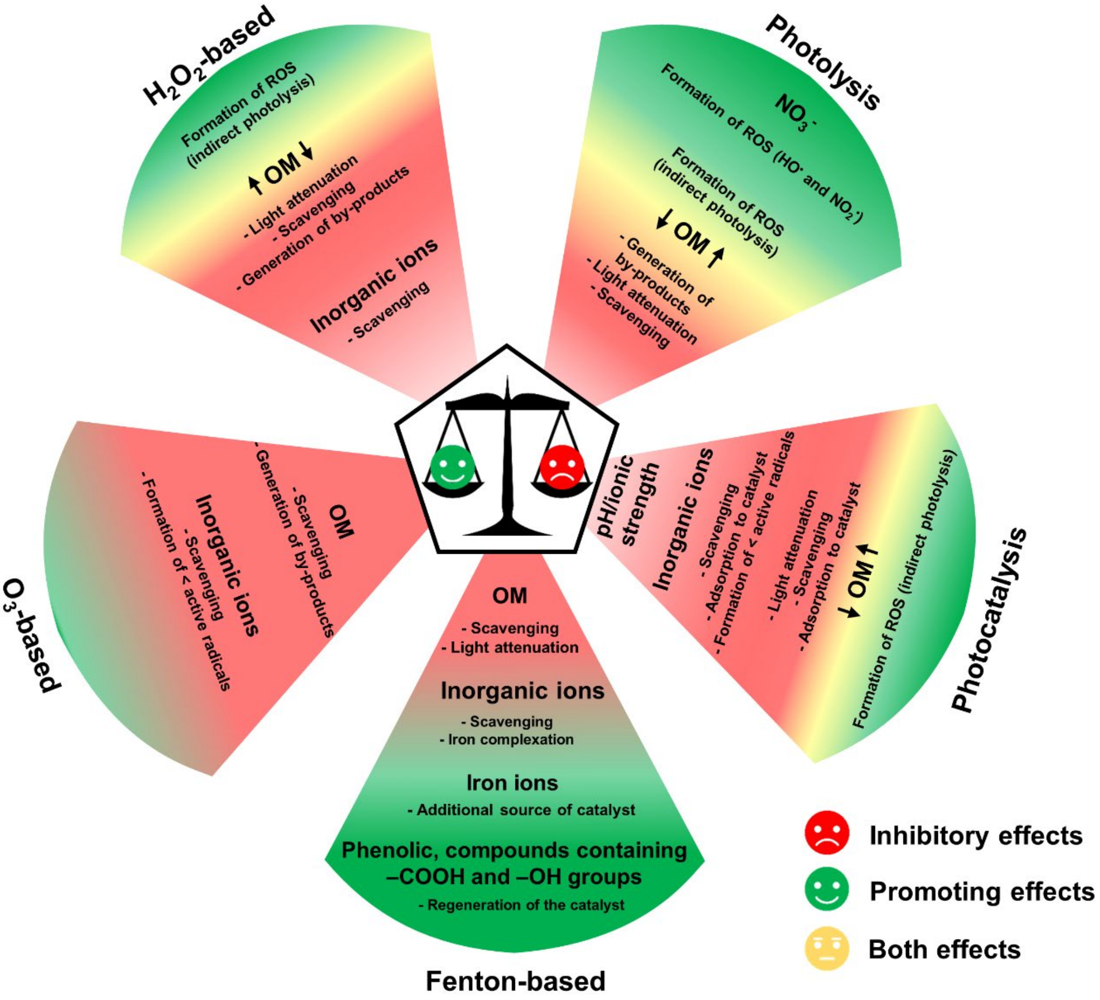

Figure 1. Schematic representation of the reported inhibitory and promoting effects of wastewater components, affecting the efficiency of photolysis, H_2O_2-based, Fenton-based, photocatalysis, and ozone-based processes.

The main scavengers of $HO^{\bullet}$ in natural waters include NOM, bromide (which forms $BrOH^{\bullet -}$ by reacting with $HO^{\bullet}$) [5], and carbonate/bicarbonate species [13]. Hence, different water matrices containing NOM exhibit different scavenging rates, reducing the fraction of ROS available to degrade MPs, which triggers the need of considering such scavengers in the optimization of AOTs. In most cases, the MPs removal kinetics decrease with an increase in the complexity of the water matrix, since this may contain numerous non-target organic and inorganic species that compete with the target contaminants for oxidants [14]. The inhibitory effects of co-existing substances in the matrix include also light absorption and attenuation in processes utilizing UV radiation. It may also result in the formation of less active complexes with iron species in Fenton-based processes and in the competition for catalytic active sites, catalyst deactivation by poisoning of the active sites or fouling of the surface area of the catalysts in heterogeneous catalytic processes, as well as the modification of the electrical surface charge due to the pH or ionic strength. However, it has been reported that non-target species may also act as promoters in selected AOTs [4, 14]. Photosensitizers organic and inorganic species in the water matrix can promote the production of ROS by UV irradiation, leading to indirect photolysis [15]. For instance, NO_3^- is able to produce $HO^•$ and $NO_2^•$ radical species, promoting the photodegradation of MPs, especially those in which indirect photolysis is the main reactive pathway (e.g., caffeine, carbamazepine, diuron, simazine, 2,4-dichlorophenoxyacetic acid) [15]. Fenton-based processes are generally promoted by natural occurring iron in the wastewater which acts as an additional catalytic source, by the presence of phenolic compounds that may reduce the ferric ions to ferrous ions regenerating the catalyst, and by dissolved compounds containing -COOH and -OH groups which complexes ferric ions in solution, where the complexes may have higher quantum yields [16].

Despite the great attention given to AOTs (**Figure 2, left**), only ca. 10% of the published papers refer to the treatment of actual wastewater and a few of them (ca. 0.2%) have addressed the impact of the water matrix (**Figure 2, right**).

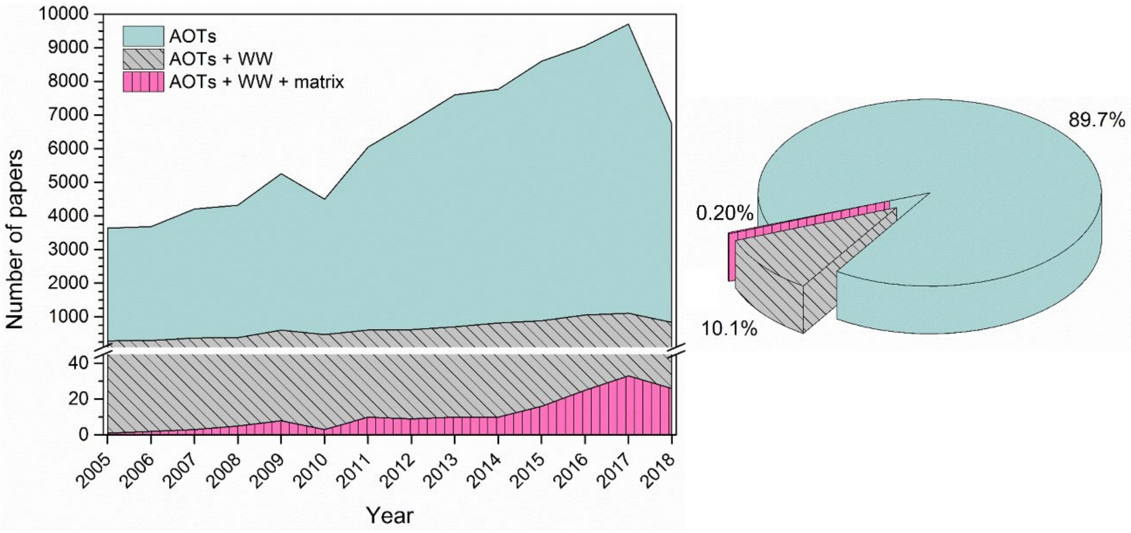

Figure 2. Number of papers published by year in the period 2005-2018 (left) and their relative frequency in the whole period (right), displayed by searching publications dealing with the different types of AOTs discussed in this review, using as keywords (abstract, title, keywords): “photolysis” or “UV/H_2O_2“ or “Fenton” or “photocatalysis” or “ozonation” or “ozonolysis” or “UV/O_3“ or “peroxone” (🟦); and “wastewater” (▨); and “matrix effect” or “matrix component” or “matrix constituent” or “water matrix” or “water matrices” or “water component” or “water constituent” (▥). Source: Scopus; July 2018.

Interestingly, although the amount of publications in this field has been markedly increasing, the number of papers dealing with wastewater treatment and the impact of the water matrix follows the same trend, with almost no variations on their relative frequency. In fact, most studies on AOTs for water/wastewater treatment have been performed using aqueous solutions spiked with model contaminants. Often, ultrapure or distilled water is spiked with the contaminant at concentration levels higher than those actually reported in environmental compartments [14]. This methodology allows: (i) to exclude the interactions between the contaminant, the oxidizing species and the matrix components; (ii) to study degradation pathways of specific compounds; (iii) to evaluate the performance of the studied treatment for target contaminants; and (iv) to use simple and widely used analytical techniques. However, the quality of the aqueous matrix for which the treatment is proposed is crucial to draw accurate conclusions about the effectiveness of the AOT, its suitability and practicability for the treatment of real contaminated waters. Therefore, this review focuses on the available data of matrix effects on the removal of MPs from effluents of UWWTPs by using photolysis, UV/H_2O_2, Fenton, photocatalysis, or ozone-based processes, and give insights about the options that improve the effectiveness of AOTs already implemented or under investigation. The search comprised publications since 2005 in Scopus database, using the following keywords (abstract, title, keywords): "photolysis" or "UV/H_2O_2" or "Fenton" or "photocatalysis" or "ozonation" or "ozonolysis" or "UV/O_3" or "peroxone" and "wastewater" and "matrix effect" or "matrix component" or "matrix constituent" or "water matrix" or "water matrices" or "water component" or "water constituent" (**Figure 2**). From this survey, only studies dealing with real wastewater were considered, namely by comparing it with ultrapure water or other matrices, testing wastewater from different origins, or by assessing the effect of adding supplementary water components.

In the last decade, many studies using actual matrices have been reported in the literature, most showing an application for a real matrix, after screening studies on synthetic aqueous solutions, and/or dealing with spiked MPs at concentration levels higher than those found in the environment. More recently, some reports have shown the influence of the quality and/or quantity of water components, on the process efficiency. Most of these works are focused on the comparison of removal efficiencies of MPs and/or dissolved organic carbon (DOC) in distilled/ultrapure water versus synthetic wastewaters [17, 18] and/or actual wastewaters [4]. Some studies comparing wastewaters from different origins [19] or at different treatment stages in the UWWTP [20], have been recently reported. Several authors have also shown the effects of wastewater components (e.g., humic acids (HA), fluvic acids, surfactants, inorganic species) on the removal of selected MPs frequently found in urban wastewater; however, these studies often address the impact on ultrapure or distilled water, rather than in real wastewater. A current approach has been performed by adding different components (organic and/or inorganic) to natural water, giving more accurate insights on the effects of wastewater components on the removal efficiencies of either MPs or DOC. Studies using environmental matrices at real concentrations and providing a deep understanding on the effects of the organics and inorganics occurring in the matrices, are still limited.

2.1. Photolysis

UV water treatment can involve two mechanisms, direct or indirect photolysis. The direct photolysis of organic substances by UV radiation (typically at $\lambda = 254$ nm) promotes the electronic excitation of the molecules, leading to: (i) electron transfer from an excited state of the organic compounds to molecular oxygen; or (ii) homolysis of the organic substance, producing organic radicals that further react with oxygen [20-22].

The water matrix can play an essential role on the yield of photodegradation reactions, depending on the presence of promoting and inhibitory substances. Table 1 summarizes the reports published since 2005 referring to the evaluation of matrix effects on photolysis (more details can be found in Table S1). Generally, lower contaminants removal rates are expected in wastewater effluents in comparison to a ultrapure water matrix, which can be enlightened by the presence of NOM absorbing a fraction of the incident radiation [23]. The main factors regulating the inhibitory effect of NOM are: (i) light attenuation caused by suspended particles; (ii) scavenging effects of NOM; and (iii) generation of NOM by-products [24]. Nevertheless, the wastewater components might enhance the removal rate of certain MPs by mean of indirect photolysis, resulting from the action of ROS originated by the irradiation of photosensitizers dissolved in the water matrix [4]. Photosensitizers comprise a wide variety of organic compounds found in DOM that can undergo diverse photochemical reactions, producing ROS that initiate MPs degradation. Such ROS may in certain cases offset the reduction of transmittance of NOM containing matrices, which in turn diminishes the degradation by direct photolysis (e.g., studies in wastewater and in drinking water) [25]. DOM photosensitizers act by absorption of light (Reaction 1) followed by excitation to a single state ($^1DOM^*$), which has typical short lifespans (ps to ns) and consequent little interaction with organic MPs. This is partially transformed to their excited triplet state ($^3DOM^*$), which has a longer lifespan (order of μs) [21, 26]. The $^3DOM^*$ species are believed to be the main reactive species in the reactive pathways and the deactivation of the excited triplet state can occur by reaction with other organic molecules (e.g., target MPs), which are consequently oxidized [24]. These species can play an important role in indirect photolysis for phenols and aromatic amines [27]. Another deactivation mechanisms of $^3DOM^*$ include the transition to their ground state or the transfer of energy to O_2 (Reaction 2), producing singlet molecular oxygen ($^1O_2$), which also act as a photo-oxidant [21].

$$DOM + hv \rightarrow {}^1DOM^* \rightarrow {}^3DOM^* \qquad (1)$$

$$^3DOM^* + O_2 \rightarrow DOM + {}^1O_2 \qquad (2)$$

For instance, the photodegradation of cocaine in a synthetic municipal wastewater effluent by direct sun-light exposure was higher (90% after 20 h of irradiation) than that observed in distilled water (22% after 60h of irradiation), without mineralization taking place in both investigated matrices [17]. This phenomenon has also been reported for the degradation of diclofenac under UVA radiation, with a higher removal rate registered in wastewater than in ultrapure water, due to some naturally occurring substances in the effluent, acting as photosensitizers [28].

The anion NO_3^- may also play an important role in the UV treatment. This inorganic species can generate $HO^•$ and $NO_2^•$ (Reactions 3-7) under direct UV photolysis (mainly at wavelength below 240 nm), consequently increasing the degradation of some compounds [24].

$$NO_3^- + hv \rightarrow NO_2^- + O \qquad (3)$$

$$NO_3^- + hv \rightarrow O^{•-} + NO_2^• \qquad (4)$$

$$O + H_2O \rightarrow 2HO^• \qquad (5)$$

$$O^{•-} + H_2O \rightarrow HO^• + HO^- \qquad (6)$$

$$2NO_2^• + H_2O \rightarrow NO_2^- + NO_3^- + 2H^+ \qquad (7)$$

This promoting effect has been observed during the degradation of several phenolic compounds [29], cytostatic drugs [24], pharmaceuticals [30] and pesticides [15]. A study on the photodegradation of antibiotics suggested that the promoting effect of NO_3^- on the photolysis of salinomycin resulted from the reaction with produced reactive nitrogen species, besides the indirect photolysis [30]. Another study reported an appreciable promoting effect of NO_3^- on those compounds which followed an indirect degradation photolytic pathway, while the impact was minor on those compounds more susceptible to direct photolysis [15]. This fact can be explained by the reduction of the photonic energy in the aqueous solution, when the target compounds strongly absorb in the same UV range as NO_3^- [31].

2.2. H_2O_2-assisted processes

UV/H_2O_2 is an AOT that combines the instantaneous UV photolytic effect (either direct or indirect) and the reaction with $HO^•$ originated from the homolytic disruption of H_2O_2 (initiation, propagation and termination, Reactions 8-12, Table S2 summarizes the reaction rate constants) [20]. UV/H_2O_2 is an alternative solution for the elimination of organic MPs with low reactivity towards O_3 and $HO^•$ and high photoactivity (e.g., N-nitrosodimethylamine) [13], as well as for the treatment of wastewaters with high concentration of bromide since this process avoids bromate formation [13].

$$H_2O_2 + hv \rightarrow 2HO^• \qquad (8)$$

$$H_2O_2 + HO^• \rightarrow HO_2^• + H_2O \qquad (9)$$

$$H_2O_2 + HO_2^• \rightarrow HO^• + O_2 + H_2O \qquad (10)$$

$$2HO_2^• \rightarrow H_2O_2 + O_2 \qquad (11)$$

$$HO^• + HO_2^• \rightarrow O_2 + H_2O \qquad (12)$$

Although H_2O_2 produces $HO^•$ under UV irradiation, at elevated concentrations it also scavenges $HO^•$ (Reactions 9-12), hindering the oxidation of the target organic MPs, therefore the dose of H_2O_2 needs to be controlled very carefully in order to maximize the removal rate of MPs [25]. Furthermore, H_2O_2 is a major contributor to the operating cost of the UV/H_2O_2 process [25].

In the H_2O_2-assisted photocatalysis, it is likely that H_2O_2 promotes the degradation of target water contaminants by reacting with conduction band electrons (Reaction 13) and the superoxide radical ($O_2^{\bullet-}$) (Reaction 14) to produce $HO^{\bullet}$ and anions [32]. The formation of additional oxidizing species and the suppression of the recombination of e^{-}/h^{+} pairs, in the case of photocatalysis, enhance the effectiveness of this AOT [32].

$$H_2O_2 + e^{-} \rightarrow HO^{-} + HO^{\bullet} \qquad (13)$$

$$H_2O_2 + O_2^{\bullet-} \rightarrow HO^{-} + HO^{\bullet} + O_2 \qquad (14)$$

Similarly to the UV/H_2O_2 process, an optimum H_2O_2 concentration can also be determined in the H_2O_2-assisted photocatalysis process, depending on the reaction and system conditions, above which H_2O_2 acts as electron and radical scavenger, ultimately reducing the degradation rate of MPs [32].

Water quality parameters, such as the specific UV absorbance and the presence of $HO^{\bullet}$ scavengers (e.g., NOM and high alkalinity), can adversely affect the degradation of MPs [33]. Diverse water matrices may have different scavenging rates since the rate constant for the reaction of DOM with $HO^{\bullet}$ depends on the nature of the DOM [13]. Table 1 summarizes the studies published since 2005 reporting the evaluation of water matrix effects on the effectiveness of H_2O_2-assisted processes (more details can be found in Table S1). In the UV/H_2O_2 process, the matrix components may: (i) absorb UV light which is required to generate $HO^{\bullet}$ from H_2O_2; and (ii) compete with the MPs for the reaction with $HO^{\bullet}$, therefore, lowering the steady-state concentration of radicals in solution [34]. The NOM competes with MPs by consuming a fraction of the oxidant, and consequently higher oxidant doses are usually required to achieve a specific removal of MPs in the presence of NOM [35]. In addition, the water components may affect the chemical nature of the oxidation by-products formed, which in turn may affect the water quality characteristics [33]. Moreover, the breakdown of DOM into smaller molecules can promote the faster decay rates of MPs due to the formation of $HO^{\bullet}$, peroxyl radicals, and excited singlet, doublet or triplet states of oxygen, which may increase the removal of organics MPs in DOC-enriched waters [36].

Another important factor that may affect the performance of H_2O_2-assisted processes is the concentration of inorganic carbon (IC) in the water sample [37]. A high carbonate/bicarbonate content may scavenge $HO^{\bullet}$, according to the following reactions (Reactions 15-16):

$$HO^{\bullet} + HCO_3^{-} \rightarrow H_2O + CO_3^{\bullet -} \qquad (15)$$

$$HO^{\bullet} + CO_3^{2-} \rightarrow HO^{-} + CO_3^{\bullet -} \qquad (16)$$

The carbonate radical ($CO_3^{\bullet -}$) can be also formed via the reaction of carbonate/bicarbonate with $^3DOM^*$ [27]. Regardless of the origin, this radical is a potent oxidant with a one electron reduction potential of 1.78 V (pH 7). It is more selective than $HO^{\bullet}$ as oxidant, mainly reacting with electron rich compounds such as phenols, S- and N-containing compounds [27].

Therefore, both effects can occur in wastewater samples with high DOC and IC: (i) carbonate/bicarbonate scavenge or compete for $HO^{\bullet}$, besides other inorganic scavengers that may interfere with the degradation of MPs [37], such as nitrate, chloride, and sulphate [25, 38]; and (ii) the $CO_3^{\bullet -}$ formed may react with those selected compounds with high second-order rate constant values [27].

Table 1. Matrix effects occurring in studies dealing with the AOTs discussed in this review, published since 2005 (* refers to different sources of wastewater and/or wastewater collected at different stages of treatment). Details of each study can be found in Supplementary Material (Tables S1/S3-S5).

AOT	**Target pollutant**	**Concentration**	**Matrices tested**						**Addition of components**						**Observed effect**	**Reference**
			UPW DI	**DW**	**GW**	**SW**	**SWW**	**WW**	**OM HA**	**NO_3^-**	**Cl^-**	**SO_4^{2-}**	**HCO_3^-**	**Other**		
UV	Bisphenol A	520 µM	X					X							Promoting effect	[4]
UV/H_2O_2	Bisphenol A	520 µM	X					X							Inhibiting effect	[4]
UV/H_2O_2	Benzoylecgonine	$2.8\times10^{-5}\pm4.0\times10^{-6}$ mol L^{-1}	X			X	X	X							Promoting effect (NO_3^-) Inhibiting effect (OM)	[39]
UV/H_2O_2	Benzoylecgonine	0.6–18.5 mg L^{-1}	X			X	X	X							Inhibiting effect (organics, inorganics)	[40]
UV/H_2O_2	Atrazine, sulfamethoxazole, N-nitrosodimethylamine	0.5 – 11 µM				X		X							Inhibiting effect (OM)	[13]
UV UV/H_2O_2	Pharmaceuticals, benzotriazole, mecoprop	ng L^{-1} to µg L^{-1} levels						X*							Dependent on the origin	[20]
UV	Hydrochlorothiazide	1 µM	X			X		X							Inhibiting effect (OM)	[23]
UV	Pharmaceuticals	100 µg L^{-1}	X					X	X	X	X	X	X		Promoting effect (NO_3^-) Inhibiting effect (HA, OM)	[24]
UV	E1, E2, EE2	1.3-1.5 mg L^{-1}		X				X							No noteworthy differences	[25]
UV/H_2O_2	E1, E2, EE2	1.3-1.5 mg L^{-1}		X				X							Inhibiting effect (OM, anions)	[25]

UV	O-phenylphenol, methyl paraben, propyl paraben, triclosan, bisphenol A	0.5 mg L^{-1}	X		X	X		X				Promoting effect (NO_3^-) Inhibiting effect	[29]
UV	Monensin, salinomycin, narasin	0.5 mg L^{-1}	X			X	X					Promoting effect (OM, NO_3^-) Inhibiting effect (OM depending on its source)	[30]
UV	Pharmaceuticals, pesticides, caffeine, triclosan, 2,4-dichlorophenoxyacetic acid	150 µg L^{-1}	X			X	X	X				Promoting effect (OM for some compounds, NO_3^-) Inhibiting effect (OM for some compounds)	[15]
UV	Monensin, salinomycin, narasin, nigericin	0.8 – 3.0 µM	X		X	X						Promoting effect (OM, NO_3^-, Cl^-)	[34]
UV/H_2O_2	Monensin, salinomycin, narasin, nigericin	0.8 – 3.0 µM	X		X	X						Inhibiting effect	[34]
UV/H_2O_2	Pharmaceuticals, bisphenol A	4 µM	X		X	X						Inhibiting effect (OM and ions)	[38]
UV	Sulfamethoxazole	1.0, 2.0, 5.0 and 10 mg L^{-1}	X			X	X	X	X	X	X	Promoting effect (Cl^-, SO_4^{2-}, NO_3^-, 5 mg L^{-1} of HA) Inhibiting effect (HCO_3^-, HA at higher concentrations)	[41]
UV UV/H_2O_2	Pharmaceuticals	0.68-1.72 µM	X			X*						Dependent on the origin	[19]
UV UV/H_2O_2	Oxytetracycline, doxycycline, ciprofloxacin	5 µM	X	X	X	X						Inhibiting effect	[35]
UV UV/H_2O_2	1-H-Benzotriazole, N,N-diethyl-m-toluamide (DEET), chlorophene, 3-methylindole, nortripty-line HCl	1 µM	X		X	X						Inhibiting effect (OM)	[42]

UV UV/H_2O_2	Fungicides	10 µg L^{-1}		X		X		X			No noteworthy differences	[43]
Fenton-like	Bisphenol A	285-14200 µg L^{-1}	X	X	X	X		X			Promoting effect (Cl^-) Inhibiting effect (OM, HCO_3^-)	[14]
Bio-electro-Fenton	Ketoprofen, diclofenac, ibuprofen and naproxen	40 µg L^{-1}	X					X			Inhibiting effect (OM, anions)	[44]
Fenton	Trimethoprim	0.05 mM	X				X	X			Inhibiting effect (OM)	[45]
Fenton Photo-Fenton UV UV/H_2O_2	Prednisolone	100 mg L^{-1}	X					X			Inhibiting effect (organics, inorganics)	[46]
Fenton Photo-Fenton	Pharmaceuticals, benzotriazole, mecoprop	ng L^{-1} to µg L^{-1} levels						X			Dependent on the origin	[20]
Photo-Fenton	Tetracycline	24 mg L^{-1}	X					X			Inhibiting effect (organics, inorganics)	[37]
Photo-Fenton	62 MPs	3-66,379 ng L^{-1}						X*		EDDS; H_2SO_4	Promoting effect (EDDS) Inhibiting effect (HA)	[47]
Photo-Fenton	Pharmaceuticals, pesticides, estrogens, triclosan, hydroxybiphenyl, caffeine	100 µg L^{-1}						X*		EDDS; H_2SO_4	No noteworthy differences	[48]
Photo-Fenton	Pharmaceuticals, pesticides, estrogens, triclosan, hydroxybiphenyl, caffeine	5 and 100 µg L^{-1}						X*	X	Oxalate; H_2SO_4	Promoting effect (HA, oxalate)	[49]
Photo-Fenton	Ofloxacin	10 mg L^{-1}	X			X	X	X			Inhibiting effect (OM, Cl^-, SO_4^{2-})	[50]

Photo-Fenton	Trimethoprim	10 mg L^{-1}	X			X	X	X							Inhibiting effect (OM, inorganics)	[12]
Fenton	Nonionic surfactants	1.4 mg L^{-1}	X					X							Inhibiting effect	[51]
Photo-Fenton	Sulfamethoxazole, clarithromycin	100 µg L^{-1}	X				X	X							Inhibiting effect (OM, Cl^{-}, SO$_4^{2-}$)	[52]
Photo-Fenton	Pharmaceuticals, pesticides, estrogens, triclosan, hydroxybiphenyl, caffeine	100 µg L^{-1}					X	X						H_2SO_4	Promoting effect (HA) Inhibiting effect (CO$_3^{2-}$, HCO$_3^{-}$)	[53]
Fenton	Hydroquinone	100 mg L^{-1}	X					X							No noteworthy differences	[54]
Fenton	51 MPs	ng L^{-1} - µg L^{-1} levels						X*							Inhibiting effect	[55]
Fenton	Pharmaceuticals, estrogens, triclosan	ng L^{-1} to µg L^{-1} levels						X*							Inhibiting effect	[56]
UV/H_2O_2 Photo-Fenton	Pharmaceuticals, methylbenzotriazole, benzotriazole	2 µM	X			X		X							Promoting effect (HA, CO$_3^{2-}$, Cl^{-})	[57]
Photocatalysis	Diclofenac	5–20 mg L^{-1}	X		X			X							Inhibiting effect (OM, other species)	[32]
Photocatalysis	Clofibric acid	1 mg L^{-1}	X					X	X		X	X	X	X	Inhibiting effect (inorganics)	[58]
Photocatalysis	Pharmaceuticals, pesticides, disinfectants	100 µg L^{-1}					X	X							Inhibiting effect	[59]
Photocatalysis UV/H_2O_2	Pharmaceuticals	100 µg L^{-1}	X					X							Inhibiting effect (OM, CO$_3^{2-}$, other anions)	[60]
Photocatalysis	Propyl paraben	420 µg L^{-1}	X	X		X		X							Inhibiting effect (HA, HCO$_3^{-}$, Cl^{-})	[61]
Photocatalysis	Pharmaceuticals, pesticides, industrial compounds	2 mg L^{-1}	X					X							Inhibiting effect (OM, ions)	[62]
Photocatalysis	E1	1000 µg L^{-1}	X				X	X							Inhibiting effect (OM, anions)	[63]

Photocatalysis	Bisphenol A, EE2	100-300 µg L^{-1}	X					X							Inhibiting effect (OM, anions)	[64]
Photocatalysis	Bisphenol A	100 µg L^{-1}	X				X	X							Inhibiting effect (CO$_3^{2-}$, Cl$^-$)	[65]
Photocatalysis	Amoxicillin, carbamazepine, diclofenac	2.5-10 mg L^{-1}					X	X							Inhibiting effect (OM, other species)	[66]
Photocatalysis	EE2	100 µg L^{-1}	X	X				X							Inhibiting effect (OM, HCO$_3^-$, Cl$^-$, SO$_4^{2-}$)	[67]
Photocatalysis	EE2	100 µg L^{-1}	X	X				X							Inhibiting effect (HA, organics, inorganics)	[68]
Photocatalysis	EE2	100–500 µg L^{-1}	X					X							Inhibiting effect (OM, HCO$_3^-$, Cl$^-$, SO$_4^{2-}$)	[69]
Photocatalysis	Ibuprofen	6 µg L^{-1} 6, 60, 213 mg L^{-1}	X					X							Inhibiting effect (OM, NO$_2^-$, NO$_3^-$, PO$_4^{3-}$)	[70]
Photocatalysis	Tetracycline	55 mg L^{-1}	X	X				X							Promoting effect (OM) Inhibiting effect (OM, HCO$_3^-$, Cl$^-$)	[71]
Photocatalysis	Azo dye congo red, carbamazepine	10 mg L^{-1}	X			X		X							Inhibiting effect (anions, Ca^{2+})	[72]
Photocatalysis	Acetaminophen, thiabendazole, imazalil, acetamiprid	100 µg L^{-1}	X				X	X							Inhibiting effect (OM, inorganics)	[73]
Photocatalysis	Metoprolol	50 mg L^{-1}	X					X							Inhibiting effect (OM, inorganics)	[74]
Photocatalysis	Carbamazepine	5 mg L^{-1}						X		X				PO$_4^{3-}$	Inhibiting effect (OM, inorganics)	[75]
Photocatalysis	Ofloxacin, atenolol	10 mg L^{-1}	X		X			X							Inhibiting effect (OM, inorganics)	[76]
Photocatalysis	Diclofenac, fluoxetine	mg L^{-1} levels	X					X							Inhibiting effect (suspended solids)	[77]

Photocatalysis	Sulfamethoxazole	10 mg L^{-1}	X		X		X		Inhibiting effect (ionic strength)	[78]
Photocatalysis	Sulfathiazole, sulfamethoxazole, sulfadiazine	5 mg L^{-1}	X				X		Inhibiting effect	[79]
Photocatalysis	Carbamazepine	133 ng L^{-1}	X				X		Inhibiting effect	[80]
Photolysis	Diclofenac, carbamazepine, ibuprofen, propranolol	5 mg L^{-1}	X				X		Promoting effect (OM, NO_3^-)	[81]
Photocatalysis	Diclofenac, carbamazepine, ibuprofen, propranolol	5 mg L^{-1}	X				X		Inhibiting effect	[81]
Photocatalysis	Pharmaceuticals	0.35-11.30 µg L^{-1}	X				X		No noteworthy differences	[82]
Photocatalysis–DCMD	Diclofenac, naproxen, ibuprofen	100 µg L^{-1}	X	X			X		Promoting effect (suspended solids) Inhibiting effect	[83]
Photocatalysis	Carbamazepine	50 µM	X				X		Inhibiting effect (OM, Cl^-)	[84]
Photocatalysis	Diatrizoate, acetaminophen, carbamazepine, atenolol	736-757 µg L^{-1}					X*		Inhibiting effect	[85]
Photocatalysis	Trimethoprim	1 mg L^{-1}		X	X		X	X	Inhibiting effect	[86]
O_3/H_2O_2	Atrazine, sulfamethoxazole, N-nitrosodimethylamine	0.5 – 11 µM				X	X		Inhibiting effect (OM, CO_3^{2-}, HCO_3^-)	[13]
Ozonation	Hydrochlorothiazide	1 µM	X			X	X		Inhibiting effect (OM)	[23]
UV Photocatalysis O_3 O_3/UV O_3/TiO_2 $O_3/UV/TiO_2$	Diclofenac, sulfamethoxazole, caffeine	10 mg L^{-1}	X				X		Inhibiting effect (OM)	[28]
Ozonation	Metoprolol, naproxen, amoxicillin, phenacetin	1 µM			X	X	X*		Inhibiting effect (OM)	[87]

UV Photocatalysis (TiO_2)	Acetamiprid	100 μg L^{-1}	X		X	X						HA, LS, lignin	Inhibiting effect (HA)	[88]
Photo-Fenton Photocatalysis (PS) UV/PS/Fe	Acetamiprid	100 μg L^{-1}	X		X	X						HA, LS, lignin	Inhibiting effect (lignin)	[88]
Photocatalysis O_3/H_2O_2	Carbamazepine, diclofenac	10-1000 μg L^{-1}	X			X							Inhibiting effect	[16]
Photo-Fenton	Carbamazepine, diclofenac	10-1000 μg L^{-1}	X			X							Promoting effect	[16]
O_3	Tetrabromobisphenol	100 mg L^{-1}	X	X		X*	X	X	X	X	X		No noteworthy differences	[89]
O_3	Flumequine	20 μg L^{-1}- 20 mg L^{-1}	X	X		X*	X		X	X	X	K^+, Ca^{2+}, Mg^{2+}	Promoting effect (OM) Inhibiting effect (OM)	[90]
O_3 O_3/H_2O_2	Metoprolol, naproxen, amoxicillin, phenacetin	1 μM	X			X*							Inhibiting effect (OM)	[91]
Photocatalytic ozonation	Diclofenac	10^{-4} and 10^{-6} M	X			X							Inhibiting effect (organics, inorganics)	[92]
O_3	APIs	1 μg L^{-1}				X*							Inhibiting effect (COD and alkalinity)	[93]
O_3	Ofloxacin	22 mg L^{-1}			X	X							Inhibiting effect (OM)	[94]
O_3	Benzalkonium chloride	10 mg L^{-1}			X	X							Inhibiting effect (OM)	[95]
O_3	Pesticides	5-20 mg L^{-1}			X	X							Inhibiting effect (COD, HCO_3^-, PO_4^{3-}, Cl^-)	[96]
O_3 Catalytic ozonation	Mesoxalic and oxalic acids	50 mg L^{-1}				X			X	X	X	PO_4^{3-}	Inhibiting effect (anions, suspended solids)	[97]
O_3 O_3/H_2O_2	Sulfamethoxazole, diclofenac	30 mg L^{-1}			X	X							Inhibiting effect (CO_3^{2-}, HCO_3^-, SO_4^{2-}, PO_4^{3-})	[98]

O_3 O_3/H_2O_2	Pharmaceuticals	ng L^{-1} levels						X*			Inhibiting effect	[99]
Catalytic ozonation	Diclofenac, sulfamethoxazole, EE2	10 mg L^{-1}						X*		H_2SO_4	No noteworthy differences	[100]
Photocatalytic ozonation	Diclofenac, amoxicillin	0.1 mM	X					X			Inhibiting effect	[101]
O_3 Catalytic ozonation	Formic, acetic, oxalic and maleic acids	7 mg L^{-1}						X*			Inhibiting effect (OM)	[102]
O_3 Photocatalysis Photocatalytic ozonation	Pharmaceuticals and hydroxyl-biphenyl	50 µg L^{-1}	X					X			Inhibiting effect (organics, inorganics)	[103]
O_3 UV UV/H_2O_2 O_3/H_2O_2	Pharmaceuticals	1 µM			X	X		X			Inhibiting effect (OM)	[104]
O_3 UV/H_2O_2	Organophosphate esters	50 µg L^{-1}	X					X	X		Inhibiting effect (OM, Cl^-, SO_4^{2-}, NO_3^{2-}, HCO_3^-)	[105]
O_3 UV UV/H_2O_2 UV/O_3, O_3/H_2O_2 $O_3/UV/H_2O_2$	E1	3 µg L^{-1} – 5 mg L^{-1}	X					X			Inhibiting effect (OM)	[106]
Catalytic ozonation	Benzotriazole	10 mg L^{-1}	X					X			No noteworthy differences	[107]

Abbreviations: API, active pharmaceutical ingredient; COD, chemical oxygen demand; DCMD, direct contact membrane distillation; DI, distilled water; DW, drinking water; E1, estrone; E2, 17-beta-estradiol; EE2, 17-alpha-ethinylestradiol; EDDS, ethylenediamine-N,N′-disuccinic acid; GW, groundwater; HA, humic acids, LS, lauryl sulphate; OM, organic matter; PS, persulphate; SW, surface water; SWW, synthetic wastewater; UPW, ultrapure water; WW, wastewater.

2.3. Fenton-based processes

The conventional Fenton process employs the “Fenton's reagent” [108], a mixture of Fe^{2+} and H_2O_2 that yields $HO^•$ and Fe^{3+} as reaction products (Reactions 17-18). This reagent combines the use of the fourth most abundant element in the earth's crust, which has environmental compatibility and low-toxicity [109], with the oxidant H_2O_2, which self-decomposition leads to non-toxic products (H_2O and O_2) [110]. The low cost of the Fenton’s reagent and the negligible activation energy, coupled to the simplicity of the process, are attractive advantages. However, the regeneration of Fe^{2+} under darkness in the conventional Fenton process is very slow and governed by the following reactions (Reactions 19-21) [20].

$$Fe^{2+} + H_2O_2 \rightarrow Fe^{3+} + HO^{-} + HO^{•} \quad (17)$$

$$Fe^{2+} + HO^{•} \rightarrow Fe^{3+} + HO^{-} \quad (18)$$

$$HO^{•} + RH \rightarrow H_2O + R^{•} \quad (19)$$

$$R^{•} + Fe^{3+} + \rightarrow R^{+} + Fe^{2+} \quad (20)$$

$$Fe^{3+} + H_2O_2 \rightarrow Fe^{2+} + HO_2^{•} + H^{+} \quad (21)$$

The main shortcomings of the Fenton process include: (i) the fast depletion of Fe^{2+} and the slow regeneration rate; (ii) the amount of sludge produced needing additional treatment; (iii) the complexation of some iron species; (iv) the potential loss of oxidants by scavenging effect or auto-degradation; and (v) the requirement of a pH between 2.5 and 3.0 to achieve optimal performance and below 4.0 to avoid the iron precipitation [111]. The latter originate the need to neutralize the wastewater with bases after treatment, but the consequent raised salt concentration would be deleterious for specific reuses of the treated water, such as for irrigation [47].

Modifications of the Fenton reaction in “Fenton-like” processes using Fe^{3+} (Reactions 22-23) [112] or zero-valent iron (Fe^{o}) (Reaction 24) [113] have also been investigated, the former producing peroxyl radicals ($HO_2^{•}$) and the latter as a source of Fe^{2+} in the Fenton reaction.

$$Fe^{3+} + H_2O_2 \rightarrow H^{+} + FeOOH^{2+} \quad (22)$$

$FeOOH^{2+} \rightarrow HO_2^{\bullet} + Fe^{2+}$ (23)

$Fe^{o} + H_2SO_4 \rightarrow Fe^{2+} + SO_4^{2-} + H_2$ (24)

Photo-Fenton based processes are assisted by UV-Vis irradiation, accelerating the regeneration rate of Fe^{2+} from Fe^{3+} complexes (Reactions 26-26). The most photoactive complex $[Fe(OH)]^{2+}$ is predominant at acidic pH, limiting the use of photo-Fenton. Temperature is also an important parameter that has an impact on both Fenton and photo-Fenton reaction rates, since raising the temperature accelerates the oxidation of Fe^{2+} by H_2O_2 (thermal Fenton) and enhances the light absorption coefficient of Fe^{3+} [44]. However, the increase of temperature may lead to higher leaching of iron and consequent deactivation of catalyst in successive cycles, as well as to the thermal decomposition of H_2O_2 to water and oxygen above 40 °C [108].

$[Fe(H_2O)]^{3+} + h\nu \rightarrow Fe^{2+} + HO^{\bullet} + H^{+}$ (25)

$[Fe(OH)]^{2+} + h\nu \rightarrow Fe^{2+} + HO^{\bullet}$ (26)

The higher costs of the photo-Fenton process in comparison to the conventional Fenton reaction, due to the use of an irradiation source, are compensated by the lower amount of catalyst required to efficiently generate $HO^{\bullet}$ and by the smaller amount of sludge produced [1], which was reported to be 25 times less in a study dealing with the treatment of landfill leachate by conventional Fenton and photo-Fenton processes [114]. It has been suggested that no supplementary iron is required in wastewater effluents containing at least 1.5 mg L^{-1} of total iron, to employ the photo-Fenton process [21, 115].

Photo-Fenton at neutral pH has been applied using chelating agents, namely ferrioxalate ($[Fe(C_2O_4)_3]^{3-}$), ethylenediamine-N,N′-disuccinic acid (EDDS), humic acids (HA) and mixing the wastewater effluents with small amounts of influent sample [47-49]. The former is a photosensitive complex with an extended absorption range, enabling the efficient use of solar light. Besides, in comparison to Fe^{2+} hydroxyl-complexes (Reaction 27), ferrioxalate gives a higher quantum yield of Fe^{2+} (Reactions 28-29) [116] and generates a higher amount of $HO^{\bullet}$

(Reactions 30-33), by providing additional sources of oxidant H_2O_2 and catalyst Fe^{2+} for the Fenton reaction [49].

$Fe(OH)_2 + h\nu \rightarrow Fe^{2+} + 2HO^{\bullet}$ (27)

$[Fe(C_2O_4)_3]^{3-} + h\nu \rightarrow Fe^{2+} + 2C_2O_4^{2-} + C_2O_4^{\bullet-}$ (28)

$C_2O_4^{\bullet-} + [Fe(C_2O_4)_3]^{3-} \rightarrow Fe^{2+} + 3C_2O_4^{2-} + 2CO_2$ (29)

$C_2O_4^{\bullet-} + O_2 \rightarrow 2CO_2 + O_2^{-}$ (30)

$O_2^{-} + H^{+} \rightarrow HO_2^{\bullet}$ (31)

$2\ HO_2^{\bullet} \rightarrow H_2O_2 + O_2$ (32)

$H_2O_2 + Fe^{2+} \rightarrow Fe^{3+} + HO^{\bullet} + HO^{-}$ (33)

Solar photo-Fenton using EDDS as an iron-complexing agent can be a feasible process to degrade contaminants (phenol, bisphenol A, sulfamethoxazole, carbamazepine and pyrimethanil) from wastewater effluents, even at neutral and slightly alkaline pH and in the presence of high DOC values [117]. HA can be also used to promote the photo-Fenton reaction due to their characteristics: (i) HA are organic substances resulting from chemical and microbiological transformation of organic matter and are ubiquitous in the environment; (ii) they have a complex chemical structure, which include carboxylic acids, phenolic, alcoholic quinine, amino and amido groups, as well as high amounts of stable free radicals; (iii) HA are able to photoinduce the transformation of non-absorbing organic chemicals due to the absorption of sunlight and consequent generation of $HO^{\bullet}$, ROS, exited triplet states ($^3HA^*$), singlet oxygen ($^1O_2$) and H_2O_2 [49]; they are able to improve the process at natural pH due to the enhanced reduction of Fe(III) humate-complexes in comparison with the Fe(III) aquo-complexes [88]. However, HA at high concentrations can also scavenge radicals [88], therefore the overall effect on the MPs removal may be either promoting, neutral or inhibitory. Table 1 summarizes the reports published since 2005 referring the evaluation of matrix effects on Fenton-based processes (more details can be found in Table S3).

Another approach commonly used in photo-Fenton like processes involves the use of radiation to assist the photo-decarboxylation of ferric carboxylates (Reaction 34) [118].

$$[Fe^{3+}L] + hv \rightarrow [Fe^{3+}L]^{*} \rightarrow Fe^{2+} + L^{\bullet} \qquad (34)$$

The photoactive ferric complexes are formed between Fe^{3+} and carboxylate or polycarboxylate groups, which are functional moieties frequently present in DOM [119]. These are soluble in wastewater under a wide pH range, avoiding the precipitation of Fe^{3+} at neutral pH and the consequent need of acidification and pH control of Fenton processes. Another main advantage is the higher molar absorption coefficients in the near UV-Vis spectral regions in comparison to the Fe(III) aquo-complexes [117, 119]. However, such compounds typically able to form photoactive $Fe^{3+}L$ (e.g., oxalic acid, lactic acid, quinolinic acid, fusaric acid, pinolenic acid) are usually highly biodegradable and often absent in wastewater effluents [119]. For this reason, the mixing of effluent with small amounts of influent (3:1 ratio) as a source of these substances has been investigated, as a mean to avoid the addition of supplementary chemical reactants during the treatment process [49]. The effectiveness of this approach for the degradation of the MPs is, however, dependent on the concentration ratio of carboxylate or polycarboxylate compounds and the organic load in the water influents [49].

The electro-Fenton process, is an eco-friendly, electrically assisted Fenton process, consisting in the use of a reactor with inert electrodes which are able to electro-regenerate Fe^{2+} from Fe^{3+}. In such process, the Fe^{2+} is provided from sacrificial cast iron anodes and the H_2O_2 is either added to the reactor or generated *in-situ* by the two-electron oxygen reduction reaction in an acidic medium (Reaction 35) [111].

$$O_2 + 2H^{+} + 2e^{-} \rightarrow H_2O_2 \qquad (35)$$

The electricity costs of the electro-Fenton (or photo-electro-Fenton) process, similarly to the photo-Fenton process, are overcome by the smaller amount of catalyst required to efficiently generate $HO^{\bullet}$ and by the smaller quantity of sludge produced, in comparison to the conventional Fenton process.

The water matrix components may raise a negative and/or a positive impact on the effectiveness of Fenton-based processes and the overall result depends on their balance [12, 16, 50]. In complex water matrices containing many species, the degradation of MPs is generally lower than in pure water when Fenton-based processes are employed, implying the use of higher doses of reactants (iron species and H_2O_2) [51]. The following factors have a negative impact: (i) light scattering inhibiting the photo-reduction of Fe^{3+}; (ii) the scavenging of $HO^{\bullet}$ by water matrix constituents, such as organic acids, NOM (e.g., humic and fulvic acids), inorganic ions (e.g., bicarbonate, carbonate) [120]; and (iii) the formation of complexes (e.g., $FeCl_2^{+}$, $FeCl^{2+}$, and $Fe(SO_4)_2^{-}$) by reaction between iron ions and inorganic anions, reducing the catalytic activity of the free iron species [16]. Specifically, chloride and sulphate can decrease the photo-Fenton reaction rate with MPs by scavenging $HO^{\bullet}$ and producing chlorine and sulphate radicals ($Cl_2^{\bullet-}$ and $SO_4^{\bullet-}$), which overall are less reactive than $HO^{\bullet}$. They can also complex the iron species (Fe^{2+} and Fe^{3+}), interfering with the reduction of Fe^{3+} to Fe^{2+} that is required to sustain an efficient Fenton mechanism [12, 52]. Very recently, these species were shown to decrease the conversion of dichlorophenoxyacetic acid from 74.25% in demineralised water to 70.98% in the presence of sulphate and 66.65% in the presence of chloride [121]. In consequence, high organic and inorganic species in water matrices may decrease the removal rates of contaminants [52] and DOC in general, interfering with the degradation pathways and consequently affecting the composition and toxicity of the by-products formed [12, 50]. For instance, the presence of chloride in the water matrix has been linked to the production of chlorinated transformation by-products [14]. Other inhibiting effect can arise from the formation of iron complexes with the by-products generated during the degradation of a certain compound, as observed in the case of prednisolone [46].

In contrast, the following factors have a positive impact on Fenton-based processes: (i) the iron ions naturally occurring in the water matrix may act as an additional source of catalyst for the Fenton reaction; (ii) inherent reductants present in the water matrix (e.g., phenolic compounds) might reduce Fe^{3+} to Fe^{2+}, increasing the regeneration rate of the catalyst; and (iii) Fe^{3+} can react with compounds containing -COOH and -OH groups, originating complexes with higher quantum yield, which might undergo photo-reduction through a ligand-to-metal charge transfer to Fe^{2+} [16, 122]. Although high content of organic species (e.g., 16.5 mg L^{-1} of DOC) may reduce the removal rates of MPs [52], some studies have demonstrated higher removal rates of MPs in actual wastewaters in comparison to simulated wastewater matrices. In a study where this phenomenon was observed for 15 compounds (pharmaceuticals, estrogens, personal care products, and pesticides), a similar DOC reduction in both matrices suggested that the HA present in the wastewater effluents probably produced solvated electrons and $HO^{\bullet}$ upon irradiation [53]. In another report, a DOM content approximately 2000 times higher than the concentration of MPs in the wastewater did not denote a shortcoming on their removal rates, since certain species in the DOM could either act as photosensitizers or complex iron to keep it dissolved, promoting the degradation of MPs by the photo-Fenton reaction mechanism [115].

2.4. Photocatalysis

Heterogeneous photocatalysis has been extensively reported in the last decades, not only for water/wastewater and air treatment, but also for production of fuels [1]. Heterogeneous photocatalysis is based on the use of wide band-gap semiconductors, which generate conduction band electrons and valence band holes, under irradiation with light energy (hv) equal to or higher than the semiconductor band-gap energy (Reaction 36) [123, 124].

$$TiO_2 + h\nu \quad \rightarrow \quad e^- + h^+ \qquad (36)$$

The photogenerated conduction band electrons and valence band holes can either recombine to dissipate heat, or migrate to the semiconductor surface, where they can react with species adsorbed on the catalyst surface [123]. The photogenerated valence band holes produce reactive $HO^{\bullet}$ which are strong oxidizing agents, by reaction with water (Reaction 37) and with hydroxide ion under alkaline conditions (Reaction 38), or can also react directly with adsorbed species (Reaction 39) [1].

$$TiO_2\ (h^+) + H_2O \rightarrow TiO_2 + HO^\bullet + H^+ \qquad (37)$$

$$TiO_2\ (h^+) + HO^- \rightarrow TiO_2 + HO^\bullet \qquad (38)$$

$$TiO_2\ (h^+) + AdsSpecies \rightarrow TiO_2 + AdsSpecies^{\bullet +} \qquad (39)$$

The photogenerated conduction band electrons usually reduce the adsorbed molecular oxygen (and/or adsorbed reducible species) and generate superoxide radicals (Reaction 40), which can further react with protons to produce peroxide radicals (Reaction 41) [123]. The substrate species then can react with the ROS generated (Reaction 42).

$$TiO_2\ (e^-) + O_2 \rightarrow TiO_2 + O_2^{\bullet -} \qquad (40)$$

$$O_2^{\bullet -} + H^+ \rightarrow HO_2^{\bullet -} \qquad (41)$$

$$ROS\ (HO^\bullet, O_2^{\bullet -}, HO_2^{\bullet -}) + Species \rightarrow Oxidation\ products \qquad (42)$$

An ideal photocatalyst should be chemically and photochemically stable, should have a high surface area for the adsorption of the reacting species, a high photon absorption coefficient, a small scattering albedo, be easily available and of low cost whenever possible. Generally, the photodegradation rate of MPs increases with catalyst loading up to an optimum concentration corresponding to the maximum amount of catalyst at which all particles are efficiently irradiated, beyond which the efficiency drops off due to the lower penetration of activating photons through the turbid water [58]. Such process is dependent on reactor geometry, the design of which has been rationalised in terms of optimum dimensionless optical thickness of photoreactors [125]. In the last decades, the most common, commercially available photocatalyst has been TiO_2, either in bulk or supported on a substrate, due to its relatively high photoactivity, high mineralization efficiency, low cost and toxicity, high photochemical stability and suitable band-gap energy [1, 124]. ZnO has also been largely used mainly due to its higher electronic conductivity and near band-gap energy [126]. However, its susceptibility to photo-corrosion limits its use and thus TiO_2 is still the most used photocatalyst. Although it has higher performance in an aqueous slurry suspension, the separation of TiO_2 from the treated water may in some cases present a minor challenge in industrial scale applications [127]. In consequence, a range of support materials have been used for the immobilization of TiO_2, including polymers, metals, silica, carbon materials or ceramics [59]. Ideally, an active support must also promote the interaction between the photocatalyst and the contaminants, without hindering the absorption of active photons, and should be resistant to the oxidizing conditions [59].

The two major shortcomings of heterogeneous photocatalysis over TiO_2 are: (i) the limited absorption of natural sunlight since near-UV radiation is needed for photo-activation and this part represents only ca. 3-5% of the solar radiation reaching the earth surface; and (ii) the relatively high rate of electron-hole pairs recombination which reduces the available charges for the redox reactions. Several studies have been published using different approaches to develop photocatalysts that can address the above shortcoming [7], by creating defect structures on the catalyst [128], by metal deposition on the catalyst surface [129], by semiconductor coupling of the energy bands [130] and by doping with metals/non-metal ions [131]. TiO_2 combinations with noble metals (e.g., silver, gold and platinum) [63] or with carbon-based materials such as graphene-based materials [132, 133], have also been examined. Other carbon materials have been widely studied, including activated carbons [134, 135], carbon xerogels [136], carbon nanotubes [137, 138], graphite [139], and more recently graphitic carbon nitride [140]. The suppression of the recombination of photo-generated charge carriers has been attempted, by adding oxidizing agents/electron acceptors (e.g., inorganic peroxides ($S_2O_8^{2-}$), Fe^{3+}, H_2O_2), doping the material with metal ions or anions, by noble metal loading, dye sensitization or using composite semiconductors [126, 141, 142].

The detrimental effect of components co-existing in the water matrix is attributed to the organic and inorganic species intrinsically present in the wastewater [64], including: (i) light attenuation by suspended particles and dissolved species [77]; (ii) the NOM partially consuming $HO^{\bullet}$ and other oxidizing species, thus competing with the degradation of MPs [32, 64-67, 69, 70]; (iii) the anions present in wastewater (e.g., bicarbonate, sulphate and chloride) which scavenge $HO^{\bullet}$ to form the respective radicals with lower oxidation potential [58, 64-67, 69-72]; and (iv) both organics and inorganics adsorbing onto the catalyst surface, fouling and/or competing for the active reaction sites [63, 73-76]. Table 1 summarizes the reports published since 2005 referring the evaluation of matrix effects on photocatalytic processes (more details can be found in Table S4).

The impact of NOM on the photocatalytic degradation of organic compounds has been recently reviewed [143]. NOM plays an important role in sunlight-induced photochemical processes, generally retarding the photocatalytic degradation of pollutants by the combination of radiation attenuation, competition for adsorption on active sites of the catalyst and surface deactivation, and by scavenging both valence band holes and conduction band electrons [144]. The water matrix may not show an effect on the degradation of the MPs, but may strongly affect the rate of mineralization, as shown in a study on solar TiO_2 photocatalytic oxidation of a mixture of four pharmaceuticals (atenolol, hydrochlorothiazide, ofloxacin and trimethoprim) in a synthetic effluent [145]. The impact of the water matrix on the photocatalytic degradation of clofibric acid resulted in a strong decrease of the photocatalytic activity resulting from the competition of NOM, for active sites on the catalyst surface and for reactive species [58]. UV light attenuation plays an additional significant role on the reduction of the rate of degradation of MPs in wastewater.

Inorganic salts in the water matrix (NaCl, $FeCl_3$, $FeCl_2$,, $AlCl_3$, $CaCl_2$) can have negative impact on the photocatalyst activity, with a generally more pronounced deactivation effects observed at higher salt concentrations [58]. The deactivation of the TiO_2 catalyst by inorganic species has been linked to the competition for free radicals and to the blockage of the active sites on the catalyst surface [58]. Sulphate and carbonate anions might cause strong catalyst deactivation, since both species are strong ROS scavengers, whereas sodium chloride can produce ambiguous effects on the photocatalytic activity of TiO_2, depending on the salt concentration [58]. The pH and the ionic strength of the wastewater play important roles on the degree of catalyst agglomeration in a suspension, which impact on the effective surface area of the photocatalyst [78] and on the rate of photon absorption [146]. High pH and/or ionic strength of the aqueous solution might result in a higher agglomeration of TiO_2, decreasing the effective surface area of the photocatalyst [147, 148]. This phenomenon has been observed for the photocatalytic degradation of sulphonamides, whose removal was favoured at acidic pH [78-80]. The photocatalytic degradation of clofibric acid was shown to be inhibited by chloride ions at low concentrations, which adsorbed on the TiO_2 surface reducing the available active sites. This is justified by the acidic nature of the contaminant and the positively charged surface of the catalyst, resulting from the sample pH lower than the point of zero charge (pH_{PZC}) of TiO_2 [58]. At high concentration of NaCl, the ionic strength was the dominant factor of the photocatalytic efficiency, since the electric double layer become more compressed and the clofibric acid could easily reach the catalyst surface [58].

Phosphate can affect positively the degradation of pollutants by generating the reactive radical $H_2PO_4^{\bullet}$ in the presence of holes (Reaction 43) which favours the photocatalytic degradation of carbamazepine over TiO_2 [72]:

$$h^+ + H_2PO_4^- \rightarrow H_2PO_4^{\bullet} \qquad (43)$$

The impact of coexisting substances on the photocatalytic degradation of bisphenol A was studied under simulated solar light irradiation and using bismuth tungstate (Bi_2WO_6) as catalyst, suggesting that photogenerated holes are predominant in the reaction system [149]. The degradation of bisphenol A was accelerated in the presence of a low concentration of HA (1 mg L^{-1}), while a hindrance was found at concentrations higher than 5 mg L^{-1}. The presence of anions (nitrate, chloride, sulphate and bicarbonate) and cations (sodium, potassium, calcium and magnesium) led to inhibitory effects, the latter being ascribed to the chloride resulting from the addition of the chloride salts of each cation [149]. At solution pH lower than 8.7 (pH_{PZC} of Bi_2WO_6), the positively charged surface of the catalyst attracted anions, decreasing the free active sites and diminishing the reaction rate of bisphenol A. Sulphate had a much stronger inhibition effect than chloride, nitrate and bicarbonate, due to its double charge and larger molecular size which increases the steric hindrance [149]. A minor impact was observed for bicarbonate and nitrate ions, the latter favouring the reaction rate at low concentrations, which can be explained by its photolysis and consequent production of $HO^{\bullet}$ [149]. At high salt concentrations, nitrate could be adsorbed on the catalyst surface, competing for the active sites with the target pollutant, while bicarbonate scavenged $HO^\bullet$, producing weakly oxidizing carbonate radicals. The impact of bicarbonate is more significant when the photocatalytic degradation of the target contaminant follows $HO^\bullet$ attack, rather than hole oxidation. On the contrary, the presence of inorganic Fe^{3+} ion in the water and the use of H_2O_2 oxidative reagent played different effects depending on their concentrations. At concentrations lower than 0.01 mmol L^{-1} Fe^{3+} or 1 mmol L^{-1} H_2O_2, there was no effect; at concentrations in the range of 0.01–0.1 mmol L^{-1} of Fe^{3+} or in the range of 0.1–3 mmol L^{-1} of H_2O_2, a suppression of the photogenerated holes (the main oxidizing species by Bi_2WO_6) was observed; however, higher concentrations of these interfering species enhanced the degradation rate of bisphenol A due to the generation of $HO^\bullet$ produced by $Fe(OH)^{2+}$ under UV irradiation or by photolysis of H_2O_2 [149].

2.5. Ozone-based processes

Ozonation is an AOT widely applied for the purification of drinking water due to the power of O_3 as disinfectant and oxidant. Ozonation has also been used for the treatment of either raw wastewaters, as pre-treatment, or secondary wastewater effluents, as post-treatment, to minimize the release of MPs into the receiving waters [89]. In Switzerland, full-scale UWWTPs have already implemented ozonation as a post-treatment process, aiming 80% average removal of target organic MPs [150].

The transformation of organic substances by ozonation occurs by either reaction with molecular O_3 or reaction with less selective $HO^\bullet$, resulting from the decomposition of O_3 at neutral and alkaline pH [13]. In comparison to molecular O_3, which is a selective oxidant attacking predominantly electron-rich organic moieties (phenols, anilines, olefins, sulphur, and amine moieties), $HO^\bullet$ are non-selective radicals, more reactive than ozone. The contribution of each pathway depends on the O_3 and $HO^\bullet$ exposures (i.e., $\int [O_3]\, dt$ and $\int [HO^\bullet]\, dt$) and second order reaction rate constants (Reaction 44-51) [151, 152]. In many cases, high pH values favour the degradation efficiency due to the decomposition of O_3 into $HO^\bullet$ [153].

$$O_3 + HO^- \rightarrow HO_2^- + O_2 \qquad \text{(basic pH)} \qquad (44)$$

$$O_3 + HO_2^- \rightarrow HO^{\bullet} + O_2^{\bullet -} + O_2 \qquad (45)$$

$$O_3 + O_2^{\bullet -} \rightarrow O_3^{\bullet -} + O_2 \qquad (46)$$

$$O_3^{\bullet -} + H^+ \leftrightarrow HO_3^{\bullet} \qquad (pH < 8) \qquad (47)$$

$$HO_3^{\bullet} \rightarrow HO^{\bullet} + O_2 \qquad (pH < 8) \qquad (48)$$

$$O_3^{\bullet -} \leftrightarrow O^{\bullet -} + O_2 \qquad (pH > 8) \qquad (49)$$

$$O^{\bullet -} + H_2O \rightarrow HO^{\bullet} + HO^- \qquad (pH > 8) \qquad (50)$$

$$HO^{\bullet} + O_3 \rightarrow HO_2^{\bullet} + O_2 \qquad (51)$$

Ozonation is an oxidation process that can take place at both the gas-liquid interface and in the bulk liquid, depending on the concentration of the reactants and on the Hatta number [154]. Therefore, the polarity can play an important role in the reaction rate, since non-polar organic compounds tend to accumulate at the interface and be more reactive, while more polar or dissociated substances remain in the bulk liquid [155].

O_3 decomposition is fast during the initial phase ($t < 20$ s) of natural water ozonation, known as ‘‘instantaneous ozone demand’’, while during the second phase ($t > 20$ s) it follows an apparent first-order rate law attributed to radical-type chain reactions, during which $HO^{\bullet}$ are generated [156]. NOM and carbonate/bicarbonate ions interfere with the rate of O_3 decomposition depending on their concentrations and pH, affecting the yield of $HO^{\bullet}$ [157]. Besides the scavenging effect of $HO^{\bullet}$ by NOM [13, 23, 87, 90-95] and carbonate/bicarbonate [13, 92, 93, 97, 98], other anions (e.g., chloride, phosphate, sulphate) can also act as ozonation inhibitors [97, 98].

The main mechanism of O_3 decomposition and generation of $HO^{\bullet}$ in wastewater is the direct reaction with specific reactive moieties of the NOM (e.g., phenolic, amino and olefinic groups), considering that the initiation step of the radical chain reaction between O_3 and hydroxide anions has a small rate constant [156]. The reactions of O_3 with DOM (Reactions 52-55) are summarized as the follows [158, 159].

$O_3 + DOM_{direct} \rightarrow$ products (52)

$O_3 + DOM_{initiator} \rightarrow HO^{\bullet}$ (53)

$HO^{\bullet} + DOM_{promoter} \rightarrow \bullet\bullet\bullet \rightarrow O_2^{\bullet -}$ (54)

$HO^{\bullet} + DOM_{inhititor} \rightarrow$ products (55)

Both the concentration and the composition of DOC determine the rate of decomposition of aqueous O_3, therefore DOC is a crucial water quality parameter that is monitored to normalize the dosing of O_3 [156]. Table 1 summarizes the reports published since 2005 referring the evaluation of matrix effects on ozone-based processes (more details can be found in Table S5). The O_3 dose required to degrade the antibiotic ofloxacin was strongly affected by the matrix (synthetic water vs wastewater effluent), showing the competition between the NOM and the target pharmaceutical for O_3 and suggesting that certain moieties of NOM present in wastewater were preferably attacked [94]. Even when the degradation rate of the organic MPs is not affected, total organic carbon (TOC) removal can be significantly affected due to the refractory nature of the organic matter, as observed in synthetic effluents treated by ozonation [145].

The impact of the inorganic ions (chloride, sulphate and bicarbonate, potassium, calcium and magnesium) or extracts of NOM, and the type of water matrices (ultrapure, river water, influent and effluent wastewaters) on the removal of flumequine by ozonation, has been shown to be insignificant [90]. However, rice straw and pig manure NOM extracts, promoted the oxidation of the target pollutant [90]. The scavenging of NOM and carbonate/bicarbonate on $HO^{\bullet}$ in different water matrices containing similar DOC and bicarbonate contents demonstrated different DOM reactivity [13]. Moreover, the higher carbonate-alkalinity led to slower kinetics of pCBA removal, ascribed to the slower kinetics of O_3 decomposition due to the inhibition by the carbonate/bicarbonate ions in the water [13].

Another study reported that nitrate enhanced the degradation rate of phenazone by ozone, whereas other anions (chlorine, sulphate and bicarbonate) reduced the rate, following the order: sulphate > chloride > bicarbonate [160]. While the scavenging of $HO^{\bullet}$ by bicarbonate is well-known, the lower degradation rate of phenazone in the presence of sulphate and chloride was attributed to the formation of weaker $Cl_2^{\bullet-}$ and $SO_4^{\bullet-}$ radicals [160].

The main drawback of the ozonation process is the generally limited rate of DOC mineralization and consequent accumulation of unknown reaction by-products, resulting from the incomplete oxidation of the target compounds and from the reaction with the water matrix constituents [161]. Undesirable toxic oxidation by-products include nitrosamines (e.g., N-Nitrosodimethylamine, NDMA), bromate and formaldehyde [161]. Although these by-products may increase the toxicity of the treated wastewater, they are typically biodegradable and therefore a biological post-filtration is usually applied [161]. The limited extent of DOC mineralization can be overcome by adding catalysts or H_2O_2.

The peroxone process combining O_3/H_2O_2 accelerates the conversion of O_3 to $HO^{\bullet}$, which can decrease the reaction time needed to degrade the MPs [13]. The degradation efficiency of the MPs reaches a maximum at certain concentration of H_2O_2 beyond which inhibition occurs [160]. Two $HO^{\bullet}$ are produced from the reaction between two O_3 and one H_2O_2 molecule, therefore the ratio between the H_2O_2 supply rate and the O_3 absorption rate should be 0.5 or slightly higher [162]. A low H_2O_2 dose can catalytically decompose O_3 to generate a substantial amount of $HO^{\bullet}$, which favours the oxidation of MPs, whereas an excessive H_2O_2 dose can favour the reaction with $HO^{\bullet}$ to form a weaker hydroperoxyl radical ($HO_2^{\bullet}$) [160].

The use of heterogeneous catalysts or photocatalysts is an attractive solution in ozonation, since the combination of two or more AOTs can lead to higher removal rates in comparison to the single processes. Usually, the application of ozonation alone rarely lead to complete mineralization of MPs, since some reaction intermediates, including specific carboxylic acids, may not be easily destroyed by O_3 or by its produced oxidizing radicals. When the organic compounds are not completely degraded, the partial oxidation may produce by-products that are more toxic than the parent pollutants [163, 164]. Thus, the addition of catalysts in catalytic ozonation can improve the oxidation efficiency of ozone and also its potential to convert oxidation by-products into CO_2 [100]. The most widely used catalysts include transition metal oxides (TiO_2, MnO_2, Al_2O_3, FeOOH, and CeO_2), metals (Cu, Ru, Pt and Co) on supports (SiO_2, TiO_2, Al_2O_3, CeO_2 and activated carbon), zeolites modified with metals, activated carbon and natural minerals [165].

Recently, photocatalytic ozonation has been studied as an alternative to photocatalysis and ozonation due to the increased production of $HO^{\bullet}$ through the formation of an ozonide radical ($O_3^{\bullet -}$) in the adsorption layer of a semiconductor (e.g., TiO_2) and lower electron–hole recombination, in comparison to ozonation and photocatalysis, respectively [1]. Specifically, the $O_3^{\bullet -}$ species (Reaction 56) generated from the reaction of ozone with the semiconductor electrons react with H^+ in the solution, forming $HO_3^{\bullet}$ radicals (Reaction 57) which then evolve to produce oxygen and $HO^{\bullet}$ (Reaction 58). In this scenario, it must be also considered that $HO^{\bullet}$ can react with ozone (Reaction 59). When ozone is completely consumed, dissolved O_2 can accept the semiconductor conduction band electrons, generating $O_2^{\bullet -}$ (Reaction 60), which in turn can be protonated (Reaction 61). $HO_2^{\bullet}$ radicals can also originate $HO^{\bullet}$, according to the pathway shown by Reactions 62-63 [166].

$O_3 + e- \rightarrow O_3^{\bullet -}$ (56)

$O_3^{\bullet -} + H^+ \rightarrow HO_3^{\bullet}$ (57)

$HO_3^{\bullet} \rightarrow O_2 + HO^{\bullet}$ (58)

$HO^{\bullet} + O_3 \rightarrow O_2 + HO_2^{\bullet}$ (59)

$O_2 + e- \rightarrow O_2^{\bullet -}$ (60)

$O_2^{\bullet -} + H^+ \rightarrow HO_2^{\bullet}$ (61)

$2HO_2^{\bullet} \rightarrow H_2O_2 + O_2$ (62)

$H_2O_2 + O_2^{\bullet -} \rightarrow HO^{\bullet} + HO^- + O_2$ (63)

Another possible reaction pathway has been proposed by Kopf et al. [167]. These authors suggested that the photocatalytic ozonation reactions are initiated by an electron transfer from TiO_2 to O_2 (Reactions 64-67), followed by reaction of $O_2^{\bullet -}$ with O_3 (Reaction 68), giving place to Reactions 57-58, as well as to Reactions 69-72.

Charge separation:

$TiO_2 + h\nu \rightarrow h^+ + e^-$ (64)

Charge transfer of positive charge:

$h^+ + H_2O \rightarrow HO^\bullet + H^+$ (65)

Electron transfer and further reactions:

$e^- + O_2 \rightarrow O_2^{\bullet-}$ (66)

$O_2^{\bullet-} + H^+ \rightleftarrows HO_2^\bullet$ (67)

$O_3 + O_2^{\bullet-} \rightarrow O_3^{\bullet-} + O_2$ (68)

$O_3^{\bullet-} + H^+ \rightleftarrows HO_3^\bullet$ (69)

$HO_3^\bullet \rightarrow HO^\bullet + O_2$ (70)

Oxidation of the organic compound R:

$HO^\bullet + R\text{–}H \rightarrow R^\bullet + H_2O$ (71)

or

$HO^\bullet + R \rightarrow R^\bullet\text{–}OH$ (72)

There are some factors that can affect the photocatalytic ozonation process, some of them similar to those affecting the single processes, such as the ozone dosage, pH and nature of the photocatalyst. The TOC removal can increase with the ozone dosage, but low ozone dosages are economically more attractive [168]. The pH of the wastewater has a stronger influence on the ozonation reactions, and may impact the degradation pathways and the kinetics in the reaction process, which can also occur in the photocatalytic ozonation process [169, 170]. The synergistic effect between both processes can reduce the treatment costs and reaction time under optimum operating conditions (e.g., ozone concentration, the catalyst properties, the loading in the reactor and the usage of more cost-efficient and long-lasting UV sources, such as UV LEDs) [165]. Catalytic and photocatalytic ozonation has been studied for the removal of pharmaceuticals in effluents from UWWTPs, however the available data about the impact of water matrix are still unclear. Catalytic ozonation was more efficient than ozonation to degrade mesoxalic and oxalic acids, being almost unaffected by the presence of the inorganic anions or suspended solids. Catalytic ozonation of oxalic acid using copper oxide supported on mesoporous silica as catalyst in the presence of inorganic anions (HCO_3^-, PO_4^{3-}, Cl^- and SO_4^{2-}), was inhibited only in the presence of PO_4^{3-}, while ozonation alone was almost inhibited by the suspended solids and strongly depended on presence of these inorganic anions [97]. In turn, in other work dealing with the degradation of carboxyl acids (formic, acetic, oxalic and maleic acid), the copper-catalysed continuous ozonation was strongly influenced by the water matrix, ascribing the negative effect to the complexation with organic matter reducing the availability of metal as catalyst [102]. Although the reaction time needed to reach 99% conversion of 3 compounds (diclofenac, sulfamethoxazole and caffeine) was similar, the removal rates were slightly slower in wastewater effluents than in ultrapure water, by catalytic and photocatalytic ozonation in the presence of TiO_2 [28]. The degradation of diclofenac and amoxicillin by photocatalytic ozonation, using TiO_2 as photocatalyst, was similar in both ultrapure and wastewater, however, the oxamic acid formed as by-product was refractory to photocatalytic ozonation in the case of spiked wastewater effluents [101]. Another study on the degradation of diclofenac by TiO_2-photocatalytic ozonation showed that it was only slightly affected by the organic–inorganic matter of the urban wastewater [92].

3. Future challenges and conclusions

Wastewater quality is critical for the performance of AOTs, namely for those here reviewed: photolysis, UV/H_2O_2, Fenton-based processes, photocatalysis, and ozone-based processes. The efficiency of each process results from the complex interplay of inhibitory and promoting effects originated by the water matrix constituents. Wastewater components leading to inhibitory effects on the removal of MPs include NOM (light attenuation; scavenging effects; generation of by-products; adsorption to catalyst in photocatalytic processes); and inorganic anions (scavenging effects; formation of less active radicals; iron complexation in the case of Fenton; adsorption to the catalyst surface or decrease of its effective surface area, in the case of photocatalytic processes). Promoting effects can result from NOM originating ROS, which enhance indirect photolysis; from nitrate ions producing ROS in the case of photolysis; iron ions as additional source of catalyst in Fenton-based processes; and phenolic or other compounds containing -COOH and -OH groups, which can regenerate the catalyst. However, it is difficult to understand and discriminate the role of each single component. Table 2 summarizes the inhibitory and promoting mechanisms of different wastewater components, aiming to provide a guide on the most suitable treatment as function of the wastewater composition. The available information on the water matrix effects on the removal efficiency of MPs in UWWTPs effluents is still limited and more studies are needed to enlighten the mechanisms and the impact of the main components of the water.

Table 2. Summary of inhibitory (-) and promoting (+) effects of wastewater components, affecting the efficiency of the processes discussed in this review, namely photolysis, UV/H_2O_2, Fenton-based, photocatalysis, and O_3-based processes.

	Photolysis	**UV/H_2O_2**	**Fenton-based**	**Heterogeneous photocatalysis**	**O_3-based**
Organic matter Humic acids	+/-	+/-	-	+/-	-
Inorganic ions	+/-	+/-	+/-	-	-
NO_3^-	+	+		-	
NO_2^-				-	
PO_4^{3-}				-	-
Cl^-	+		+/-	-	-
SO_4^{2-}	+		-	-	-
HCO_3^-	-		-	-	-
CO_3^-			-	-	-
Ca^{2+}				-	
Iron ions			+		

Phenolic compounds (containing –COOH and –OH groups			+		
pH/ionic strength				-	
Number of papers (2005-2018)	19	18	20	32	24

On the other hand, it is well known that removal efficiencies of MPs depend on their chemical nature and on the AOT under study, but limited information is available on the effect of wastewater coexisting substances on the elimination of different types of substances by different AOTs. For instance, under UV, UV/H_2O_2, and photo-Fenton, gabapentin and metformin were found as the most recalcitrant compounds from a set of 8 MPs, which followed the same order of degradation [57]. Another report on the degradation of pharmaceuticals showed the same trend for UV-C radiation, heterogeneous photocatalysis, Fenton and photo-Fenton systems (amoxicillin > naproxen > metoprolol > phenacetin), but metoprolol was the most recalcitrant in the ozone-based processes [91], showing that the removal depends also on the MP nature. A recent study on UV/chlorine treatment showed that the degradation of MPs having electron-withdrawing groups (e.g., $-NO_2$, $-Cl$, $-F$) was largely attributed to $HO^{\bullet}$, while the degradation of those containing electron-donating groups (e.g., phenol, aniline, alkyl-/alkoxy aromatics, or olefins) was highly ascribed to other reactive species such as $Cl^{\bullet}$, $Cl_2^{\bullet-}$ and $ClO^{\bullet}$ [6]. In the same study, it was shown that the scavenging of NOM on $ClO^{\bullet}$ was much higher than that observed on $HO^{\bullet}$ and $Cl^{\bullet}$, suggesting that the removal of MPs that are readily degradable by $ClO^{\bullet}$ can be largely inhibited by the presence of NOM. On the contrary, alkaline components were ascribed to scavenge $HO^{\bullet}$ and $Cl^{\bullet}$ at higher extent and thus the MPs degraded primarily by these radicals are those which removal is most inhibited by alkalinity [6].

Moreover, the scarce data available on the effects of wastewater components on the removal of MPs with different chemical nature by hydroxyl radical-mediated AOTs show ambiguous results. For example, a better performance was reported for UV/H_2O_2 to degrade several organophosphate esters and some of them (chlorinated and one aliphatic) were recalcitrant to ozonation, but the presence of HA improved only the ozonation process, with an opposite trend observed in UV/H_2O_2 treatment [105]. On the contrary, the same order of degradation rates ($UV < UV/H_2O_2 < $ Fenton < solar irradiation < photo-Fenton) was observed regardless of the type of WW analysed, in a study comparing the effluents from activated sludge, moving bed bioreactor and coagulation-flocculation treatments [20].

Besides interfering with the process performance, the water matrix might also have an impact on the production and on the nature of the transformation by-products. The degradation of MPs is usually accompanied by the formation of numerous transformation by-products through unaccountable pathways and the matrix components may impact these pathways. For example, reactions in the presence of chlorides are prone to originate toxic chlorinated by-products. However, more studies addressing the effect of diverse water matrix components on the transformation products, are still needed to better understand their possible impacts. Other important parameters that are important to consider for the evaluation of the impact of the water matrix are the biodegradability and the toxicity of the effluents that are generated. A thorough investigation on the nature of the wastewater components is required not only to improve the performance of advanced water treatment systems, but also to minimize the formation of toxic reaction by-products, to enhance the biodegradability of the treated effluents and to reduce the ecotoxicity of the treated effluents. Complete mineralization of the organic matter is difficult and in general not needed if the by-products formed are biodegradable and non-toxic. Standard biodegradability and toxicity tests may be used to establish the levels of treatment needed to achieve a safe effluent.

Future research on treatment technologies should consider the complex interactions between matrix constituents and the oxidative species formed, aiming to maximize the performance of AOTs, since lower efficiencies and higher costs could be expected in real case scenario. With this review, we attempted to provide a comprehensive data analysis of the available studies using real water matrices, showing the lack of systematic understanding of the role of each wastewater component for all AOTs herein reviewed and encouraging the need of more studies applying real matrices. Although complex, the role of matrix constituents is fundamental for future employment of AOTs in industrial-scale water treatment processes to remove MPs and to protect the environment.

Acknowledgments

This work was financially supported by Projects: POCI-01-0145-FEDER-006984 – Associate Laboratory LSRE-LCM funded by European Regional Development Fund (ERDF) through COMPETE2020-Programa Operacional Competitividade e Internacionalização (POCI) – and by national funds through FCT - Fundação para a Ciência e a Tecnologia; Project POCI-01-0145-FEDER-030521 funded by ERDF funds through COMPETE2020 - POCI and by national funds (PIDDAC) through FCT/MCTES; and Project NORTE-01-0145-FEDER-031049 funded by ERDF funds through NORTE 2020 and by national funds (PIDDAC) through FCT/MCTES. NFFM acknowledge the research grant from FCT (PD/BD/114318/2016), with financing from the European Social Fund and the Human Potential Operational Programme. The authors would like to acknowledge the financial support provided by COST-European Cooperation in Science and Technology, to the COST Action ES1403: New and emerging challenges and opportunities in wastewater reuse (NEREUS). Disclaimer: The content of this article is the authors' responsibility and neither COST nor any person acting on its behalf is responsible for the use, which might be made of the information contained in it.

References

[1] A.R. Ribeiro, O.C. Nunes, M.F.R. Pereira, A.M.T. Silva, An overview on the advanced oxidation processes applied for the treatment of water pollutants defined in the recently launched Directive 2013/39/EU, Environ. Int., 75 (2015) 33-51.

[2] M.O. Barbosa, N.F.F. Moreira, A.R. Ribeiro, M.F.R. Pereira, A.M.T. Silva, Occurrence and removal of organic micropollutants: An overview of the watch list of EU Decision 2015/495, Water Res., 94 (2016) 257-279.

[3] J.C.G. Sousa, A.R. Ribeiro, M.O. Barbosa, M.F.R. Pereira, A.M.T. Silva, A review on environmental monitoring of water organic pollutants identified by EU guidelines, J. Hazard. Mater., 344 (2018) 146-162.

[4] M. Neamtu, F.H. Frimmel, Degradation of endocrine disrupting bisphenol A by 254 nm irradiation in different water matrices and effect on yeast cells, Water Res., 40 (2006) 3745-3750.

[5] L. Lian, B. Yao, S. Hou, J. Fang, S. Yan, W. Song, Kinetic Study of Hydroxyl and Sulfate Radical-Mediated Oxidation of Pharmaceuticals in Wastewater Effluents, Environ. Sci. Technol., 51 (2017) 2954-2962.

[6] K. Guo, Z. Wu, C. Shang, B. Yao, S. Hou, X. Yang, W. Song, J. Fang, Radical Chemistry and Structural Relationships of PPCP Degradation by UV/Chlorine Treatment in Simulated Drinking Water, Environ. Sci. Technol., 51 (2017) 10431-10439.

[7] R. Dewil, D. Mantzavinos, I. Poulios, M.A. Rodrigo, New perspectives for Advanced Oxidation Processes, J. Environ. Manage., 195 (2017) 93-99.

[8] I. García-Fernández, S. Miralles-Cuevas, I. Oller, S. Malato, P. Fernández-Ibáñez, M.I. Polo-López, Inactivation of *E. coli* and *E. faecalis* by solar photo-Fenton with EDDS complex at neutral pH in municipal wastewater effluents, J. Hazard. Mater., (2018).

[9] I. García-Fernández, I. Fernández-Calderero, M.I. Polo-López, P. Fernández-Ibáñez, Disinfection of urban effluents using solar TiO_2 photocatalysis: A study of significance of dissolved oxygen, temperature, type of microorganism and water matrix, Catal. Today, 240 (2015) 30-38.

[10] I. Michael-Kordatou, C. Michael, X. Duan, X. He, D.D. Dionysiou, M.A. Mills, D. Fatta-Kassinos, Dissolved effluent organic matter: Characteristics and potential implications in wastewater treatment and reuse applications, Water Res., 77 (2015) 213-248.

[11] M. Wang, Y. Chen, Generation and characterization of DOM in wastewater treatment processes, Chemosphere, 201 (2018) 96-109.

[12] I. Michael, E. Hapeshi, V. Osorio, S. Perez, M. Petrovic, A. Zapata, S. Malato, D. Barceló, D. Fatta-Kassinos, Solar photocatalytic treatment of trimethoprim in four environmental matrices at a pilot scale: Transformation products and ecotoxicity evaluation, Sci. Total Environ., 430 (2012) 167-173.

[13] I.A. Katsoyiannis, S. Canonica, U. von Gunten, Efficiency and energy requirements for the transformation of organic micropollutants by ozone, O_3/H_2O_2 and UV/H_2O_2, Water Res., 45 (2011) 3811-3822.

[14] A. Outsiou, Z. Frontistis, R.S. Ribeiro, M. Antonopoulou, I.K. Konstantinou, A.M.T. Silva, J.L. Faria, H.T. Gomes, D. Mantzavinos, Activation of sodium persulfate by magnetic carbon xerogels (CX/CoFe) for the oxidation of bisphenol A: Process variables effects, matrix effects and reaction pathways, Water Res., 124 (2017) 97-107.

[15] Y. Wang, F.A. Roddick, L. Fan, Direct and indirect photolysis of seven micropollutants in secondary effluent from a wastewater lagoon, Chemosphere, 185 (2017) 297-308.

[16] M. Tokumura, A. Sugawara, M. Raknuzzaman, M. Habibullah-Al-Mamun, S. Masunaga, Comprehensive study on effects of water matrices on removal of pharmaceuticals by three different kinds of advanced oxidation processes, Chemosphere, 159 (2016) 317-325.

[17] C. Postigo, C. Sirtori, I. Oller, S. Malato, M.I. Maldonado, M. López de Alda, D. Barceló, Solar transformation and photocatalytic treatment of cocaine in water: Kinetics, characterization of major intermediate products and toxicity evaluation, Appl. Catal. B, 104 (2011) 37-48.

[18] J. Radjenović, C. Sirtori, M. Petrović, D. Barceló, S. Malato, Solar photocatalytic degradation of persistent pharmaceuticals at pilot-scale: Kinetics and characterization of major intermediate products, Appl. Catal. B, 89 (2009) 255-264.

[19] O.S. Keen, K.G. Linden, Degradation of antibiotic activity during UV/H_2O_2 advanced oxidation and photolysis in wastewater effluent, Environ. Sci. Technol., 47 (2013) 13020-13030.

[20] S. Giannakis, F.A. Gamarra Vives, D. Grandjean, A. Magnet, L.F. De Alencastro, C. Pulgarin, Effect of advanced oxidation processes on the micropollutants and the effluent organic matter contained in municipal wastewater previously treated by three different secondary methods, Water Res., 84 (2015) 295-306.

[21] N. De la Cruz, L. Esquius, D. Grandjean, A. Magnet, A. Tungler, L.F. de Alencastro, C. Pulgarin, Degradation of emergent contaminants by UV, UV/H_2O_2 and neutral photo-Fenton at pilot scale in a domestic wastewater treatment plant, Water Res., 47 (2013) 5836-5845.

[22] O. Legrini, E. Oliveros, A.M. Braun, Photochemical processes for water treatment, Chem. Rev., 93 (1993) 671-698.

[23] F.J. Real, J.L. Acero, F.J. Benitez, G. Roldán, L.C. Fernández, Oxidation of hydrochlorothiazide by UV radiation, hydroxyl radicals and ozone: Kinetics and elimination from water systems, Chem. Eng. J., 160 (2010) 72-78.

[24] Y. Zhang, J. Zhang, Y. Xiao, V.W. Chang, T.T. Lim, Direct and indirect photodegradation pathways of cytostatic drugs under UV germicidal irradiation: Process kinetics and influences of water matrix species and oxidant dosing, J. Hazard. Mater., 324 (2017) 481-488.

[25] B. Cedat, C. de Brauer, H. Metivier, N. Dumont, R. Tutundjan, Are UV photolysis and UV/H_2O_2 process efficient to treat estrogens in waters? Chemical and biological assessment at pilot scale, Water Res., 100 (2016) 357-366.

[26] M. Schmitt, P.R. Erickson, K. McNeill, Triplet-State Dissolved Organic Matter Quantum Yields and Lifetimes from Direct Observation of Aromatic Amine Oxidation, Environ. Sci. Technol., 51 (2017) 13151-13160.

[27] W.A. Arnold, One electron oxidation potential as a predictor of rate constants of N-containing compounds with carbonate radical and triplet excited state organic matter, Environmental Science: Processes & Impacts, 16 (2014) 832-838.

[28] F.J. Beltrán, A. Aguinaco, J.F. García-Araya, Application of Ozone Involving Advanced Oxidation Processes to Remove Some Pharmaceutical Compounds from Urban Wastewaters, Ozone Sci. Eng., 34 (2012) 3-15.

[29] G. Castro, I. Rodriguez, M. Ramil, R. Cela, Evaluation of nitrate effects in the aqueous photodegradability of selected phenolic pollutants, Chemosphere, 185 (2017) 127-136.

[30] P. Sun, S.G. Pavlostathis, C.H. Huang, Photodegradation of veterinary ionophore antibiotics under UV and solar irradiation, Environ. Sci. Technol., 48 (2014) 13188-13196.

[31] R. Andreozzi, M. Raffaele, P. Nicklas, Pharmaceuticals in STP effluents and their solar photodegradation in aquatic environment, Chemosphere, 50 (2003) 1319-1330.

[32] A. Achilleos, E. Hapeshi, N.P. Xekoukoulotakis, D. Mantzavinos, D. Fatta-Kassinos, Factors affecting diclofenac decomposition in water by UV-A/TiO_2 photocatalysis, Chem. Eng. J., 161 (2010) 53-59.

[33] P.J. Chen, E.J. Rosenfeldt, S.W. Kullman, D.E. Hinton, K.G. Linden, Biological assessments of a mixture of endocrine disruptors at environmentally relevant concentrations in water following UV/H_2O_2 oxidation, Sci. Total Environ., 376 (2007) 18-26.

[34] H. Yao, P. Sun, D. Minakata, J.C. Crittenden, C.H. Huang, Kinetics and modeling of degradation of ionophore antibiotics by UV and UV/H_2O_2, Environ. Sci. Technol., 47 (2013) 4581-4589.

[35] F. Yuan, C. Hu, X. Hu, D. Wei, Y. Chen, J. Qu, Photodegradation and toxicity changes of antibiotics in UV and UV/H_2O_2 process, J. Hazard. Mater., 185 (2011) 1256-1263.

[36] B. Verma, J.V. Headley, R.D. Robarts, Behaviour and fate of tetracycline in river and wetland waters on the Canadian Northern Great Plains, J. Environ. Sci. Health., Part A, 42 (2007) 109-117.

[37] I.R. Bautitz, R.F.P. Nogueira, Degradation of tetracycline by photo-Fenton process—Solar irradiation and matrix effects, J. Photochem. Photobiol. A: Chem., 187 (2007) 33-39.

[38] C. Baeza, D.R. Knappe, Transformation kinetics of biochemically active compounds in low-pressure UV photolysis and UV/H_2O_2 advanced oxidation processes, Water Res., 45 (2011) 4531-4543.

[39] D. Russo, D. Spasiano, M. Vaccaro, K.H. Cochran, S.D. Richardson, R. Andreozzi, G. Li Puma, N.M. Reis, R. Marotta, Investigation on the removal of the major cocaine metabolite (benzoylecgonine) in water matrices by UV_{254}/H_2O_2 process by using a flow microcapillary film array photoreactor as an efficient experimental tool, Water Res., 89 (2016) 375-383.

[40] D. Spasiano, D. Russo, M. Vaccaro, A. Siciliano, R. Marotta, M. Guida, N.M. Reis, G. Li Puma, R. Andreozzi, Removal of benzoylecgonine from water matrices through UV_{254}/H_2O_2 process: Reaction kinetic modeling, ecotoxicity and genotoxicity assessment, J. Hazard. Mater., 318 (2016) 515-525.

[41] M.V. Mouamfon, W. Li, S. Lu, Z. Qiu, N. Chen, K. Lin, Photodegradation of sulphamethoxazole under UV-light irradiation at 254 nm, Environ. Technol., 31 (2010) 489-494.

[42] F.J. Benitez, J.L. Acero, F.J. Real, G. Roldan, E. Rodriguez, Modeling the photodegradation of emerging contaminants in waters by UV radiation and UV/H_2O_2 system, J. Environ. Sci. Health., Part A, 48 (2013) 120-128.

[43] M. Celeiro, R. Facorro, T. Dagnac, V.J.P. Vilar, M. Llompart, Photodegradation of multiclass fungicides in the aquatic environment and determination by liquid chromatography-tandem mass spectrometry, Environ. Sci. Pollut. R., 24 (2017) 19181-19193.

[44] H. Nadais, X. Li, N. Alves, C. Couras, H.R. Andersen, I. Angelidaki, Y. Zhang, Bio-electro-Fenton process for the degradation of Non-Steroidal Anti-Inflammatory Drugs in wastewater, Chem. Eng. J., 338 (2018) 401-410.

[45] S. Wang, J. Wang, Trimethoprim degradation by Fenton and Fe(II)-activated persulfate processes, Chemosphere, 191 (2018) 97-105.

[46] A.M. Díez, A.S. Ribeiro, M.A. Sanromán, M. Pazos, Optimization of photo-Fenton process for the treatment of prednisolone, Environ. Sci. Pollut. R., (2018) *in press*.

[47] N. Klamerth, S. Malato, A. Aguera, A. Fernandez-Alba, Photo-Fenton and modified photo-Fenton at neutral pH for the treatment of emerging contaminants in wastewater treatment plant effluents: a comparison, Water Res., 47 (2013) 833-840.

[48] N. Klamerth, S. Malato, A. Aguera, A. Fernandez-Alba, G. Mailhot, Treatment of municipal wastewater treatment plant effluents with modified photo-Fenton as a tertiary treatment for the degradation of micro pollutants and disinfection, Environ. Sci. Technol., 46 (2012) 2885-2892.

[49] N. Klamerth, S. Malato, M.I. Maldonado, A. Agüera, A. Fernández-Alba, Modified photo-Fenton for degradation of emerging contaminants in municipal wastewater effluents, Catal. Today, 161 (2011) 241-246.

[50] I. Michael, E. Hapeshi, J. Acena, S. Perez, M. Petrovic, A. Zapata, D. Barcelo, S. Malato, D. Fatta-Kassinos, Light-induced catalytic transformation of ofloxacin by solar Fenton in various water matrices at a pilot plant: mineralization and characterization of major intermediate products, Sci. Total Environ., 461-462 (2013) 39-48.

[51] M. Pagano, A. Lopez, A. Volpe, G. Mascolo, R. Ciannarella, Oxidation of nonionic surfactants by Fenton and H_2O_2/UV processes, Environ. Technol., 29 (2008) 423-433.

[52] P. Karaolia, I. Michael, I. Garcia-Fernandez, A. Aguera, S. Malato, P. Fernandez-Ibanez, D. Fatta-Kassinos, Reduction of clarithromycin and sulfamethoxazole-resistant *Enterococcus* by pilot-scale solar-driven Fenton oxidation, Sci. Total Environ., 468-469 (2014) 19-27.

[53] N. Klamerth, L. Rizzo, S. Malato, M.I. Maldonado, A. Aguera, A.R. Fernandez-Alba, Degradation of fifteen emerging contaminants at mg L^{-1} initial concentrations by mild solar photo-Fenton in MWTP effluents, Water Res., 44 (2010) 545-554.

[54] V.N. Lima, C.S.D. Rodrigues, L.M. Madeira, Application of the Fenton's process in a bubble column reactor for hydroquinone degradation, Environ. Sci. Pollut. R., (2017).

[55] E.B. Estrada-Arriaga, J.E. Cortes-Munoz, A. Gonzalez-Herrera, C.G. Calderon-Molgora, M. de Lourdes Rivera-Huerta, E. Ramirez-Camperos, L. Montellano-Palacios, S.L. Gelover-Santiago, S. Perez-Castrejon, L. Cardoso-Vigueros, A. Martin-Dominguez, L. Garcia-Sanchez, Assessment of full-scale biological nutrient removal systems upgraded with physico-chemical

processes for the removal of emerging pollutants present in wastewaters from Mexico, Sci. Total Environ., 571 (2016) 1172-1182.

[56] G.T. Chi, J. Churchley, K.D. Huddersman, Pilot-Scale Removal of Trace Steroid Hormones and Pharmaceuticals and Personal Care Products from Municipal Wastewater Using a Heterogeneous Fenton's Catalytic Process, Int. J. Chem. Eng., 2013 (2013) 1-10.

[57] M. Neamţu, D. Grandjean, A. Sienkiewicz, S. Le Faucheur, V. Slaveykova, J.J.V. Colmenares, C. Pulgarín, L.F. de Alencastro, Degradation of eight relevant micropollutants in different water matrices by neutral photo-Fenton process under UV_{254} and simulated solar light irradiation – A comparative study, Appl. Catal. B, 158-159 (2014) 30-37.

[58] N. Rioja, S. Zorita, F.J. Peñas, Effect of water matrix on photocatalytic degradation and general kinetic modeling, Appl. Catal. B, 180 (2016) 330-335.

[59] N. Miranda-García, S. Suárez, B. Sánchez, J.M. Coronado, S. Malato, M.I. Maldonado, Photocatalytic degradation of emerging contaminants in municipal wastewater treatment plant effluents using immobilized TiO_2 in a solar pilot plant, Appl. Catal. B, 103 (2011) 294-301.

[60] M. Bosio, S. Satyro, J.P. Bassin, E. Saggioro, M. Dezotti, Removal of pharmaceutically active compounds from synthetic and real aqueous mixtures and simultaneous disinfection by supported TiO_2/UV-A, H_2O_2/UV-A, and TiO_2/H_2O_2/UV-A processes, Environ. Sci. Pollut. R., (2018).

[61] S. Kotzamanidi, Z. Frontistis, V. Binas, G. Kiriakidis, D. Mantzavinos, Solar photocatalytic degradation of propyl paraben in Al-doped TiO_2 suspensions, Catal. Today, 313 (2018) 148-154.

[62] M. Sarro, N.P. Gule, E. Laurenti, R. Gamberini, M.C. Paganini, P.E. Mallon, P. Calza, ZnO-based materials and enzymes hybrid systems as highly efficient catalysts for recalcitrant pollutants abatement, Chem. Eng. J., 334 (2018) 2530-2538.

[63] K. Sornalingam, A. McDonagh, J.L. Zhou, M.A.H. Johir, M.B. Ahmed, Photocatalysis of estrone in water and wastewater: Comparison between Au-TiO_2 nanocomposite and TiO_2, and degradation by-products, Sci. Total Environ., 610-611 (2018) 521-530.

[64] H. Dimitroula, V.M. Daskalaki, Z. Frontistis, D.I. Kondarides, P. Panagiotopoulou, N.P. Xekoukoulotakis, D. Mantzavinos, Solar photocatalysis for the abatement of emerging micro-contaminants in wastewater: Synthesis, characterization and testing of various TiO_2 samples, Appl. Catal. B, 117-118 (2012) 283-291.

[65] E.M. Saggioro, A.S. Oliveira, T. Pavesi, M.J. Tototzintle, M.I. Maldonado, F.V. Correia, J.C. Moreira, Solar CPC pilot plant photocatalytic degradation of bisphenol A in waters and wastewaters using suspended and supported-TiO_2. Influence of photogenerated species, Environ. Sci. Pollut. R., 21 (2014) 12112-12121.

[66] L. Rizzo, S. Meric, M. Guida, D. Kassinos, V. Belgiorno, Heterogenous photocatalytic degradation kinetics and detoxification of an urban wastewater treatment plant effluent contaminated with pharmaceuticals, Water Res., 43 (2009) 4070-4078.

[67] Z. Frontistis, V.M. Daskalaki, E. Hapeshi, C. Drosou, D. Fatta-Kassinos, N.P. Xekoukoulotakis, D. Mantzavinos, Photocatalytic (UV-A/TiO_2) degradation of 17α-ethynylestradiol in environmental matrices: Experimental studies and artificial neural network modeling, J. Photochem. Photobiol. A: Chem., 240 (2012) 33-41.

[68] Z. Frontistis, C. Drosou, K. Tyrovola, D. Mantzavinos, D. Fatta-Kassinos, D. Venieri, N.P. Xekoukoulotakis, Experimental and Modeling Studies of the Degradation of Estrogen Hormones in Aqueous TiO_2 Suspensions under Simulated Solar Radiation, Ind. Eng. Chem. Res., 51 (2012) 16552-16563.

[69] Z. Frontistis, D. Fatta-Kassinos, D. Mantzavinos, N.P. Xekoukoulotakis, Photocatalytic degradation of 17α-ethynylestradiol in environmental samples by ZnO under simulated solar radiation, J. Chem. Technol. Biotechnol., 87 (2012) 1051-1058.

[70] N. Jallouli, L.M. Pastrana-Martínez, A.R. Ribeiro, N.F.F. Moreira, J.L. Faria, O. Hentati, A.M.T. Silva, M. Ksibi, Heterogeneous photocatalytic degradation of ibuprofen in ultrapure water, municipal and pharmaceutical industry wastewaters using a TiO_2/UV-LED system, Chem. Eng. J., 334 (2018) 976-984.

[71] G.H. Safari, M. Hoseini, M. Seyedsalehi, H. Kamani, J. Jaafari, A.H. Mahvi, Photocatalytic degradation of tetracycline using nanosized titanium dioxide in aqueous solution, Int. J. Environ. Sci. Technol. (Tehran), 12 (2014) 603-616.

[72] G. Laera, B. Jin, H. Zhu, A. Lopez, Photocatalytic activity of TiO_2 nanofibers in simulated and real municipal effluents, Catal. Today, 161 (2011) 147-152.

[73] M. Jiménez, M. Ignacio Maldonado, E.M. Rodríguez, A. Hernández-Ramírez, E. Saggioro, I. Carra, J.A. Sánchez Pérez, Supported TiO_2 solar photocatalysis at semi-pilot scale: degradation of pesticides found in citrus processing industry wastewater, reactivity and influence of photogenerated species, J. Chem. Technol. Biotechnol., 90 (2015) 149-157.

[74] R.P. Cavalcante, R.F. Dantas, H. Wender, B. Bayarri, O. González, J. Giménez, S. Esplugas, A. Machulek, Photocatalytic treatment of metoprolol with B-doped TiO_2: Effect of water matrix, toxicological evaluation and identification of intermediates, Appl. Catal. B, 176-177 (2015) 173-182.

[75] M.N. Chong, B. Jin, G. Laera, C.P. Saint, Evaluating the photodegradation of Carbamazepine in a sequential batch photoreactor system: Impacts of effluent organic matter and inorganic ions, Chem. Eng. J., 174 (2011) 595-602.

[76] E. Hapeshi, A. Achilleos, M.I. Vasquez, C. Michael, N.P. Xekoukoulotakis, D. Mantzavinos, D. Kassinos, Drugs degrading photocatalytically: Kinetics and mechanisms of ofloxacin and atenolol removal on titania suspensions, Water Res., 44 (2010) 1737-1746.

[77] E. Marquez Brazon, C. Piccirillo, I.S. Moreira, P.M. Castro, Photodegradation of pharmaceutical persistent pollutants using hydroxyapatite-based materials, J. Environ. Manage., 182 (2016) 486-495.

[78] N.P. Xekoukoulotakis, C. Drosou, C. Brebou, E. Chatzisymeon, E. Hapeshi, D. Fatta-Kassinos, D. Mantzavinos, Kinetics of UV-A/TiO_2 photocatalytic degradation and mineralization of the antibiotic sulfamethoxazole in aqueous matrices, Catal. Today, 161 (2011) 163-168.

[79] J. Ziemianska, E. Adamek, A. Sobczak, I. Lipska, A. Makowski, W. BARAN, The study of photocatalytic degradation of sulfonamides applied to municipal wastewater, Physicochem. Probl. Mi., 45 (2010) 127-140.

[80] H. Gulyas, M.K. Ogun, W. Meyer, M. Reich, R. Otterpohl, Inadequacy of carbamazepine-spiked model wastewaters for testing photocatalysis efficiency, Sci. Total Environ., 542 (2016) 612-619.

[81] Y. He, N.B. Sutton, H.H.H. Rijnaarts, A.A.M. Langenhoff, Degradation of pharmaceuticals in wastewater using immobilized TiO_2 photocatalysis under simulated solar irradiation, Appl. Catal. B, 182 (2016) 132-141.

[82] S. Teixeira, R. Gurke, H. Eckert, K. Kühn, J. Fauler, G. Cuniberti, Photocatalytic degradation of pharmaceuticals present in conventional treated wastewater by nanoparticle suspensions, J. Environ. Chem. Eng., 4 (2016) 287-292.

[83] D. Darowna, S. Grondzewska, A.W. Morawski, S. Mozia, Removal of non-steroidal anti-inflammatory drugs from primary and secondary effluents in a photocatalytic membrane reactor, J. Chem. Technol. Biotechnol., 89 (2014) 1265-1273.

[84] R. Matta, S. Tlili, S. Chiron, S. Barbati, Removal of carbamazepine from urban wastewater by sulfate radical oxidation, Environ. Chem. Lett., 9 (2010) 347-353.

[85] G. Plantard, A. Azais, J. Mendret, S. Brosillon, V. Goetz, Coupling of photocatalytic and separation processes as a contribution to mineralization of wastewater, Chemical Engineering and Processing - Process Intensification, 134 (2018) 115-123.

[86] E. Grilla, V. Matthaiou, Z. Frontistis, I. Oller, I. Polo, S. Malato, D. Mantzavinos, Degradation of antibiotic trimethoprim by the combined action of sunlight, TiO_2 and persulfate: A pilot plant study, Catal. Today, (2018).

[87] F.J. Benitez, J.L. Acero, F.J. Real, G. Roldan, Ozonation of pharmaceutical compounds: Rate constants and elimination in various water matrices, Chemosphere, 77 (2009) 53-59.

[88] I. Carra, J.A. Sánchez Pérez, S. Malato, O. Autin, B. Jefferson, P. Jarvis, Performance of different advanced oxidation processes for tertiary wastewater treatment to remove the pesticide acetamiprid, J. Chem. Technol. Biotechnol., 91 (2014) 72-81.

[89] R. Qu, M. Feng, X. Wang, Q. Huang, J. Lu, L. Wang, Z. Wang, Rapid Removal of Tetrabromobisphenol A by Ozonation in Water: Oxidation Products, Reaction Pathways and Toxicity Assessment, PLoS One, 10 (2015) e0139580.

[90] M. Feng, L. Yan, X. Zhang, P. Sun, S. Yang, L. Wang, Z. Wang, Fast removal of the antibiotic flumequine from aqueous solution by ozonation: Influencing factors, reaction pathways, and toxicity evaluation, Sci. Total Environ., 541 (2016) 167-175.

[91] F.J. Benitez, J.L. Acero, F.J. Real, G. Roldan, F. Casas, Comparison of different chemical oxidation treatments for the removal of selected pharmaceuticals in water matrices, Chem. Eng. J., 168 (2011) 1149-1156.

[92] A. Aguinaco, F.J. Beltrán, J.F. García-Araya, A. Oropesa, Photocatalytic ozonation to remove the pharmaceutical diclofenac from water: Influence of variables, Chem. Eng. J., 189-190 (2012) 275-282.

[93] M.G. Antoniou, G. Hey, S. Rodriguez Vega, A. Spiliotopoulou, J. Fick, M. Tysklind, J. la Cour Jansen, H.R. Andersen, Required ozone doses for removing pharmaceuticals from wastewater effluents, Sci. Total Environ., 456-457 (2013) 42-49.

[94] J.B. Carbajo, A.L. Petre, R. Rosal, S. Herrera, P. Leton, E. Garcia-Calvo, A.R. Fernandez-Alba, J.A. Perdigon-Melon, Continuous ozonation treatment of ofloxacin: transformation products, water matrix effect and aquatic toxicity, J. Hazard. Mater., 292 (2015) 34-43.

[95] J.B. Carbajo, A.L. Petre, R. Rosal, A. Berná, P. Letón, E. García-Calvo, J.A. Perdigón-Melón, Ozonation as pre-treatment of activated sludge process of a wastewater containing benzalkonium chloride and NiO nanoparticles, Chem. Eng. J., 283 (2016) 740-749.

[96] P. Westlund, S. Isazadeh, A. Therrien, V. Yargeau, Endocrine Activities of Pesticides During Ozonation of Waters, Bull. Environ. Contam. Toxicol., 100 (2018) 112-119.

[97] A.L. Petre, J.B. Carbajo, R. Rosal, E. Garcia-Calvo, J.A. Perdigón-Melón, CuO/SBA-15 catalyst for the catalytic ozonation of mesoxalic and oxalic acids. Water matrix effects, Chem. Eng. J., 225 (2013) 164-173.

[98] D.S. Gomes, L.M. Gando-Ferreira, R.M. Quinta-Ferreira, R.C. Martins, Removal of sulfamethoxazole and diclofenac from water: strategies involving O_3 and H_2O_2, Environ. Technol., (2017) 1-12.

[99] R. Rosal, A. Rodriguez, J.A. Perdigon-Melon, M. Mezcua, M.D. Hernando, P. Leton, E. Garcia-Calvo, A. Aguera, A.R. Fernandez-Alba, Removal of pharmaceuticals and kinetics of mineralization by O_3/H_2O_2 in a biotreated municipal wastewater, Water Res., 42 (2008) 3719-3728.

[100] P. Pocostales, P. Álvarez, F.J. Beltrán, Catalytic ozonation promoted by alumina-based catalysts for the removal of some pharmaceutical compounds from water, Chem. Eng. J., 168 (2011) 1289-1295.

[101] N.F.F. Moreira, C.A. Orge, A.R. Ribeiro, J.L. Faria, O.C. Nunes, M.F.R. Pereira, A.M.T. Silva, Fast mineralization and detoxification of amoxicillin and diclofenac by photocatalytic ozonation and application to an urban wastewater, Water Res., 87 (2015) 87-96.

[102] A.L. Petre, J.B. Carbajo, R. Rosal, E. García-Calvo, P. Letón, J.A. Perdigón-Melón, Influence of water matrix on copper-catalysed continuous ozonation and related ecotoxicity, Appl. Catal. B, 163 (2015) 233-240.

[103] Á. Encinas, F.J. Rivas, F.J. Beltrán, A. Oropesa, Combination of Black-Light Photo-catalysis and Ozonation for Emerging Contaminants Degradation in Secondary Effluents, Chem. Eng. Technol., 36 (2013) 492-499.

[104] F.J. Real, F.J. Benitez, J.L. Acero, G. Roldan, Combined chemical oxidation and membrane filtration techniques applied to the removal of some selected pharmaceuticals from water systems, J. Environ. Sci. Health., Part A, 47 (2012) 522-533.

[105] X. Yuan, S. Lacorte, J. Cristale, R.F. Dantas, C. Sans, S. Esplugas, Z. Qiang, Removal of organophosphate esters from municipal secondary effluent by ozone and UV/H_2O_2 treatments, Sep. Purif. Technol., 156 (2015) 1028-1034.

[106] S. Sarkar, S. Ali, L. Rehmann, G. Nakhla, M.B. Ray, Degradation of estrone in water and wastewater by various advanced oxidation processes, J. Hazard. Mater., 278 (2014) 16-24.

[107] N.H.S. Javadi, M. Baghdadi, N. Mehrdadi, M. Mortazavi, Removal of benzotriazole from secondary municipal wastewater effluent by catalytic ozonation in the presence of magnetic alumina nanocomposite, J. Environ. Chem. Eng., 6 (2018) 6421-6430.

[108] A. Mirzaei, Z. Chen, F. Haghighat, L. Yerushalmi, Removal of pharmaceuticals from water by homo/heterogonous Fenton-type processes – A review, Chemosphere, 174 (2017) 665-688.

[109] A.D. Bokare, W. Choi, Review of iron-free Fenton-like systems for activating H_2O_2 in advanced oxidation processes, J. Hazard. Mater., 275 (2014) 121-135.

[110] F. Duarte, F.J. Maldonado-Hódar, L.M. Madeira, Influence of the characteristics of carbon materials on their behaviour as heterogeneous Fenton catalysts for the elimination of the azo dye Orange II from aqueous solutions, Appl. Catal. B, 103 (2011) 109-115.

[111] P.V. Nidheesh, R. Gandhimathi, Trends in electro-Fenton process for water and wastewater treatment: An overview, Desalination, 299 (2012) 1-15.

[112] R. Andreozzi, V. Caprio, A. Insola, R. Marotta, Advanced oxidation processes (AOP) for water purification and recovery, Catal. Today, 53 (1999) 51-59.

[113] T. Mackul'ak, J. Prousek, L.u. Švorc, Degradation of atrazine by Fenton and modified Fenton reactions, Monatsh. Chem., 142 (2011) 561-567.

[114] D. Hermosilla, M. Cortijo, C.P. Huang, Optimizing the treatment of landfill leachate by conventional Fenton and photo-Fenton processes, Sci. Total Environ., 407 (2009) 3473-3481.

[115] N. De la Cruz, J. Gimenez, S. Esplugas, D. Grandjean, L.F. de Alencastro, C. Pulgarin, Degradation of 32 emergent contaminants by UV and neutral photo-fenton in domestic wastewater effluent previously treated by activated sludge, Water Res., 46 (2012) 1947-1957.

[116] P.R. Gogate, A.B. Pandit, A review of imperative technologies for wastewater treatment II: hybrid methods, Adv. Environ. Res., 8 (2004) 553-597.

[117] S. Papoutsakis, S. Miralles-Cuevas, I. Oller, J.L. Garcia Sanchez, C. Pulgarin, S. Malato, Microcontaminant degradation in municipal wastewater treatment plant secondary effluent by EDDS assisted photo-Fenton at near-neutral pH: An experimental design approach, Catal. Today, 252 (2015) 61-69.

[118] M. Umar, H.A. Aziz, M.S. Yusoff, Trends in the use of Fenton, electro-Fenton and photo-Fenton for the treatment of landfill leachate, Waste Manage., 30 (2010) 2113-2121.

[119] I. Michael, E. Hapeshi, C. Michael, A.R. Varela, S. Kyriakou, C.M. Manaia, D. Fatta-Kassinos, Solar photo-Fenton process on the abatement of antibiotics at a pilot scale: Degradation kinetics, ecotoxicity and phytotoxicity assessment and removal of antibiotic resistant enterococci, Water Res., 46 (2012) 5621-5634.

[120] N. Klamerth, N. Miranda, S. Malato, A. Agüera, A.R. Fernández-Alba, M.I. Maldonado, J.M. Coronado, Degradation of emerging contaminants at low concentrations in MWTPs effluents with mild solar photo-Fenton and TiO_2, Catal. Today, 144 (2009) 124-130.

[121] L.O. Conte, A.V. Schenone, B.N. Giménez, O.M. Alfano, Photo-Fenton degradation of a herbicide (2,4-D) in groundwater for conditions of natural pH and presence of inorganic anions, J. Hazard. Mater., (2018).

[122] L. Clarizia, D. Russo, I. Di Somma, R. Marotta, R. Andreozzi, Homogeneous photo-Fenton processes at near neutral pH: A review, Appl. Catal. B, 209 (2017) 358-371.

[123] T. Papadam, N.P. Xekoukoulotakis, I. Poulios, D. Mantzavinos, Photocatalytic transformation of acid orange 20 and Cr(VI) in aqueous TiO_2 suspensions, J. Photochem. Photobiol. A: Chem., 186 (2007) 308-315.

[124] G. Li Puma, A. Bono, D. Krishnaiah, J.G. Collin, Preparation of titanium dioxide photocatalyst loaded onto activated carbon support using chemical vapor deposition: A review paper, J. Hazard. Mater., 157 (2008) 209-219.

[125] I. Grčić, G. Li Puma, Photocatalytic Degradation of Water Contaminants in Multiple Photoreactors and Evaluation of Reaction Kinetic Constants Independent of Photon Absorption, Irradiance, Reactor Geometry, and Hydrodynamics, Environ. Sci. Technol., 47 (2013) 13702-13711.

[126] J. Fenoll, P. Sabater, G. Navarro, G. Pérez-Lucas, S. Navarro, Photocatalytic transformation of sixteen substituted phenylurea herbicides in aqueous semiconductor suspensions: Intermediates and degradation pathways, J. Hazard. Mater., 244-245 (2013) 370-379.

[127] L. Prieto-Rodríguez, S. Miralles-Cuevas, I. Oller, A. Aguera, G. Li Puma, S. Malato, Treatment of emerging contaminants in wastewater treatment plants (WWTP) effluents by solar photocatalysis using low TiO_2 concentrations, J. Hazard. Mater., 211-212 (2012) 131-137.

[128] M.J. Lima, A.M.T. Silva, C.G. Silva, J.L. Faria, Graphitic carbon nitride modified by thermal, chemical and mechanical processes as metal-free photocatalyst for the selective synthesis of benzaldehyde from benzyl alcohol, J. Catal., 353 (2017) 44-53.

[129] S. Sakthivel, M.V. Shankar, M. Palanichamy, B. Arabindoo, D.W. Bahnemann, V. Murugesan, Enhancement of photocatalytic activity by metal deposition: characterisation and photonic efficiency of Pt, Au and Pd deposited on TiO_2 catalyst, Water Res., 38 (2004) 3001-3008.

[130] S.B. Rawal, S. Bera, D. Lee, D.-J. Jang, W.I. Lee, Design of visible-light photocatalysts by coupling of narrow bandgap semiconductors and TiO_2: effect of their relative energy band positions on the photocatalytic efficiency, Catalysis Science & Technology, 3 (2013) 1822-1830.

[131] A.M.T. Silva, C.G. Silva, G. Dražić, J.L. Faria, Ce-doped TiO2 for photocatalytic degradation of chlorophenol, Catal. Today, 144 (2009) 13-18.

[132] M. Pedrosa, L.M. Pastrana-Martínez, M.F.R. Pereira, J.L. Faria, J.L. Figueiredo, A.M.T. Silva, N/S-doped graphene derivatives and TiO_2 for catalytic ozonation and photocatalysis of water pollutants, Chem. Eng. J., 348 (2018) 888-897.

[133] N.F.F. Moreira, C. Narciso-da-Rocha, M.I. Polo-López, L.M. Pastrana-Martínez, J.L. Faria, C.M. Manaia, P. Fernández-Ibáñez, O.C. Nunes, A.M.T. Silva, Solar treatment (H_2O_2, TiO_2-P25 and GO-TiO_2 photocatalysis, photo-Fenton) of organic micropollutants, human pathogen indicators, antibiotic resistant bacteria and related genes in urban wastewater, Water Res., 135 (2018) 195-206.

[134] S. Morales-Torres, A.M.T. Silva, F.J. Maldonado-Hódar, B.F. Machado, A.F. Pérez-Cadenas, J.L. Faria, J.L. Figueiredo, F. Carrasco-Marín, Pt-catalysts supported on activated carbons for catalytic wet air oxidation of aniline: Activity and stability, Appl. Catal. B, 105 (2011) 86-94.

[135] S. Morales-Torres, A.M.T. Silva, A.F. Pérez-Cadenas, J.L. Faria, F.J. Maldonado-Hódar, J.L. Figueiredo, F. Carrasco-Marín, Wet air oxidation of trinitrophenol with activated carbon catalysts: Effect of textural properties on the mechanism of degradation, Appl. Catal. B, 100 (2010) 310-317.

[136] M.E. Metheniti, Z. Frontistis, R.S. Ribeiro, A.M.T. Silva, J.L. Faria, H.T. Gomes, D. Mantzavinos, Degradation of propyl paraben by activated persulfate using iron-containing magnetic carbon xerogels: investigation of water matrix and process synergy effects, Environ. Sci. Pollut. R., (2017) 1-10.

[137] D.F.M. Santos, O.S.G.P. Soares, A.M.T. Silva, J.L. Figueiredo, M.F.R. Pereira, Catalytic wet oxidation of organic compounds over N-doped carbon nanotubes in batch and continuous operation, Appl. Catal. B, 199 (2016) 361-371.

[138] R.S. Ribeiro, A.M.T. Silva, J.L. Figueiredo, J.L. Faria, H.T. Gomes, Catalytic wet peroxide oxidation: A route towards the application of hybrid magnetic carbon nanocomposites for the degradation of organic pollutants. A review, Appl. Catal. B, 187 (2016) 428-460.

[139] R.S. Ribeiro, R.O. Rodrigues, A.M.T. Silva, P.B. Tavares, A.M.C. Carvalho, J.L. Figueiredo, J.L. Faria, H.T. Gomes, Hybrid magnetic graphitic nanocomposites towards catalytic wet peroxide oxidation of the liquid effluent from a mechanical biological treatment plant for municipal solid waste, Appl. Catal. B, 219 (2017) 645-657.

[140] L. Svoboda, P. Praus, M.J. Lima, M.J. Sampaio, D. Matýsek, M. Ritz, R. Dvorský, J.L. Faria, C.G. Silva, Graphitic carbon nitride nanosheets as highly efficient photocatalysts for phenol degradation under high-power visible LED irradiation, Mater. Res. Bull., 100 (2018) 322-332.

[141] A.L. Linsebigler, G. Lu, J.T. Yates, Photocatalysis on TiO_2 Surfaces: Principles, Mechanisms, and Selected Results, Chem. Rev., 95 (1995) 735-758.

[142] S. Morales-Torres, L.M. Pastrana-Martínez, J.L. Figueiredo, J.L. Faria, A.M.T. Silva, Design of graphene-based TiO_2 photocatalysts—a review, Environ. Sci. Pollut. R., 19 (2012) 3676-3687.

[143] C.S. Uyguner-Demirel, N.C. Birben, M. Bekbolet, Elucidation of background organic matter matrix effect on photocatalytic treatment of contaminants using TiO_2: A review, Catal. Today, 284 (2017) 202-214.

[144] T.E. Doll, F.H. Frimmel, Photocatalytic degradation of carbamazepine, clofibric acid and iomeprol with P25 and Hombikat UV100 in the presence of natural organic matter (NOM) and other organic water constituents, Water Res., 39 (2005) 403-411.

[145] G. Márquez, E.M. Rodríguez, M.I. Maldonado, P.M. Álvarez, Integration of ozone and solar TiO_2-photocatalytic oxidation for the degradation of selected pharmaceutical compounds in water and wastewater, Sep. Purif. Technol., 136 (2014) 18-26.

[146] D. Friedmann, C. Mendive, D. Bahnemann, TiO_2 for water treatment: Parameters affecting the kinetics and mechanisms of photocatalysis, Appl. Catal. B, 99 (2010) 398-406.

[147] G. Li, L. Lv, H. Fan, J. Ma, Y. Li, Y. Wan, X.S. Zhao, Effect of the agglomeration of TiO_2 nanoparticles on their photocatalytic performance in the aqueous phase, J. Colloid Interface Sci., 348 (2010) 342-347.

[148] R.A. French, A.R. Jacobson, B. Kim, S.L. Isley, R.L. Penn, P.C. Baveye, Influence of Ionic Strength, pH, and Cation Valence on Aggregation Kinetics of Titanium Dioxide Nanoparticles, Environ. Sci. Technol., 43 (2009) 1354-1359.

[149] C. Wang, L. Zhu, M. Wei, P. Chen, G. Shan, Photolytic reaction mechanism and impacts of coexisting substances on photodegradation of bisphenol A by Bi_2WO_6 in water, Water Res., 46 (2012) 845-853.

[150] M. Bourgin, B. Beck, M. Boehler, E. Borowska, J. Fleiner, E. Salhi, R. Teichler, U. von Gunten, H. Siegrist, C.S. McArdell, Evaluation of a full-scale wastewater treatment plant upgraded with ozonation and biological post-treatments: Abatement of micropollutants, formation of transformation products and oxidation by-products, Water Res., 129 (2018) 486-498.

[151] W.T. Li, M. Majewsky, G. Abbt-Braun, H. Horn, J. Jin, Q. Li, Q. Zhou, A.M. Li, Application of portable online LED UV fluorescence sensor to predict the degradation of dissolved organic matter and trace organic contaminants during ozonation, Water Res., 101 (2016) 262-271.

[152] Y. Lee, D. Gerrity, M. Lee, A.E. Bogeat, E. Salhi, S. Gamage, R.A. Trenholm, E.C. Wert, S.A. Snyder, U. von Gunten, Prediction of Micropollutant Elimination during Ozonation of Municipal Wastewater Effluents: Use of Kinetic and Water Specific Information, Environ. Sci. Technol., 47 (2013) 5872-5881.

[153] U. von Gunten, Ozonation of drinking water: Part I. Oxidation kinetics and product formation, Water Res., 37 (2003) 1443-1467.

[154] M.S. Lucas, J.A. Peres, B.Y. Lan, G. Li Puma, Ozonation kinetics of winery wastewater in a pilot-scale bubble column reactor, Water Res., 43 (2009) 1523-1532.

[155] J. Santiago-Morales, M.J. Gomez, S. Herrera-Lopez, A.R. Fernandez-Alba, E. Garcia-Calvo, R. Rosal, Energy efficiency for the removal of non-polar pollutants during ultraviolet irradiation, visible light photocatalysis and ozonation of a wastewater effluent, Water Res., 47 (2013) 5546-5556.

[156] M.-O. Buffle, J. Schumacher, S. Meylan, M. Jekel, U. von Gunten, Ozonation and Advanced Oxidation of Wastewater: Effect of O_3 Dose, pH, DOM and HO•- Scavengers on Ozone Decomposition and HO• Generation, Ozone Sci. Eng., 28 (2006) 247-259.

[157] M. Saquib, C. Vinckier, B. Van der Bruggen, The effect of UF on the efficiency of O_3/H_2O_2 for the removal of organics from surface water, Desalination, 260 (2010) 39-42.

[158] Y. Liu, J. Jiang, J. Ma, Y. Yang, C. Luo, X. Huangfu, Z. Guo, Role of the propagation reactions on the hydroxyl radical formation in ozonation and peroxone (ozone/hydrogen peroxide) processes, Water Res., 68 (2015) 750-758.

[159] E.L. Yong, Y.-P. Lin, Kinetics of Natural Organic Matter as the Initiator, Promoter, and Inhibitor, and Their Influences on the Removal of Ibuprofen in Ozonation, Ozone Sci. Eng., 35 (2013) 472-481.

[160] H.-F. Miao, M. Cao, D.-Y. Xu, H.-Y. Ren, M.-X. Zhao, Z.-X. Huang, W.-Q. Ruan, Degradation of phenazone in aqueous solution with ozone: Influencing factors and degradation pathways, Chemosphere, 119 (2015) 326-333.

[161] J. Margot, C. Kienle, A. Magnet, M. Weil, L. Rossi, L.F. de Alencastro, C. Abegglen, D. Thonney, N. Chèvre, M. Schärer, D.A. Barry, Treatment of micropollutants in municipal wastewater: Ozone or powdered activated carbon?, Sci. Total Environ., 461–462 (2013) 480-498.

[162] N. Takeuchi, H. Mizoguchi, Study of optimal parameters of the H_2O_2/O_3 method for the decomposition of acetic acid, Chem. Eng. J., 313 (2017) 309-316.

[163] T.E. Agustina, H.M. Ang, V.K. Vareek, A review of synergistic effect of photocatalysis and ozonation on wastewater treatment, J Photochem. Photobiol. C: Photochem. Rev., 6 (2005) 264-273.

[164] F. Thevenet, O. Guaïtella, J.M. Herrmann, A. Rousseau, C. Guillard, Photocatalytic degradation of acetylene over various titanium dioxide-based photocatalysts, Appl. Catal. B, 61 (2005) 58-68.

[165] J. Xiao, Y. Xie, H. Cao, Organic pollutants removal in wastewater by heterogeneous photocatalytic ozonation, Chemosphere, 121 (2015) 1-17.

[166] L. Sánchez, J. Peral, X. Domènech, Aniline degradation by combined photocatalysis and ozonation, Appl. Catal. B, 19 (1998) 59-65.

[167] P. Kopf, E. Gilbert, S.H. Eberle, TiO_2 photocatalytic oxidation of monochloroacetic acid and pyridine: influence of ozone, J. Photochem. Photobiol. A: Chem., 136 (2000) 163-168.

[168] L. Li, W. Zhu, L. Chen, P. Zhang, Z. Chen, Photocatalytic ozonation of dibutyl phthalate over TiO_2 film, J. Photochem. Photobiol. A: Chem., 175 (2005) 172-177.

[169] D.S. Bhatkhande, V.G. Pangarkar, A.A.C.M. Beenackers, Photocatalytic degradation for environmental applications – a review, J. Chem. Technol. Biotechnol., 77 (2002) 102-116.

[170] T.S. Müller, Z. Sun, G. Kumar, K. Itoh, M. Murabayashi, The combination of photocatalysis and ozonolysis as a new approach for cleaning 2,4-dichlorophenoxyaceticacid polluted water, Chemosphere, 36 (1998) 2043-2055.

[171] G.V. Buxton, C.L. Greenstock, W.P. Helman, A.B. Ross, Critical Review of rate constants for reactions of hydrated electrons, hydrogen atoms and hydroxyl radicals (·OH/·O− in Aqueous Solution, J. Phys. Chem. Ref. Data, 17 (1988) 513-886.

[172] W.H. Koppenol, J. Butler, J.W.v. Leeuwen, THE HABER-WEISS CYCLE, Photochem. Photobiol., 28 (1978) 655-658.

[173] Y. Liu, X. He, X. Duan, Y. Fu, D. Fatta-Kassinos, D.D. Dionysiou, Significant role of UV and carbonate radical on the degradation of oxytetracycline in UV-AOPs: Kinetics and mechanism, Water Res., 95 (2016) 195-204.

[174] C. Walling, A. Goosen, Mechanism of the ferric ion catalyzed decomposition of hydrogen peroxide. Effect of organic substrates, J. Am. Chem. Soc., 95 (1973) 2987-2991.

[175] B.H.J. Bielski, D.E. Cabelli, R.L. Arudi, A.B. Ross, Reactivity of HO_2/O_{-2} Radicals in Aqueous Solution, J. Phys. Chem. Ref. Data, 14 (1985) 1041-1100.

[176] N.M. Ram, R.F. Christman, K.P. Cantor, Significance and treatment of volatile organic compounds in water supplies, in, Chelsea, MI (US); Lewis Publishers, Inc., 1990, pp. 339.

Supplementary Information

Impact of water matrix on the removal of micropollutants by advanced oxidation technologies

Ana R. Ribeiro[1,*], Nuno F.F. Moreira[1], Gianluca Li Puma[2,*], Adrián M.T. Silva[1]

[1]Laboratory of Separation and Reaction Engineering - Laboratory of Catalysis and Materials (LSRE-LCM), Faculdade de Engenharia, Universidade do Porto, Rua Dr. Roberto Frias s/n, 4200-465 Porto, Portugal

[2]Environmental Nanocatalysis & Photoreaction Engineering, Department of Chemical Engineering, Loughborough University, Loughborough, United Kingdom

*Corresponding authors: ritalado@fe.up.pt (A.R. Ribeiro), G.Lipuma@lboro.ac.uk (G. Li Puma)

Table S1. Matrix effects occurring in studies dealing with photolysis and UV/H_2O_2, published since 2005. Unless otherwise stated, the experimental conditions refer to the tested conditions for the evaluation of matrix effects.

AOT	Target pollutant Concentration	Matrices	Experimental conditions	Main conclusions	Reference
UV **UV/H_2O_2**	Bisphenol A 520 µM	- UPW; - WW effluent (pH 7.43; DOC 10.74 mg L^{-1}; conductivity 1180 µS cm^{-1}; Cl^- 111.9 mg L^{-1}: NO_3^- 47.5 mg L^{-1}; SO_4^{2-} 121.8 mg L^{-1}), Germany.	- Stirred batch photoreactor; - V 750 mL; T 298 K; - Optical path length 4 cm; - Irradiation source: UV immersed LP Heraeus Hg lamp TN 15/35 with a nominal output of 15 W (λ_{max} = 254 nm), located at the centre axis of the reactor, in a quartz sleeve; - 0, 250, 500, 750 µM H_2O_2.	The matrix played an important role on the photodegradation yield. The removal rate of bisphenol A by photolysis was slightly higher in WW than in UPW, probably due to the ROS produced in the effluent. On the contrary, the removal rate by UV/H_2O_2 was lower in the WW.	[4]
UV/H_2O_2	Benzoylecgonine 2.8×10^{-5} ± 4.0×10^{-6} mol L^{-1}	- UPW (pH 6.0; conductivity 2.5 µS cm^{-1}; TOC 0.248 mg L^{-1}; NO_3^- 1.0 mg L^{-1}); - SW (pH 7.8; conductivity 930 µS cm^{-1}; TOC 46.37 mg L^{-1}; NO_3^- 25.8 mg L^{-1}; NO_2^- 0.17 mg L^{-1}), Grand Union Canal, UK; - SWW (pH 6.0; conductivity 80 µS cm^{-1}; TOC 20.79 mg L^{-1}; NO_3^- 1.0 mg L^{-1}); - WW effluent (pH 7.8; conductivity 960 µS cm^{-1}; TOC 43.25 mg L^{-1}; NO_3^- 52.4 mg L^{-1}; NO_2^- 0.17 mg L^{-1}), Leicestershire, UK.	- Microcapillary film array photoreactor; - Irradiation source: UV monochromatic lamp (Germicidal G8T5, 8W) emitting at 253.7 nm; - $[H_2O_2]/[BE] \sim 500$.	The removal of benzoylecgonine was affected by the matrix, mainly due to the presence of different xenobiotics and natural compounds that can act as $HO^\bullet$ scavengers and as inner filters. Moreover, the presence of NO_3^- in higher concentration in WW promoted the removal, in comparison to SW.	[39]
UV/H_2O_2	Benzoylecgonine 0.6–18.5 mg L^{-1}	- UPW (pH 6.0; conductivity 2.5 µS cm^{-1}; TOC 0.248 mg L^{-1}; NO_3^- 1.0 mg L^{-1}); - SW (pH 7.8; conductivity 930 µS cm^{-1}; TOC 46.37 mg L^{-1}; NO_3^- 25.8 mg L^{-1}; NO_2^- 0.17 mg L^{-1}), Grand Union Canal, UK; - SWW (pH 6.0; conductivity 80 µS cm^{-1}; TOC 20.79 mg L^{-1}; NO_3^- 1.0 mg L^{-1}); - WW effluent (pH 7.8; conductivity 960 µS cm^{-1}; TOC 43.25 mg L^{-1}; NO_3^- 52.4 mg L^{-1}; NO_2^- 0.17 mg L^{-1}), Leicestershire, UK.	- Microcapillary film array photoreactor; - Irradiation source: UV monochromatic lamp (Germicidal G8T5, 8W) emitting at 253.7 nm; - H_2O_2 concentration: 10^{-4} - 10^{-3} M..	The removal efficiency was affected by organic and inorganic compounds present in the matrices.	[40]
UV/H_2O_2	Atrazine, sulfamethoxazole and N-nitrosodimethylamine 0.5 – 11 µM	- 3 lake waters, Switzerland and Norway; - WW effluent (DOM 3.9 mg C L^{-1}; alkalinity 6.5 mg $CaCO_3$ L^{-1}), Switzerland.	- 500 mL cylindrical glass vessel filled with 350 mL of solution; - Irradiation source: UV immersed LP Heraeus Hg lamp TN 15/35 with a nominal output of 15 W (λ_{max} 254 nm), with a quartz cooling jacket; - MP Hg arc lamp (Heraeus Noble-light model TQ718, nominal power 500 – 700 W) and a UV W-55 glass band pass filter (λ 308 – 410 nm) in the cooling jacket.	The degradation rate was higher in waters with lower DOM concentration and/or lower $HO^\bullet$ scavenging rates. The reactivity of DOM was different in different waters with the same DOC concentration.	[13]

UV **UV/H_2O_2**	Carbamazepine, clarithromycin, diclofenac, metoprolol, benzotriazole, mecoprop ng L^{-1} to µg L^{-1} levels	- WW effluents with different secondary treatment, namely activated sludge (pH 7.8; TOC 37 mg L^{-1}; COD 63 mg L^{-1}; alkalinity 273 mg $CaCO_3$ L^{-1}; Fe_{total} 0.9 mg L^{-1}; TSS 12 mg L^{-1}); moving bed bioreactor (pH 7.4; TOC 20.2 mg L^{-1}; COD 35 mg L^{-1}: alkalinity 85 mg $CaCO_3$ L^{-1}; Fe_{total} 1.6 mg L^{-1}; TSS 14 mg L^{-1}) and coagulation flocculation (pH 7.9; TOC 57.2 mg L^{-1}; COD 90 mg L^{-1}; alkalinity 231 mg $CaCO_3$ L^{-1}; Fe_{total} 1.9 mg L^{-1}; TSS 30 mg L^{-1}), Lausanne, Switzerland.	- 300 mL double-wall, water-jacketed glass batch stirred reactors; - UV-C irradiation source: 36 W, low-pressure amalgam lamp (λ_{max} 254 nm); - H_2O_2: 25 mg L^{-1}.	Regardless the type of secondary treatment, the degradation rates were higher when using UV/H_2O_2 than UV-C. Both UV-based processes removed 80% of the selected MPs. Comparing matrices, the higher removal of both pollutants and TOC was achieved when using effluents resulting from moving bed bioreactor, following by activated sludge and coagulation flocculation. The UV/H_2O_2 process led to a higher degradation rate of the MPs and TOC abatement.	[20]
UV	Hydrochlorothiazide 1 µM	- UPW; - SW from a public reservoir, Spain; - WW effluent (pH 8.0; TOC 23.3 mg L^{-1}; alkalinity 250 mg $CaCO_3$ L^{-1}), Spain.	- 500 mL cylindrical glass vessel filled with 350 mL of solution; - Irradiation source: UV immersed LP Heraeus Hg lamp TN 15/35 with a nominal output of 15 W (λ_{max} 254 nm), located at the centre axis of the reactor, in a quartz sleeve; - T 20 °C.	Photodegradation led to a lower removal rate in the WW, intermediate in the SW and higher in UPW, which can be explained by the DOM present in the studied matrices, absorbing part of UV radiation.	[23]
UV	Azathioprine, cyclophosphamide, cytarabine, doxorubicin, methotrexate, 5-fluorouracil, flutamide and mitotane 100 µg L^{-1}	- DI (pH 6.0; turbidity <0.1 NTU; TOC 0.08 mg L^{-1}; Total alkalinity <5.0 mg L^{-1}; NO_3^- <0.05 mg L^{-1}; SO_4^{2-} <0.05 mg L^{-1}, Cl^- <5.0 mg L^{-1}); - Treated water from water treatment plant (pH 8.0; turbidity 0.2 NTU; TOC 0.8 mg L^{-1}; alkalinity 13.0 mg L^{-1}; NO_3^- 3.2 mg L^{-1}; SO_4^{2-} 21.6 mg L^{-1}, Cl^- 10.0 mg L^{-1}); - WW effluent (pH 6.7; turbidity 5.3 NTU; TOC 10.6 mg L^{-1}; alkalinity 54.9 mg L^{-1}; $NO_3^{-\,6.3}$ mg L^{-1}; SO_4^{2-} 45.1 mg L^{-1}, Cl^- 145.5 mg L^{-1}).	- Cylindrical photoreactor (1 L) - Irradiation source: 5 W Philips UV lamp (λ = 254 nm); Addition of HA, $HCO_3^−$, $NO_3^−$, $Cl^−$, and $SO_4^{2−}$.	The presence of HA decreased the degradation rates of the target pollutants. NO_3^- (0.5 to 5 mg L^{-1}) promoted their photodegradation; whereas HCO_3^-, SO_4^{2-} and Cl^- did not affect it. The performance of the UV treatment was not reduced when applied to treated water since the TOC content of this matrix was very low. However, the degradation efficiency decreased in the WW effluent, with a much higher TOC content (10.6 mg L^{-1}). Furthermore, the addition of $S_2O_8^{2−}$and H_2O_2 increased the degradation efficiency.	[24]
UV **UV/H_2O_2**	E1, E2, EE2 1.3-1.5 mg L^{-1}	- DW; - WW effluent (pH 7.5-7.8; DOC 6.1-11 mg L^{-1}; COD 18.5-21.7 mg L^{-1}; BOD_5 3-5.8 mg L^{-1}; SS 2.0-4.7 mg L^{-1}: NH_4^+ 0.6-4.24 mg L^{-1}; NO_2^- 0.09-0.54 mg L^{-1}; NO_3^- 3.68-4.54 mg L^{-1}), France.	- Commercial UVC reactor (COMAP WT) and a 55 W LP lamp (λ_{max} 254 nm); - Reactor: 81.5 cm long, 5.4 cm diameter, 1 cm distance between the lamp sleeve and the inner side of the chamber; - V 1.12 L; T 20 °C;. - H_2O_2: 10, 40 and 90 mg L^{-1}.	UV photolysis was more efficient to degrade E1 than E2 and EE2 in both matrices, being the degradation rate constants in the same order of magnitude, regardless the matrix. This low impact of the matrix on degradation rates was attributed to: (i) ROS formed by the action of UV on organic components of the matrices, probably balancing the low transmittance of the WW; and (ii) $NO_3^−$ content, known to act as $HO^•$ precursor. UV/H_2O_2 process highly increased the removals of all hormones, but it was significantly affected by the water matrix, with lower degradation rate constants obtained in treated WW. The NOM competing for UV irradiation, and scavengers competing for $HO^•$ (e.g., humic substances, $Cl^−$, $HCO_3^−$, $SO_4^{2−}$, and $NO_3^−$) were suggested as main factors impacting the removals.	[25]

UV	O-phenylphenol, methyl paraben, propyl paraben, triclosan, bisphenol A 0.5 mg L^{-1}	- UPW; - River water (pH 6.8; DOC 1.42 mg L^{-1}; TC 3.70 mg L^{-1}; NO_3^- 8.40 mg L^{-1}; Cl^- 8.37 mg L^{-1} ; PO_4^{3-} < 0.044 mg L^{-1}; SO_4^{2-} 7.0 mg L^{-1}), Northwest of Spain; - WW effluent (pH 7.1; DOC 3.61 mg L^{-1}; TC 12.8 mg L^{-1}; NO_3^- 4.7 mg L^{-1}; Cl^- 23.1 mg L^{-1} ; PO_4^{3-} 1.32 mg L^{-1}; SO_4^{2-} 30.4 mg L^{-1}).	- Homemade photoreactor with 20 mL of selected water matrix exposed; - UV Irradiation source: two 8 W LP lamps (254 nm); - Effect of NO_3^- addition (25 mg L^{-1}).	Overall, the removal efficiencies were in the following order: UP > SW > WW. NO_3^- had a positive effect in the removal of the investigated pollutants under sunlight and UV radiation, mainly by the enhancement of transformation routes involving $HO^•$. In ultrapure and river water, NO_3^- addition reduced the compounds stability, while not significant changes were found in WW. However, reactive species could be partially consumed by DOC, reducing the removal efficiency.	[29]
UV	Monensin, salinomycin, narasin 0.5 mg L^{-1}	- DI; - WW effluent (pH 7.4; Cl^- 23.1 mg L^{-1} DOC 0.435 mg L^{-1}; NO_3^- 1.45 mM; HCO_3^- 0.120 mM; CO_3^{2-} 0.000141 mM).	- Cylindrical quartz reactor (100 mL) kept in a photochamber; - Irradiation source: 4-W LP UV lamp (λ = 254 nm); - Addition of DOM, NO_3^-.	The photodegradation rate of monensin was significantly increased in WW in comparison with deionized water while the photodegradation of salinomycin was not enhanced. The overall photodegradation of studied compounds in real water matrices is a result of both direct and indirect photolysis. NO_3^- and DOM increased the photodegradation of monensin and salinomycin. An exception was found for the degradation of salinomycin in the presence of one type of DOM.	[30]
UV	Caffeine, carbamazepine, diuron, simazine, sulfamethoxazole, triclosan, 2,4-dichlorophenoxyacetic acid 150 µg L^{-1}	- UPW; - WW effluent (pH 7.85±0.21; DOC 11.55±2.05 mg L^{-1}; COD 33.00±5.65 mg L^{-1}; NO_3^- 26.25±0.64 mg L^{-1}; UVA_{254} 0.36±0.02 cm^{-1}; UVA_{254}/DOC 3.10±0.28 m^{-1} mg^{-1}), Victoria, Australia	- Sealed quartz test tubes (20 mL); - Irradiation source: natural (average solar irradiance 7.7-9.2 KW m^{-2}) and simulated sunlight xenon arc lamp with an UV range of 290–400 nm; - Effect of HA (DOC of 0, 2 and 4 mg L^{-1}) or NO_3^- (10 mg L^{-1} and 20 mg L^{-1}) addition.	The photodegradation rates of the studied compounds were significantly greater in the WW than in the UPW, indicating they primarily degraded via indirect photolysis. However, sulfamethoxazole and triclosan were mainly degraded via direct photolysis. NO_3^- could act as photosensitizer and produce $HO^•$, promoting the photodegradation of the MPs. The addition of NO_3^- promoted the photolysis of all compounds, with minor effect on those which indirect photolysis was not the main degradation pathway. HA enhanced the degradation of caffeine, diuron and sulfamethoxazole, inhibiting the photolysis of the other compounds.	[15]
UV **UV/H_2O_2**	Monensin, salinomycin, narasin, nigericin 0.8 – 3.0 µM	- Deionized water (buffered at pH 7.0); - SW (SW); - WW effluent (pH 7.4; DOC 0.435 mg L^{-1}; Cl^- 0.41 mM; NO_3^- 1.45 mM; PO_4^{3-} 0.95 mM; HCO_3^- 0.00011 mM; CO_3^{2-} 0.12 mM).	- 60 mL cylindrical quartz reactor with a 4-W LP UV lamp (λ_{max} 254 nm); - Incident light intensity 2.0 mW·cm^{-2} (≈ to a photo fluence rate of 3.36 × 10^{-6} Einstein·L^{-1}·s^{-1}); - Fluences from 0 to 6.05 × 10^{-4} Einstein·L^{-1}; - 30 mg L^{-1} H_2O_2; - T 22 °C.	Under UV irradiation, the degradation of the antibiotics in SW and WW was faster than in buffered DI. In this case, the degradation occurred by direct UV photolysis, whereas indirect photolysis contributed to the faster degradation in the actual matrices. Matrix components such as NO_3^-, Cl^- and DOM may produce certain radicals and reactive transient species under UV irradiation, reacting quickly. However, the degradation rates by UV/H_2O_2 were lower in SW and WW than in DI. The authors attributed this behaviour to matrix effects, mostly $HO^•$ scavengers and competitors for UV absorption. Since the direct photolysis was significantly slower than the reaction of the compounds with $HO^•$, the direct photolysis by UV can be considered negligible in the UV/H_2O_2 process.	[34]

UV **UV/H_2O_2**	Sulfamethoxazole, sulfamethazine, sulfadiazine, trimethoprim, bisphenol A, diclofenac 4 µM	- UPW; - Lake water (pH 6.84; DOC 5.1 mg L^{-1}; alkalinity 24.4 mg $CaCO_3$ L^{-1}; NO_3^- 1.9 mg L^{-1}: NO_2^- < 0.25 mg L^{-1}; Cl^- 5.8 mg L^{-1}: Br^- < 0.25 mg L^{-1}; SO_4^{2-} 4.6 mg L^{-1}); - WW effluent (pH 6.84; DOC 7.3 mg L^{-1}; alkalinity 73.4 mg $CaCO_3$ L^{-1}; NO_3^- 4.9 mg L^{-1}: NO_2^- < 0.25 mg L^{-1}; Cl^- 59.2 mg L^{-1}: Br^- < 0.25 mg L^{-1}; SO_4^{2-} 47.5 mg L^{-1}).	- Bench scale quasi-collimated beam apparatus equipped with 4 LP UV lamps; - pH in UPW experiments: 3.6, 7.85, 9.7 (only for UV); - pH in water matrices experiments: 7.85; - H_2O_2: 2, 6, 10 mg L^{-1}.	UV/H_2O_2 treatment led to removals ranging from 43% for trimethoprim to 98% for diclofenac in lake water. In WW, the removals were lower (31-97%), suggesting a superior scavenging rate of $HO^\bullet$, namely DOC, alkalinity, Cl^-, SO_4^{2-} and NO_3^-.	[38]
UV	Sulfamethoxazole 1.0, 2.0, 5.0 and 10 mg L^{-1}	- UPW; - WW effluent (pH 7.0; DOC 16 mg L^{-1}; COD 21.2 mg L^{-1}; turbidity 2.0 NTU; N_{total} 23 mg L^{-1}; P_{total} 0.4 mg L^{-1}), Shanghai, China.	- 0.8 L a cylindrical glass-jacketed reactor ; - 10 W power input LP Hg lamp (Shanghai, China) (λ_{max} 254 nm); - Effect of organic anions (Cl^-, SO_4^{2-}, NO_3^-, HCO_3^-) and HA.	The removal of sulfamethoxazole (10 mg L^{-1}) in UPW was completed in 30 min, but the degradation rate decreased in WW, with almost total removal after 60 min. The degradation was slightly improved in water matrices containing 1.0 mM of Cl^-, SO_4^{2-} and NO_3^-, and 5 mg L^{-1} of HA. In turn, HA at higher concentrations and HCO_3^- reduced the degradation rate.	[41]
UV **UV/H_2O_2**	Erythromycin, doxycycline, clindamycin, ciprofloxacin, penicillin-G, trimethoprim 0.68-1.72 µM	- UPW; - WW effluent 1 (pH 6.84; DOC 5.8 mg L^{-1}; alkalinity 123 mg $CaCO_3$ L^{-1}; NO_3^- 4.04 mg L^{-1}: NO_2^- < 0.015 mg L^{-1}); - WW effluent 1 (pH 6.58; DOC 4.9 mg L^{-1}; alkalinity 88 mg $CaCO_3$ L^{-1}; NO_3^- 10.3 mg L^{-1}: NO_2^- 0.021 mg L^{-1}).	- MP lamp system consisting of a 1-kW lamp emitting a polychromatic spectrum > 200 nm; - LP lamp system consisting of four 15-W lamps emitting monochromatic light at λ 253.7 nm; - H_2O_2: 10 mg L^{-1}.	Photolysis and UV/ H_2O_2 experiments showed the matrix influence. UV-photosensitized reactions were recorded for clindamycin. In UV/H_2O_2 process, erythromycin and doxycycline originated some active intermediates at low treatment doses of UV_{254} and only in WW effluents, suggesting that these by-products does not result from direct reaction with $HO^\bullet$. The reactions seem to be controlled by some components of the matrix by the following mechanisms: (i) reaction initiated when $HO^\bullet$ interact with the pollutant in the presence of other matrix components; (ii) result of dark reactions of photoproducts; or (iii) result from photosensitized reactions in complex matrices under UV, namely with $^1O_2$ or $^3DOM^*$.	[19]
UV **UV/H_2O_2**	Oxytetracycline, doxycycline, ciprofloxacin 5 µM	- UPW; - SW; - DW; - WW effluent (pH 7.84; DOC 5.0 mg L^{-1}; alkalinity 1.58 mM HCO_3^-; NO_3^- 132 mg L^{-1}; Cl^- 107.3 mg L^{-1}; F^- 0.4 mg L^{-1}; SO_4^{2-} 60.7 mg L^{-1}).	- 11W LP Hg lamp emitting monochromatic light at λ 254 nm; - H_2O_2: 1mM.	The performance of UV/H_2O_2 process was influenced by water matrix. For all target antibiotics, the DW was the matrix which led to faster degradation and the opposite occurred in WW due to the higher background $HO^\bullet$ radical scavenging in this matrix.	[35]
UV **UV/H_2O_2**	1-H-Benzotriazole, N,N-diethyl-m-toluamide (DEET), Chlorophene, 3-Methylindole, Nortripty-line HCl 1 µM	- UPW; - Lake water (pH 7.4; TOC 5.2 mg L^{-1}; COD 18 mg L^{-1}; conductivity 80.2 µS cm^{-1}; alkalinity 30 mg $CaCO_3$ L^{-1}; N_{total} 1.51 mg L^{-1}; P_{total} 0.041 mg L^{-1}); - WW effluent (pH 7.9-8.3; TOC 2.8-11.1 mg L^{-1}; COD 7-56 mg L^{-1}; conductivity 550-570 µS cm^{-1}; alkalinity 325-335 mg $CaCO_3$ L^{-1}; N_{total} 21.3-35.5 mg L^{-1}: P_{total} 0.156-1.76 mg L^{-1}), Spain.	- Irradiation source: UV immersed LP Heraeus Hg lamp TN 15/35 with a nominal output of 15 W (λ_{max} 254 nm); - H_2O_2: 1 and 5 x 10^{-5} M; - Natural pH of each water ; - Temperature of 20 °C.	In the simultaneous photodegradation by UV and UV/H_2O_2, the removal rate of all compounds decreased with the relative organic matter contents of the different water matrices.	[42]

UV **UV/H_2O_2**	Benalaxyl, cyprodinil, dimethomorph, fenhexamide, iprovalicarb, kresoxim-methyl, metalaxyl, myclobutanil, tebuconazole $10\ \mu g\ L^{-1}$	- Tap water; - Swimming pool water; - River water; - WW effluent (composition not provided).	- Middle-scale photoreactor with water recirculation to simulate real conditions; - Irradiation source: UVC 6W lamp ($\lambda = 254$ nm) - H_2O_2: 20 mg L^{-1}.	Under UVC radiation, degradation occurred in all water samples and was quite similar despite of the studied matrices, removing approximately >50% (except for benalaxyl, iprovalicarb and myclobutanil) after 30 min. Regarding the removal efficiency by UVC/H_2O_2, an average removal of 75% was verified for all the water matrices in less than 6 min. The addition of H_2O_2 under UVC light allowed an improvement of the reaction kinetics.	[43]

Abbreviations: BOD_5, biochemical oxygen demand; COD, chemical oxygen demand; DI, distilled water; DOC, dissolved organic carbon; DOM, dissolved organic matter; DW, drinking water; E1, estrone; E2, 17-beta-estradiol; EE2, 17-alpha-ethinylestradiol; HA, humic acids; LP, low pressure; MP, micropollutants; NOM, natural organic matter; NTU, nephelometric turbidity unit; ROS, reactive oxidation species; SS, suspended solids; SW, surface water; SWW, synthetic wastewater; TC, total carbon; TOC, total organic carbon; TSS, total suspended solids; UPW, ultrapure water; WW, wastewater.

Table S2. Reaction rate constants (*k*).

Reaction		*k*	Reference
9	$H_2O_2 + HO^\bullet \rightarrow HO_2^\bullet + H_2O$	$3.3 \times 10^{7}\ M^{-1}\ s^{-1}$	[171]
10	$H_2O_2 + HO_2^\bullet \rightarrow HO^\bullet + O_2 + H_2O$	$3\ M^{-1}\ s^{-1}$	[172]
15	$HO^\bullet + HCO_3^- \rightarrow H_2O + CO_3^{\bullet-}$	$8.5 \times 10^{6}\ M^{-1}\ s^{-1}$	[173]
16	$HO^\bullet + CO_3^{2-} \rightarrow HO^- + CO_3^{\bullet-}$	$3.9 \times 10^{8}\ M^{-1}\ s^{-1}$	[173]
17	$Fe^{2+} + H_2O_2 \rightarrow Fe^{3+} + HO^- + HO^\bullet$	$76\ M^{-1}\ s^{-1}$	[37]
18	$Fe^{2+} + HO^\bullet \rightarrow Fe^{3+} + HO^-$	$3.2 \times 10^{8}\ M^{-1}\ s^{-1}$	[118]
19	$HO^\bullet + RH \rightarrow H_2O + R^\bullet$	$10^{7}\ M^{-1}\ s^{-1}$	[118]
21	$Fe^{3+} + H_2O_2 \rightarrow Fe^{2+} + HO_2^\bullet + H^+$	$0.001 - 0.01\ M^{-1}\ s^{-1}$	[174]
41	$O_2^{\bullet-} + H^+ \rightarrow HO_2^{\bullet-}$	$2 \times 10^{9}\ M^{-1}\ s^{-1}$	[175]
44	$O_3 + HO^- \rightarrow HO_2^- + O_2$ (basic pH)	$70\ M^{-1}\ s^{-1}$	[153]
45	$O_3 + HO_2^- \rightarrow HO^\bullet + O_2^{\bullet-} + O_2$	$2.8 \times 10^{6}\ M^{-1}\ s^{-1}$	[153]
46	$O_3 + O_2^{\bullet-} \rightarrow O_3^{\bullet-} + O_2$	$1.6 \times 10^{9}\ M^{-1}\ s^{-1}$	[153]
47	$O_3^{\bullet-} + H^+ \leftrightarrow HO_3^\bullet$ (pH < 8)	$k+ = 5 \times 10^{10}\ M^{-1}\ s^{-1}$ $k- = 3.3 \times 10^{2}\ s^{-1}$	[153]
48	$HO_3^\bullet \rightarrow HO^\bullet + O_2$ (pH < 8)	$1.4 \times 10^{5}\ s^{-1}$	[153]
49	$O_3^{\bullet-} \leftrightarrow O^{\bullet-} + O_2$ (pH > 8)	$k+ = 2.1 \times 10^{3}\ M^{-1}\ s^{-1}$ $k- = 3.3 \times 10^{9}\ s^{-1}$	[153]
50	$O^{\bullet-} + H_2O \rightarrow HO^\bullet + HO^-$ (pH > 8)	$10^{8}\ s^{-1}$	[153]
51	$HO^\bullet + O_3 \rightarrow HO_2^\bullet + O_2$	$1 \times 10^{8}\ M^{-1}\ s^{-1} - 2 \times 10^{9}\ M^{-1}\ s^{-1}$	[153]
57	$O_3^{\bullet-} + H^+ \rightarrow HO_3^\bullet$	$5 \times 10^{10}\ M^{-1}\ s^{-1}$	[176]
58	$HO_3^\bullet \rightarrow O_2 + HO^\bullet$	$1.4 \times 10^{5}\ s^{-1}$	[176]
59	$HO^\bullet + O_3 \rightarrow O_2 + HO_2^\bullet$	$2 \times 10^{9}\ M^{-1}\ s^{-1}$	[175]

Table S3. Matrix effects occurring in studies dealing with Fenton-based processes, published since 2005. Unless otherwise stated, the experimental conditions refer to the tested conditions for the evaluation of matrix effects.

AOT	Target pollutant Concentration	Matrices	Experimental conditions	Main conclusions	Reference
Fenton-like	Bisphenol A 285-14200 µg L^{-1}	- UPW; - DW; - GW; - SW; - WW effluent (pH 8; TOC 7 mg L^{-1}; conductivity 311 µS cm^{-1}; Cl^- 0.5 mg L^{-1}: NO_3^- 57 mg L^{-1}; HCO_3^- 182 mg L^{-1}; SO_4^{2-} 30 mg L^{-1}).	- Glass cylindrical reaction vessel; - 20 mL of an aqueous solution containing Bisphenol A; - Magnetic stirring, open air equilibrium; - Catalyst: sodium persulphate (SPS) and a magnetic carbon xerogel, consisting of interconnected carbon microspheres with embedded iron and cobalt microparticles.	The elimination rate in UPW was always lower than in any other matrices. This resulted from an interplay among many effects, namely: (i) the presence of HA and low molecular weight organic acids (e.g., oxalate) able to form complexes with iron species, promoting the Fenton-like reactions; and (ii) the presence of organic/inorganic species that could led to competitive adsorption onto the xerogel surface, as well as scavenging effects. The experiments performed in spiked UPW showed that organics and HCO_3^- hindered the degradation, by acting as scavengers of $SO_4^{\bullet-}$ and $HO^\bullet$, whereas Cl^- (> 50 mg/L) had a positive effect, maybe due to the formation $Cl_2^{\bullet-}$.	[14]
Bio-electro-Fenton	Ketoprofen, diclofenac, ibuprofen and naproxen 40 µg L^{-1}	- DI; - WW after primary clarifier (COD 186 mg l-1; pH 7.9; conductivity 1.3 µS cm^{-1}; NH_4^+-N 0.08 g L^{-1}; PO_4^{3-}-P 0.01 g L^{-1}; Cl^- 0.1 g L^{-1}; SO_4^{2-} 0.03 g L^{-1}), Copenhagen, Denmark.	- Lab-scale rectangular bio-electrochemical system; - Reactors were maintained with 90 mL of WW; -Voltage: 0.5 V; - pH 2; - Airflow rate: 8 mL min^{-1}; - $FeSO_4$: 5 mM.	Lower removal rates were found when actual WW was used as matrix. Regarding ketoprofen, diclofenac and naproxen the k_{app} were 30-65% lower, which can be explained by the presence of organic matter present in WW competing with the targeted compounds for $HO^\bullet$. Fenton reactions can be inhibited by inorganic ions. Ferric ion can form complexes with PO_4^{3-}. SO_4^{2-}, Cl^- and F^- can reduce the reactivity of ferric ion.	[44]
Fenton **Fe(II)-activated persulfate**	Trimethoprim 0.05 mM	- DI; - SWW; - WW effluent, Beijing.	- Glass bottle (150 mL) fill with 100 mL; - Fe^{2+}: 0.05 mM; - H_2O_2: 1 mM. - pH 3.	Complete degradation of trimethoprim was obtained when using DI. A decrease in the treatment efficiency was found in actual WW, with 35.8% and 43.6% removal for Fenton and the Fe (II)-activated persulfate processes, respectively. Furthermore, the decomposition efficiencies for H_2O_2 was lower in comparison to DI and SWW, which may be due the formation of Fe(II) complexes with organic matter present in actual WW, decreasing the amount of Fe(II) available for reaction with H_2O_2. The removal efficiency in the presence of persulfate decreased in WW, possibly due to the reaction between the sulphate radicals and organic MPs.	[45]
Fenton **Photo-Fenton**	Prednisolone 100 mg L^{-1}	- DI;	- Cylindrical glass reactor (550 mL); - Irradiation source: LED (40 W, λ_{max}=360 nm);	Matrix constituents affected the mineralization rates, with only 10% removal after 1 hour treatment, while	[46]

UV **UV/H_2O_2**		- WW effluent (pH 6.9; COD 35 mg O_2 L^{-1}; TOC 52.7 mg L^{-1}; BOD_5 2 mg O_2 L^{-1}: SS 12 mg L^{-1}), Spain.	- Solution pH 3; - Fe^{2+}: 3 mM; - H_2O_2: 3 mM.	50% was obtained in DI. The presence of inorganic and organic compounds in the WW may reduce the concentration of oxidant species by reacting with $HO^•$.	
Solar irradiation **Fenton** **Solar photo-Fenton**	Carbamazepine, clarithromycin, diclofenac, metoprolol, benzotriazole, mecoprop ng L^{-1} to µg L^{-1} levels	- WW effluents with different secondary treatment, namely activated sludge (pH 7.8; TOC 37 mg L^{-1}; COD 63 mg L^{-1}: alkalinity 273 mg $CaCO_3$ L^{-1}; Fe_{total} 0.9 mg L^{-1}; TSS 12 mg L^{-1}), moving bed bioreactor (pH 7.4; TOC 20.2 mg L^{-1}; COD 35 mg L^{-1}; alkalinity 85 mg $CaCO_3$ L^{-1}; Fe_{total} 1.6 mg L^{-1}; TSS 14 mg L^{-1}) and coagulation flocculation (pH 7.9; TOC 57.2 mg L^{-1}; COD 90 mg L^{-1}: alkalinity 231 mg $CaCO_3$ L^{-1}; Fe_{total} 1.9 mg L^{-1}; TSS 30 mg L^{-1}), Lausanne, Switzerland.	- 100-mL brown bottles; - Irradiation source: solar simulator; - H_2O_2: 25 mg L^{-1}; - Fe^{2+}: 5 mg L^{-1}.	Regardless the type of secondary treatment, the order of degradation rates was photo-Fenton > solar irradiation > Fenton. In general, the higher abatement of both pollutants and TOC was reached when using effluents from moving bed bioreactor, following by activated sludge. Although the moving bed bioreactor effluents led to a higher removal by Fenton process than the other matrices, the consumption of peroxide was inferior due to the lower alkalinity, showing the HCO_3^- effect.	[20]
Photo-Fenton	Tetracycline 24 mg L^{-1}	- UPW; - SW; - WW effluent (pH 8.0; TOC 10.6 mg L^{-1}; IC 52.4 mg L^{-1}; COD 136 mg L^{-1}; BOD 30.0 mg L^{-1}; DO 5.0 mg L^{-1}; Cl^- 54.4 mg L^{-1}; NO_3^- 0.73 mg L^{-1}; turbidity 134 NTU; TDS 510 mg L^{-1}), Brazil.	- Iron (0.2 mM) source: $Fe(NO_3)_3$ or potassium ferrioxalate; - H_2O_2: 3, 10 mM; *Black-light irradiation* - Upflow reactor; V 280 mL; - Irradiation source: 15W black-light lamp (λ_{max} 365 nm), with an irradiance of 19 W m^{-2}; - Recirculation of the solution at a flow rate of 80 mL min^{-1}, after addition of iron, pH adjustment to 2.5 and addition of H_2O_2; *Solar irradiation* - Transparent glass vessel; V 500 mL; - Direct sunlight, during summer between 10 a.m. and 14 p.m., in Brazil (22°S 48°W); - Irradiance: 15 to 20 W m^{-2}.	The SW matrix did not decrease the degradation efficiency, in comparison to UPW, under either black-light or solar irradiation. In the case of WW under solar irradiation in the presence of ferrioxalate, no influence of the matrix was also observed. However, lower efficiency was obtained under black-light, indicating the interference of the matrix components on the efficiency of the process. This effect could be originated by the high TOC and/or IC content of 52.4 mg L^{-1} at pH 8. The increase of H_2O_2 resulted in an even lower efficiency, suggesting the influence of other matrix constituents.	[37]
Photo-Fenton	62 MPs 3-66,379 ng L^{-1}	- WW effluent (pH 7.6–8.3; TOC 16-18 mg L^{-1}; IC 69-116 mg L^{-1}; COD 20-29 mg L^{-1}), Almería, Spain. - Stripped WW: 0.4–0.5 g H_2SO_4 L^{-1} effluent) was added to reduce HCO_3^-/CO_3^- content to less than 5 mg L^{-1} as IC, with no significant decrease on the pH.	- CPC plant under natural solar irradiation; - Fe(II): 5 mg L^{-1}; - H_2O_2: 50 mg L^{-1}; - Complexing agents (HA and EDDS); - pH: 3 (classical photo-Fenton), 6.5 (modified photo-Fenton).	Modified photo-Fenton with HA at neutral pH resulted in a longer treatment time required to reach a similar degradation to that observed on conventional photo-Fenton. Modified photo-Fenton with EDDS showed promising results, with lower consumption of H_2O_2 and keeping the pH.	[47]
Photo-Fenton	Acetaminophen, antipyrine, atrazine, caffeine, carbamazepine, diclofenac, flumequine, hydroxybiphenyl, ibuprofen, isoproturon,	- WW effluent (pH 7.6–8.3; TC 87-132 mg L^{-1}; IC 69-116 mg L^{-1}; COD 20-19 mg L^{-1}), Almería, Spain. - Stripped WW: 0.4–0.5 g H_2SO_4 L^{-1} effluent was added to reduce HCO_3^-/CO_3^- content to less than 5 mg L^{-1} as IC, with no significant decrease on the pH.	CPC solar plant; Solution of Fe:EDDS (molar ratio 1:2 or 1:1); H_2O_2: 50 mg L^{-1}.	The removal rate by photo-Fenton was only slightly lower in the WW effluent than in the stripped effluent, since the first radical formed with Fe:EDDS during Fenton-like or photoactivated Fe is the $O_2^{•-}$. The reactivity of $HCO_3^-$with the $O_2^{•-}$ is much lower than with the $HO^•$, turning its influence negligible.	[48]

	ketorolac, ofloxacin, progesterone, sulfamethoxazole, and triclosan 100 μg L^{-1}				
Photo-Fenton	Acetaminophen, antipyrine, atrazine, caffeine, carbamazepine, diclofenac, flumequine, hydroxybiphenyl, ibuprofen, isoproturon, ketorolac, ofloxacin, progesterone, sulfamethoxazole and triclosan 5 and 100 μg L^{-1}	- WW effluent (pH 7.6−8.3; DOC 10-24 mg L^{-1}; IC 91-120 mg L^{-1}; COD 26-63 mg L^{-1}), Almería, Spain. - Stripped WW: 0.4−0.5 g H_2SO_4 L^{-1} effluent) was added to reduce HCO_3^-/CO_3^- content to less than 1 mg L^{-1} as IC.	Modified solar photo-Fenton; - 5mg L^{-1} of Fe(II); - 50 mg L^{-1} of H_2O_2; - pH ≈7; - Addition of 35 mg L^{-1} oxalic acid; - Addition of HA (10, 25, 50 mg L^{-1}); - Mixing 31% of WWTP influent and 69% effluent.	The use of ferrioxalate, humic substances and mixing the WWTP effluent with a percentage of influent, were attempted to form photoactive Fe(III) complexes. Both oxalate- and HA-enhanced processes provided higher degradation of MPs, but mixing influent was not successful.	[49]
Photo-Fenton	Ofloxacin 10 mg L^{-1}	- Demineralized water; - Simulated natural freshwater; - Simulated municipal WW; - WW effluent (pH 7.8; DOC 10.72 mg L^{-1}; COD 63.7 mg L^{-1}; conductivity 3.05 μS cm^{-1}; Cl^- 0.54 mg L^{-1}; NO_3^- 0.02 mg L^{-1}; SO_4^{2-} 1.05 mg L^{-1}; Na^+ 0.37 mg L^{-1}; NH_4^+ 0.11 mg L^{-1}; K^+ 0.045 mg L^{-1}; Ca^{2+} 0.12 mg L^{-1}; Mg^{2+} 0.064 mg L^{-1}), Almería, Spain.	- CPC plant under natural solar irradiation; - pH 2.8–2.9, - Fe(II): 2 mg L^{-1}; - H_2O_2: 2.5 mg L^{-1}.	The process was efficient to remove ofloxacin. DOC removal and the formation of by-products were dependent on the chemical composition of the matrix, with a lower mineralization of ofloxacin observed in the WW, due to the higher concentration of inorganic (i.e. Cl^- and SO_4^{2-}) and organic species in the more complex matrix. The presence of inorganic ions in the simulated natural freshwater also affected the mineralization.	[50]
Photo-Fenton	Trimethoprim 10 mg L^{-1}	- Demineralized water; - Simulated natural freshwater; - SWW; - WW effluent (pH 7.8; DOC 10.72 mg L^{-1}; COD 63.7 mg L^{-1}; conductivity 3.05 μS cm^{-1}; Cl^- 0.54 mg L^{-1}: NO_3^- 0.02 mg L^{-1}; SO_4^{2-} 1.05 mg L^{-1}; Na^+ 0.37 mg L^{-1}; NH_4^+ 0.11 mg L^{-1}; K^+ 0.045 mg L^{-1}; Ca^{2+} 0.12 mg L^{-1}; Mg^{2+} 0.064 mg L^{-1}), Almería, Spain.	- CPC plant under natural solar irradiation; - pH 2.8–2.9, - Fe(II): 2 mg L^{-1}; - H_2O_2: 2.5 mg L^{-1}.	In comparison to demineralized water and simulated natural freshwater, the higher organic carbon and salt content in simulated/real effluents reduced the mineralization per dose of H_2O_2. A slightly higher amount of H_2O_2 was required in the case of simulated freshwater. The organic/inorganic content of WW competed with the target pollutant and interfered with its degradation pathways.	[12]
Fenton	Nonionic surfactants (6 alcohol ethoxylates and 4 alkylphenol ethoxylates) 1.4 mg L^{-1}	- UPW; - WW effluent (pH 7.6; TOC 13 mg L^{-1}; COD 42 mg L^{-1}; conductivity 540 μS cm^{-1}; Cl^- 124 mg L^{-1}; HCO_3^- 232 mg L^{-1}; Na^+ 74 mg L^{-1}; Ca^{2+} 77 mg L^{-1}; Mg^{2+} 11 mg L^{-1}), Como, Italy.	- 29 ml of solution in 40 ml glass vials to which acidic Fe(II) sulphate solution and H_2O_2 were added; - H_2O_2/Fe ratio: 1.4; - Fe^{2+}: 14 mg L^{-1} (WW) and 10.5 mg L^{-1} (UPW); - H_2O_2: 12 mg L^{-1} (WW) and 9 mg L^{-1} (UPW); - pH range: 3–4.	The efficiency of Fenton process decreased when using the real effluents and higher doses of reactants were required in order to achieve the same removal reached in UPW, maintaining the H_2O_2/Fe ratio.	[51]

Photo-Fenton	Sulfamethoxazole and clarithromycin 100 µg L^{-1}	- DI; - Simulated effluents; - WW effluent (pH 7.4; DOC 16.5 mg L^{-1}; conductivity 602 µS cm^{-1}; Cl^- 295.7 mg L^{-1}; NO_3^- 42.0 mg L^{-1}; SO_4^{2-} 128.6 mg L^{-1}; PO_4^{3-} 6.2 mg L^{-1}; Na^+ 172.2 mg L^{-1}; NH_4^+ 22.6 mg L^{-1}; K^+ 24.8 mg L^{-1}; Ca^{2+} 79.8 mg L^{-1}; Mg^{2+} 26.1 mg L^{-1}; turbidity 10.7 NTU), Almería, Spain.	CPC plant under solar irradiation; Fe^{3+}: 5 mg L^{-1}; H_2O_2: 50 mg L^{-1}.	Sulfamethoxazole was completely removed from all matrices by Solar Fenton, with a removal of 93% in actual effluents ($t_{30\ W,n}$ = 250 min) and a complete removal in simulated effluents ($t_{30\ W,n}$ = 198 min) and DI ($t_{30\ W,n}$ = 85 min). A lower removal (77%) was observed for clarithromycin at the end of the treatment time ($t_{30\ W,n}$ = 252 min), but it was totally eliminated in the other matrices. The lower removal in the real effluents was related to the high concentrations of DOM and inorganic ions, specifically Cl^- and SO_4^{2-} anions that can complex iron and scavenge $HO^{\bullet}$, forming less oxidative radicals ($Cl_2^{\bullet-}$ and $SO_4^{\bullet-}$), compared to $HO^{\bullet}$.	[52]
Photo-Fenton	Acetaminophen, antipyrine, atrazine, caffeine, carbamazepine, diclofenac, flumequine, hydroxybiphenyl, ibuprofen, isoproturon, ketorolac, ofloxacin, progesterone, sulfamethoxazole and triclosan 100 µg L^{-1}	- Synthetic water; - Simulated effluent; - WW effluent (DOC 25 mg L^{-1}; IC 106 mg L^{-1}; COD 60 mg L^{-1}), Almería, Spain.	CPC reactor under solar irradiation; H_2O_2: 0–50 mg L^{-1}; Iron: 5 mg L^{-1}; Unchanged pH; Addition of 406 mg L^{-1} H_2SO_4 to reach an IC < 20 mg L^{-1}.	The MPs were successfully degraded to negligible concentrations with mild solar photo-Fenton at low iron concentrations (5 mg L^{-1}) and 50 mg L^{-1} of H_2O_2, without adjusting the pH. The degradation was dependent on the type of matrix and scavengers present in the matrix, such as CO_3^{2-} and HCO_3^-. The removal was faster in the WW effluent than in the simulated one, but the DOC decrease was similar, which suggests that HA present in the actual matrix might produce solvated electrons and $HO^{\bullet}$ upon irradiation.	[53]
Fenton	Hydroquinone 100 mg L^{-1}	- DI; - WW effluent 2 (pH 7.6, TOC 88.9 mg L^{-1}; COD 308.7 mg L^{-1}; TN 12.14 mg L^{-1}; TP 13.22 mg L^{-1}; TSS 22.0 mg L^{-1}; NO_3^- < 0.18 mg L^{-1}; NO_2^- 0.007 mg L^{-1}), Portugal.	- Bubble column reactor (10 L) fill with 5 L; - Solution pH 3; - Fe^{2+}: 45 mg L^{-1}; - H_2O_2: 500 mg L^{-1}.	No reduction in terms of MP removal from WW and mineralization was observed, in comparison to the solution prepared in DI.	[54]
Fenton	51 MPs ng L^{-1} - µg L^{-1} levels	- WW effluent 1 (pH ≈ 7, DOC 3-5 mg L^{-1}; COD 25 mg L^{-1}; BOD_5 < 5 mg L^{-1}; TN 20-30 mg L^{-1}; TP 10-14 mg L^{-1}; TSS 35 mg L^{-1}; (49-51 MPs detected up to 3770 ng L^{-1}), Mexico; - WW effluent 2 (pH ≈ 7, DOC 2-4 mg L^{-1}; COD 20-35 mg L^{-1}; BOD_5 < 5 mg L^{-1} TN 6-8 mg L^{-1}; TP 4-10 mg L^{-1}; TSS 9 mg L^{-1}; 11-16 MPs detected up to 210 ng L^{-1}), Mexico.	- Jar Test stirred at 220 rpm during 2 min, followed by slow stirring at 20 rpm during 10 min, and a final step of settling during 60 min; - Natural pH; - Fe(II): 30 mg L^{-1}; - H_2O_2: 25 mg L^{-1}.	The use of Fenton as post-treatment of secondary effluents from WWTPs increased the removal efficiencies of various contaminants up to 100%, but some compounds such as metformin (44%) and dehydronifedipine (29-71%, depending on the effluent), were not completely removed. The Fenton process was more efficient to treat the WW effluent 2, since WW effluent 1 had a higher content of the main chemical parameters and MPs analysed.	[55]
Fenton	E1, E2, EE2, carbamazepine, triclosan and acetylsalicylic acid ng L^{-1} to µg L^{-1} levels	- WW effluents from 3 different locations; United Kingdom.	- Continuous stir tank reactor (31.34 dm^{-3}) containing the modified polyacrylonitrile (PAN) catalyst, corresponding to 1.31 moles of iron catalyst; - Residence time 3 h; - Flow rate 10.6 L h^{-1}; - H_2O_2 mass flow rate 4.7 mg min^{-1};	A modified PAN catalyst system was effective in the removal of the target pollutants in WW, at ambient temperature and natural pH: > 80% of the estrogens were removed; > 84% of triclosan; 46-84.5% of carbamazepine; depending on the sampling location and consequent different characteristics of the WW effluents.	[56]

			- Room temperature; natural pH.		
UV/H_2O_2 **Photo-Fenton**	Gabapentin, metformin, metoprolol, atenolol, clarithromycin, primidone, methylbenzotriazole, and benzotriazole 2 µM	- UPW; - Lake water (pH 8.02; TOC 2.96 mg L^{-1}; conductivity 285 µS cm^{-1}; Cl^- 12.39 mg L^{-1}; NO_3^- 2.26 mg L^{-1}; SO_4^{2-} 47.07 mg L^{-1}; NH_4^+ 0.19 mg L^{-1}); - WW effluents (pH 7.47; TOC 9.31 mg L^{-1}; conductivity 1068 µS cm^{-1}; Cl^- 156.8 mg L^{-1}: NO_3^- 69.65 mg L^{-1}; SO_4^{2-} 63.47 mg L^{-1}; NH_4^+ 4.91 mg L^{-1}), Lausanne, Switzerland.	- UVC light LP Hg lamp ((λ_{max} 365 nm); - Solar UV-simulator: irradiation source 1.8 kW Xe lamp; - Fe(II): 30 µM; - H_2O_2: 300 µM.	The lower removal was observed in WWTP effluents and lake water, which was suggested to be due to light absorption at 253.7 nm and competition for $HO^{\bullet}$ by scavengers occurring in water (e.g., CO_3^{2-}, Cl^-, or humic-like substances). The high Cl^- content in the WWTP effluent was suggested to originate coordinating effect over ferric ions.	[57]

Abbreviations: BOD, biochemical oxygen demand; COD, chemical oxygen demand; CPC, compound parabolic concentrator; DI, distilled water; DO, dissolved oxygen; DW, drinking water; E1, estrone; E2, 17-beta-estradiol; EE2, 17-alpha-ethinylestradiol; EDDS, ethylenediamine-N,N′-disuccinic acid; GW, groundwater; HA, humic acids, IC, inorganic carbon; MP, micropollutants; NTU, nephelometric turbidity unit; PAN, polyacrylonitrile; PS, persulphate; SS, suspended solids; SW, surface water; SWW, synthetic wastewater; TC, total carbon; TDS, total dissolved solids; TOC, total organic carbon; TSS, total suspended solids; UPW, ultrapure water; WW, wastewater; WWTP, wastewater treatment plant.

Table S4. Matrix effects occurring in studies dealing with photocatalysis, published since 2005. Unless otherwise stated, the experimental conditions refer to the tested conditions for the evaluation of matrix effects.

AOT	Target pollutant Concentration	Matrices	Experimental conditions	Main conclusions	Reference
Photocatalysis	Diclofenac 5–20 mg L^{-1}	- DI; - GW (characterization not provided), Cyprus; - WW effluent (characterization not provided), Cyprus.	- Immersion well reactor; - V 350 mL; - T 23 °C; pH 6; - Irradiation source: 9 W UV-A lamp (350–400 nm); - TiO_2:TOC ratio: 79 (GW) and 32 (WW); - H_2O_2:TOC ratio: 0.8 (GW) and 0 (WW).	UV-A/TiO_2 was efficient for the degradation and mineralization of diclofenac in treated municipal effluents. NOM and other species present in the effluent reduced the degradation in comparison with DI. The effect of water matrix on mineralization was negligible since the TOC reduction was 45±5% regardless the matrix and the addition or not of H_2O_2. TOC analysis showed that macromolecules (e.g., humic and fulvic acids, biopolymers) were stable to the AOT.	[32]
Photocatalysis	Clofibric acid 1 mg L^{-1}	- DI; - WW effluent (pH 7.54; conductivity 818 µS cm^{-1}; TOC 27.1mg L^{-1}).	- 150 mL reaction cells; - Irradiation source: UV-A lamp (λ 365nm, 0.89 mW cm^{-2}); - Catalyst: 500 mg L^{-1} of Aeroxide P25 and P90 and titania–P25/silica particles; - Addition of inorganic (NaCl, $FeCl_3$, $FeCl_2$, $AlCl_3$, $CaCl_2$, $Al_2(SO_4)_3$, $Fe_2(SO_4)_3$, Na_2SO_4, $NaHCO_3$, and Na_2CO_3) or organic compounds (HA, surfactant).	Generally, the removal efficiency decreased by adding inorganic salts to UPW, especially SO_4^{2-} and CO_3^{2-} ions, which are good scavengers of ROS, leading to more than 70% of deactivation. Overall, the environmental waters led to a higher deactivation (> 90%).	[58]
Photocatalysis	Acetaminophen, antipyrine, atrazine, carbamazepine, diclofenac, flumequine, hydroxybiphenyl, ibuprofen, isoproturon, ketorolac, ofloxacin, progesterone, sulfamethoxazole, triclosan 100 µg L^{-1}	- Simulated water; - SWW; - WW effluent (DOC 13 mg L^{-1}), Almería, Spain.	- CPC solar pilot plant; - Catalyst: TiO_2 immobilized on a glass substrate; - Natural pH.	MPs were removed using immobilized TiO_2 under solar irradiation in the following order of efficiency removal: simulated water > simulated WW > WW effluent. The photocatalyst remained active even after five cycles of reuse and degraded most of the MPs in the actual WW, however the time required was longer.	[59]

Photocatalysis **UV/H_2O_2**	Alprazolam, clonazepam, diazepam, lorazepam, and Carbamazepine 100 µg L^{-1}	- UPW; - WW effluent (pH 7.55; COD 37.2 mg L^{-1}; IC 3.72 mg L^{-1}; TOC 37.14 mg L^{-1}; N_{total} 17.18 mg L^{-1}; conductivity 506.0 µS cm^{-3}; turbidity 11.13 NTU; DO 6.1 mg L^{-1}; alkalinity 133.0 mg L^{-1}; TS 281.0 mg L^{-1}; VSS 121.0 mg L^{-1}; Total fixed solids 160.0 mg L^{-1}; Cl^- 54.3 mg L^{-1}; NO_3^- 1.8 mg L^{-1}; F^- 0.6 mg L^{-1}; PO_4^{3-} 26.4 mg L^{-1}; SO_4^{2-} 28.4 mg L^{-1}), Rio de Janeiro, Brazil.	- Batch magnetically stirred reactor (500 mL); -Irradiation source: Polychromatic high pressure 125 W mercury vapor lamp (λ_{max} = 365nm) and solar radiation; - Catalyst: 0.1, 0.05, and 0.005 g L^{-1} TiO_2; - H_2O_2: 250, 200, 100, 50, 25, and 10 mg L^{-1}.	A strong matrix effect was found when WW effluents were used, with a decrease in efficiency of approximately 50%. This effect might be due to the presence of radical scavenger species such as, DOC, CO_3^{2-} and anions. These species can also absorb UV light decreasing the activation of TiO_2 and H_2O_2. Moreover, anions can compete for the absorption site on the catalyst.	[60]
Photocatalysis	Propyl paraben 420 µg L^{-1}	- UPW (pH 6, , conductivity 0.56 µS cm^{-1}); - Bottled water (pH 7.5, conductivity 396 µS cm^{-1}, HCO_3^- 15 mg L^{-1}, SO_4^{2-} 15 mg L^{-1}, Cl^- 9.8 mg L^{-1}); - River water (pH 7.5, conductivity 491 µS cm^{-1}, TOC 2.7 mg L-1, SO_4^{2-} 274 mg L^{-1}, Cl^- 5 mg L^{-1}), Athens, Greece; - Diluted WW (50% water); - WW effluent (pH 8, TOC 7 mg L^{-1}, TSS 1.1 mg L^{-1}, COD 21 mg L^{-1}, conductivity 311 µS cm^{-1}, SO_4^{2-} 30 mg L^{-1}, Cl^- 0.44 mg L^{-1}), Patras, Greece.	- Glass cylindrical vessel (120 mL); - Catalyst: 500 mg L^{-1} of Al-doped TiO_2; - Solar simulator equipped with a 100 W xenon ozone-free lamp.	Water matrix played a considerable role on the degradation efficiency, decreasing with an increase of water matrix complexity. HA decreased greatly the degradation of propyl paraben, since it has high light absorbing capacity and can also occupy the active sites of the catalyst. Other organics can also compete for oxidizing species. A slightly negative effect was found for HCO_3^- and Cl^-. Moreover, the performance was enhanced in the presence of persulfate.	[61]
Photocatalysis	Diclofenac, naproxen, iopamidol, imidacloprid, bisphenol A and 2,4 dichlorophenol 2 mg L^{-1}	- UPW; - WW effluent (pH 6.5, COD 35 mg L^{-1}), Italy.	- Pyrex glass cells (5 mL); - ZnO based materials and enzyme hybrid materials (1 g L^{-1}); - Irradiation source: 40 Watt Philips TLK/05 lamp (λ_{max} = 365 nm); - Soybean peroxidase (1 × 10^{-8} M); - H_2O_2: 1 × 10^{-4} M.	A complete removal of all studied compounds was found for both matrices, however a loss of efficiency was found when using WW, mainly due to the presence of DOM and inorganic ions.	[62]
Photocatalysis	E1 1000 µg L^{-1}	- UPW; - SWW (pH 7.41; conductivity 56.3 µS cm^{-1}; DOC 5.40 mg L^{-1}; IC 3.71 mg L^{-1}; COD 23.6 mg L^{-1}; alkalinity 6.0 mg $CaCO_3$ L^{-1}; Cl^- 1.47 mg L^{-1}; SO_4^{2-} 6.95 mg L^{-1}; PO_4^{3-} 3.82 mg L^{-1}; NO_3^- 0.34 mg L^{-1}; NO_2^- 0.04 mg L^{-1}; Br^- 0.65 mg L^{-1}). - WW effluent (pH 7.55, conductivity 621 µS cm^{-1}; DOC 8.04 mg L^{-1}; IC 39.23 mg L^{-1}; COD 26.2 mg L^{-1}; alkalinity 27.5 mg $CaCO_3$ L^{-1}; Cl^- 32.68 mg L^{-1}; SO_4^{2-} 33.03 mg L^{-1}; PO_4^{3-} 0.21 mg L^{-1}; NO_3^- 36.30 mg L^{-1}; NO_2^- n.d.; Br^- 0.54 mg L^{-1}), Sidney.	- 11W UV LED (λ = 365 410 or 523 nm) placed 5 cm above the liquid surface of the reactor; - 500 mL; - 50 mg L^{-1} of catalyst (gold-modified TiO_2 (Au-TiO_2) or TiO_2 P25).	The Au-TiO_2 catalyst showed better photocatalytic activity than P25 TiO_2, for all the water matrices under all light sources. The removal rate of E1 decreased in the order: ultrapure > synthetic water ≈ WW. The differences between UPW and actual matrices were attributed to the NOM whereas the lower removal in WW was ascribed to the higher content of anions in comparison to synthetic water.	[63]
Photocatalysis	Bisphenol A, EE2 100-300 µg L^{-1}	- UPW; - WW effluent (pH 8; conductivity 820µS cm^{-1}; DOC 7.8 mg L^{-1}; COD 24 mg L^{-1}; Cl^- 220 mg L^{-1}; SO_4^{2-} 60 mg L^{-1};	- 150 mL reaction cells filled with 60 mL; - 150 W xenon lamp (solar radiation simulator: 5% UV-A radiation, 0.1% UV-	Degradation in WW was estimated as one order of magnitude lower than those obtained for UPW, which was attributed to the scavenging of $HO^•$ by	[64]

		HCO_3^- 188 mg L^{-1}; NO_3^- 26 mg L^{-1}; NO_2^- 57 mg L^{-1}), Greece.	B radiation, equipped with a 280 nm cut-off); - Incident photon flux 58 × 10^{-8} einstein $L^{-1}s^{-1}$; - [0.5% Pt/TiO_2] = 500 mg L^{-1} (ten titania catalysts were synthesized, characterized and tested); - T 25 °C; Matrix inherent pH (i.e., ca. 8 for WW and 6.2 for UPW).	inorganic anions present in WW and also to the NOM that could compete with the spiked contaminants for oxidizing species.	
Photocatalysis	Bisphenol A 100 µg L^{-1}	- DI; - Synthetic freshwater (pH 7.58; TOC 3.4 mg L^{-1}; conductivity 241 µS cm^{-1}; Na^+ 1.09 mM; Ca^{2+} 0.34 mM; Mg^{2+} 0.44 mM; K^+ 0.07 mM; Cl^- 0.06 mM; SO_4^{2-} 1.18 mM); - SWW secondary effluent (pH 7.75; TOC 17.76 mg L^{-1}; conductivity 301 µS cm^{-1}; Na^+ 1.23 mM; Ca^{2+} 0.34 mM; Mg^{2+} 0.45 mM; K^+ 0.17 mM; NH_4^+ 0.32 mM; PO_4^{3-} 0.03 mM; Cl^- 0.04 mM; SO_4^{2-} 1.38 mM); - Real municipal WWTP secondary effluent (pH 8.54; TOC 24.0 mg L^{-1}; conductivity 564 µS cm^{-1}; Na^+ 22.3 mM; Ca^{2+} 65.6 mM; Mg^{2+} 4.82 mM; K^+ 0.68 mM; NH_4^+ 1.38 mM; PO_4^{3-} 12.92 mM; Cl^- 13.0 mM; SO_4^{2-} 1.85 mM), Almeria, Spain.	- CPC solar pilot plant; - Catalyst: TiO_2 immobilized in glass spheres (~0.6 mg of TiO_2 was supported on the surface of each glass sphere);	Water matrix affected drastically the photocatalytic degradation of bisphenol A, remaining in water approximately 30%. This results could be explained by the presence of substances, such as, organics, CO_3^{2-} and Cl^- in the matrix, acting as radical scavengers.	[65]
Photocatalysis	Amoxicillin (10 mg L^{-1}), carbamazepine (5 mg L^{-1}), diclofenac (2.5 mg L^{-1})	- DI; - WW effluent (pH 8.1; TOC 4.51 mg L^{-1}; BOD_5 10 mg L^{-1}; TSS 11 mg L^{-1}), Italy.	- 125 W black-light fluorescent lamp (300–420 nm); - Catalyst: 0.2–0.8 g L^{-1} of TiO_2.	The half-life of diclofenac was lower than that of carbamazepine. The mineralization of the spiked urban WW was lower than that of the spiked DI due to interference of scavengers (e.g., CO_3^{2-}) and other oxidizable compounds, typically occurring in WWs.	[66]
Photocatalysis	EE2 100 µg L^{-1}	- UPW - DW (pH 7.9; conductivity 5.5 µS cm^{-1}; HCO_3^- 152 mg L^{-1}); - WW effluent (pH 8.0; COD 24 mg L^{-1}; DOC 8.4 mg L^{-1}; conductivity 820 µS cm^{-1} ; Cl^- 172 mg L^{-1}; NO_3^- 37 mg L^{-1}; NO_2^- 37 mg L^{-1}; SO_4^{2-} 54 mg L^{-1}; HCO_3^- 194 mg L^{-1}).	- Immersion well, batch type, lab scale photoreactor; - Irradiation source: 9 W UV-A lamp (350–400 nm); - Catalyst load: 750 mg L^{-1} of TiO_2.	Water matrix showed a negative effect on conversion and reaction rate. To achieve a complete removal of EE2 in WW, the treatment was three times longer in comparison with UPW and twice longer the needed for WW diluted with an equal volume of UPW, mainly due to the reactions involving the residual organic fraction present in WW and oxidizing agents. Moreover, HCO_3^-, Cl^- and SO_4^{2-} present in WW and DW can act as scavengers of $HO^\bullet$. Similar removal values to those obtained for diluted WW were found for DW samples.	[67]

Photocatalysis	EE2 100 µg L^{-1}	- UPW (pH 6.1; conductivity 5.5 µS cm^{-1}) - DW (pH 7.9; conductivity 308 µS cm^{-1}; HCO_3^- 152 mg L^{-1}); - WW effluent (pH 7.5, COD 24 mg L^{-1}, DOC 8.4 mg L^{-1}; conductivity 810 µS cm^{-1}; NO_3^- 37 mg L^{-1}; NO_2^- 37 mg L^{-1}; Cl^- 172 mg L^{-1}; SO_4^{2-} 54 mg L^{-1}; HCO_3^- 194 mg L^{-1}), W. Crete, Greece; - Diluted WW effluent.	- Cylindrical glass cell with a useful volume of 300 ml; - Solar irradiation simulator (5% UV-A radiation and 0.1% UV-B radiation) equipped with a 150 W xenon ozone-free lamp and an AirMass 1.5 Global Filter; - Catalyst load: 250 mg L^{-1} of TiO_2.	Solar-driven heterogeneous photocatalysis was efficient on the removal of estrogen hormones in distinct water matrices. However, the removal efficiency decreased in the following order: UPW > DW > diluted WW > WW. The organic and inorganic constituents typically found in WW and DW impeded degradation presumably due to the scavenging of oxidizing species. Moreover, the presence of HA affected in a greater extent the removal efficiency in comparison to a mixture of anions in UPW experiments.	[68]
Photocatalysis	EE2 100–500 µg L^{-1}	- UPW; - WW effluent (pH 8; DOC 7.8 mg L^{-1}; COD 24 mg L^{-1}; Cl^- 220 mg L^{-1}; SO_4^{2-} 60 mg L^{-1}; HCO_3^- 188 mg L^{-1}; conductivity 820 µS cm^{-1}), Greece.	- Cylindrical Pyrex cell with a useful volume of 300 ml; - Solar irradiation simulator (5% UV-A radiation and 0.1% UV-B radiation) equipped with a 150 W xenon ozone-free lamp and an AirMass 1.5 Global Filter; - Catalyst load: 50–500 mg L^{-1} ZnO.	Among the five different operating variables, the water matrix was the only with a negative effect on the removal efficiency. Since usually estrogens are found in WW effluents, water matrix can have an important role on their treatment, mainly by the presence of organic and inorganic matter. Furthermore, $HO^\bullet$ may be scavenged by HCO_3^-, Cl^- and SO_4^{2-} present in WW.	[69]
Photocatalysis	Ibuprofen 6 µg L^{-1} 6, 60, 213 mg L^{-1}	- UPW; - WW effluent (pH 7.3; DOC 215 mg L^{-1}; conductivity 610 µS cm^{-1}; Cl^- 58 mg L^{-1}; SO_4^{2-} 34 mg L^{-1}; NO_3^- 19 mg L^{-1}; NO_2^- 30 mg L^{-1}; PO_4^{3-} 7 mg L^{-1}; Na^+ 40 mg L^{-1}; NH_4^+ 22 mg L^{-1}; K^+ 10 mg L^{-1}; Ca^{2+} 21 mg L^{-1}); Portugal. - Pharmaceutical WW (pH 7.9; DOC 170 mg L^{-1}; conductivity 3770 µS cm^{-1}; Cl^- 978 mg L^{-1}; SO_4^{2-} 661 mg L^{-1}; Na^+ 310 mg L^{-1}; Mg^{2+} 27 mg L^{-1}), Sfax, Tunisia.	- Spiked WW and UPW (250 mL): Photoreactor equipped with four 10 W UV high intensity LEDs (λ_{max} 382 nm); - Catalyst load: 0.5, 1.0, 1.5 g L^{-1} TiO_2; - Pharmaceutical WW and WW effluent (7.5 mL): Quartz cylindrical reactor equipped with a single LED; - Catalyst load: 0.5, 1.0, 2.0, 2.5, 3.0, 4.0 g L^{-1} TiO_2.	Lower ibuprofen removals were found when treating WW effluents and pharmaceutical WW in comparison to UPW. Moreover, ibuprofen was more difficult to be removed in the case of WW effluent mainly due to the higher DOC, NO_2^-, NO_3^- and PO_4^{3-}.	[70]

Photocatalysis	Tetracycline 55 mg L^{-1}	- UPW (pH 6.6; DOC 8.4 mg L^{-1}; conductivity 0.067 µS cm^{-1}; transmittance (at 254 nm) 100%); - DW (pH 7.8; conductivity 334 µS cm^{-1}; Cl^- 5.8 mg L^{-1}; NO_3^- <5 mg L^{-1}; NO_2^- <0.1 mg L^{-1}; SO_4^{2-} 47 mg L^{-1}; HCO_3^- 63 mg L^{-1}; Ca^{2+} 68 mg L^{-1}; Mg^{2+} 11.5 mg L^{-1}; transmittance (at 254 nm) 97.6%); - WW effluent (pH 8; conductivity 855 µS cm^{-1}; COD 24 mg L^{-1};Cl^- 92 mg L^{-1}; NO_3^- 23 mg L^{-1}; NO_2^- 48 mg L^{-1}; SO_4^{2-} 74 mg L^{-1}; HCO_3^- 156 mg L^{-1}; Ca^{2+} 88 mg L^{-1}; Mg^{2+} 54 mg L^{-1}; transmittance (at 254 nm) 61.6%).	- Photocatalytic reactor (500 mL); - Irradiation source: 18 W lamp emitting at 254 nm; - Catalyst load: 1 g L^{-1} of TiO_2.	The removal efficiency of tetracycline was higher in DW in comparison with UPW, which could be explained by the presence of dissolved organic matter acting as photosensitizer with the generation of reactive species. However, the removal decreased when WW was used as matrix. The organic matter could act as a filter for UV radiation and $HO^{\bullet}$ can be scavenged by the high concentration of HCO_3^- and Cl^- present in the WW effluent.	[71]
Photocatalysis	Azo dye congo red, carbamazepine 10 mg L^{-1}	- DI; - Saline water (pH 7.5; conductivity 1300 818 µS cm^{-1}, NaCl 1 g L^{-1}, KH_2PO_4 6 mg P L^{-1}); - WW effluent (pH 7.5; conductivity 1700 818 µS cm^{-1}, COD 30 mg L^{-1}; PO_4^{-3} 6 mg P L^{-1}; NO_3^- 30 mg N L^{-1}), collected from a lab-scale MBR system fed on real municipal primary effluent.	- Glass cylinder (1 L) photo-reactor, equipped with an axial quartz tube holding the UV lamp; - Catalysts: Hydrogen titanate nanofiber and commercial TiO_2 (P25); - 8W lamp (λ 360nm).	The photocatalytic activity of both catalysts was similar in saline water and effluent, but the degradation of the target compounds had an opposite trend regarding the matrix effects. Matrix effect on the dark adsorption of congo red was higher in real effluents than in saline water, while carbamazepine had negligible adsorption, explained by the different polarity, which causes different adsorption and interaction with the catalyst surface. Anions affected slightly the removal rates, whereas calcium had a pronounced negative effect on the photocatalytic performance using nanofiber catalyst.	[72]
Photocatalysis	Acetaminophen, thiabendazole, imazalil, acetamiprid 100 µg L^{-1}	- DI; - Synthetic freshwater; - SWW; - WW effluent (pH 8.4; conductivity 2670 µS cm^{-1}, DOC 21.10 mg L^{-1}; IC 60.4 mg L^{-1}; Cl^- 12.9 mg L^{-1}; SO_4^{2-} 1.85 mg L^{-1}; Na^+ 23.0 mg L^{-1}; NH_4^+ 0.06 mg L^{-1}; K^+ 0.68 mg L^{-1}; Ca^{2+} 65.7 mg L^{-1}; Mg^{2+} 4.82 mg L^{-1}), Spain.	- CPC solar pilot plant; - Solar simulator equipped with a Xenon lamp and a 290 nm cut-off filter; - Catalyst: TiO_2-coated glass beads.	The matrix effect led to a reduction of degradation rate due to the presence of other substances in the matrix (organics, CO_3^{2-}, etc.), which can be adsorbed onto the catalyst surface (blocking and/or competing for reaction sites) and/or compete for $HO^{\bullet}$ in the bulk.	[73]

Photocatalysis	Metoprolol 50 mg L^{-1}	- UPW; - WW effluent (pH 7.56; TOC 18.8 mg C L^{-1}; COD 44.6 mg L^{-1}; BOD_5 8.4 mg L^{-1}; UV_{254} 0.235 cm^{-1}; turbidity 10.4 NTU; alkalinity 471 mg $CaCO_3$ L^{-1}; TSS 18.8 mg L^{-1}; VSS 14.6 mg L^{-1}; Cl^- 745 mg L^{-1}; NO_3^- 3.0 mg L^{-1}; NO_2^- n.d.; PO_4^{3-} 15 mg L^{-1}; SO_4^{2-} 232 mg L^{-1}; NH_4^+ 57.1 mg L^{-1}; Na^+ 495 mg L^{-1}; K^+ 45.9 mg L^{-1}; Ca^{2+} 138 mg L^{-1}; Mg^{2+} 59.6 mg L^{-1}), Spain.	- Solar simulator equipped with a Xenon lamp and an optical filter (cut-off < 280 nm); - Photon flux 2.99×10^{-6} Einstein s^{-1} (290–400 nm); Duran tubular photoreactor (24 cm length, 2.11 cm diameter, 0.078 L illuminated volume) placed at the bottom of the solarbox in the axis of a parabolic mirror; Recirculation at a flow rate of 0.65 L min^{-1}; - Catalyst: boron-modified TiO_2 (5% w/w of B); - V 1.0 L; T 25 °C.	The optimal photocatalyst concentration was higher in WW due to the competition of organic matter for active species generated and for adsorption in the photocatalyst surface. Inorganic ions may also interfere, by deactivation of the catalyst surface.	[74]
Photocatalysis	Carbamazepine 5 mg L^{-1}	- WW effluent from a lab-scale MBR used to treat primary WWs from a WWTP (COD 13.5-22 mg L^{-1}; PO_4^{3-} 21.7-23.8 mg L^{-1}; NO_3^- 210-238 mg L^{-1}), South Australia	- Sequential batch annular slurry photoreactor; - Low-intensity (11 W) UV-C lamp; - Catalysts: immobilized TiO_2, namely anatase titanate nanofiber and mesoporous TiO_2 impregnated kaolinite; - Presence of effluent organic matter and inorganic ions.	The sequential batch annular slurry photoreactor system was successfully applied for the elimination of carbamazepine from WW, but high molecular weight effluent organic matter competed for the photocatalytic reaction. The presence of inorganic ions interfered with the surface fouling of immobilized photocatalysts, reducing their photoactivity.	[75]
Photocatalysis	Ofloxacin, atenolol 10 mg L^{-1}	- UPW; - GW; - WW effluent (pH 8.22; TOC 11 mg L^{-1}; COD 6 mg L^{-1}; turbidity 1.9 NTU; conductivity 1424 µS cm^{-1}; TSS 4.5 mg L^{-1}; N_{total} 3.7 mg L^{-1}; P_{total} 2.96 mg L^{-1}; N-NH_4^+ 0.16 mg L^{-1}; Cl^- 196 mg L^-), Cyprus.	- 9W lamp emitting predominantly at 350–400 nm; -Catalyst: 0.25 g L^{-1} of TiO_2.	The extent of mineralization followed the decreasing order: UPW > GW > WW. This could be attributed to the corresponding TOC increment and other species present in the actual matrices, which are able to scavenge radicals or other reactive moieties.	[76]
Photocatalysis	Diclofenac, fluoxetine mg L^{-1} levels	- DI; - WW effluent (pH 6.15; TOC 5.15 mg L^{-1}; DOC 4.65 mg L^{-1}; SS 11 mg L^{-1}), Portugal.	- XX-15 BLB UV lamp (λ 365 nm), - Catalysts: Single-phase Hydroxyapatite (HAp) and HAp-titania (TiHAp) materials (1 wt% TiO_2); - DI: spiked with 2-8 mg L^{-1}; catalyst load between 1 and 4 g L^{-1}; Effluents: spiked with 5 mg L^{-1} of both contaminants; 4 g L^{-1} of TiHAp.	The HAp-titania photocatalyst was effective when using actual treated WW, but the removal efficiency decreased by 20% for diclofenac and by 4% for fluoxetine, probably due to the suspended solids present in the WW. The degradation rate using centrifuged WW was comparable to that observed in DI.	[77]
Photocatalysis	Sulfamethoxazole 10 mg L^{-1}	- UPW; - GW; - WW effluent (pH 8.22; TOC 11 mg L^{-1}; COD 6 mg L^{-1}; turbidity 1.9 NTU; conductivity 1424 µS cm^{-1}; TSS 4.5 mg L^{-1}; N_{total} 3.7 mg L^{-1}; P_{total} 2.96 mg L^{-1}; N-NH_4^+ 0.16 mg L^{-1}; Cl^- 196 mg L^-), Cyprus.	- 9W lamp emitting predominantly at 350–400 nm; -Catalyst: 0.5 g L^{-1} of TiO_2.	The degradation was favoured at acidic pH. Comparing to UPW, the matrix effects on degradation were negligible, even for WW with high TOC and GW with high content of HCO_3^-, both known scavengers of radicals. At near-neutral pH, the	[78]

				presence of co-existing substances in environmental samples slightly affected the degradation of the pharmaceutical, suggesting that the ionic strengths of both environmental matrices had a role on promoting the agglomeration of TiO_2 particles, decreasing the effective surface area.	
Photocatalysis	Sulfonamides (sulfathiazole, sulfamethoxazole, sulfadiazine) 5 mg L^{-1}	- DI; - Influents (with and without preliminary filtration and coagulation); - WW effluents (pH 7.10-7.66; conductivity 1204-1722 µS cm^{-1}; COD 137-774 mg L^{-1}; BOD_5 60-89 mg L^{-1}; turbidity 4-50), Poland.	- 4 UV lamps emitting at λ_{max} 366 nm; -Catalyst: 0.5 g L^{-1} of TiO_2 and/or 1 mM of $FeCl_3$; - pH 3.	The optimum photocatalytic system was $TiO_2/FeCl_3$ under acid pH. The degradation rate was significantly lower in WW than in DI. Similar results were obtained using the model WW. Preliminary microfiltration and coagulation of the influents did not improved the photocatalytic efficiency, in comparison to untreated influents.	[79]
Photocatalysis	Carbamazepine 133 ng L^{-1}	- Deionized water; - WW effluent from a sequential batch reactor (SBR) activated sludge process with phosphate precipitation by Fe^{3+} (pH 7.7; TOC 10 mg L^{-1}, electrical conductivity 803 µmho cm^{-1}; IC 26.3 mg L^{-1}; alkalinity 139 mg $CaCO_3$ L^{-1})	- Temperature: between 21 and 25 °C; - Catalyst: 100 mg L^{-1} of TiO_2; - pH 7.3; - Presence and absence of powdered activated carbon.	The photocatalytic efficiency was matrix and pH dependent. Carbamazepine present in the WW (pH 7.3) was not completely removed by photocatalysis with a UV dose of about 6 kJ L^{-1}. In contrast, spiking carbamazepine at 10 mg L^{-1} in deionized water and in acidic effluent led to an efficient removal with the same UV dose. Under alkaline conditions, the UV dose needed for the same removal from the spiked effluent was 10 times higher.	[80]
Photocatalysis	Diclofenac, carbamazepine, ibuprofen and propranolol 5 mg L^{-1}	- DI; - WW effluent (pH 7.3; DOC 12.2 mg L^{-1}; COD 35.2 mg L^{-1}; BOD_5 6 mg L^{-1}; Cl^- 49.5 mg L^{-1}; SO_4^{2-} 24.4 mg L^{-1}; NO_3^- 4.5 mg L^{-1}; TN 7.2 mg L^{-1}; TP 0.55 mg L^{-1}), The Netherlands.	- Simulated solar irradiation (96 h): Xenon high-intensity discharge lamps (55 W) emitting at λ range of 300–800 nm; - Stirring at 75 rpm; - Catalyst: 25 g of immobilized TiO_2.	Photolysis efficiency was enhanced by the DOM present in WW effluent, organic matter, which might absorb light to excite triplet states of DOM ($^3DOM^*$) and further to reactive radicals. NO_3^- could also play a role by adsorption of light < 350 nm and production of $HO^•$, accelerating the indirect photolysis. Photocatalysis led to superior removal efficiencies for all pharmaceuticals. However, carbamazepine and ibuprofen were degraded at less extent in WW, probably due a proposed partial or selective reduction of the oxidized intermediates back to parent compounds.	[81]

Photocatalysis	Carbamazepine, gabapentin, lamotrigine, oxcarbazepine, venlafaxine, bisoprolol, celiprolol, talinolol, bezafibrate, tramadol, candesartan, eprosartan, irbesartan and valsartan 0.35-11.30 µg L^{-1}levels	- UPW; - WW effluent (pH 7.5; COD 37 mg L^{-1}; BOD_5 4 mg L^{-1}; TN 12.0 mg L^{-1}; NO_3^- 7.4 mg L^{-1}; NO_2^- 0.03 mg L^{-1}; NH_4^+ 0.31 mg L^{-1}; TP 0.86 mg L^{-1}; PO_4^{3-} 0.56 mg L^{-1}), Dresden, Germany.	- UVA radiation: six 8W Hg fluorescent tubes (365 nm); - Catalyst load: 1 g L^{-1} of TiO_2 P25 or ZnO.	UVA/TiO_2 and UVA/ZnO systems led to a significant degradation of the analysed pharmaceuticals and in the particular case of carbamazepine, for which the matrix effect was also studied. Similar results were obtained when comparing UPW and WW for each photocatalytic system, but ZnO nanoparticles showed a better performance.	[82]
Photocatalysis–DCMD (direct contact membrane distillation)	Diclofenac, naproxen and ibuprofen 100 µg L^{-1}	- UPW; - DW; - Primary WW effluents; - Secondary WW effluents, Poland.	- Photoreactor equipped with an UV-C germicidal lamp (λ_{max} 254 nm) located between a feed tank and a membrane module; - Catalyst load: 0.5 g L^{-1} of TiO_2; - DCDM: hydrophobic polypropylene membranes, with an area of 0.014 m^2 and nominal pore size of 0.2 µm; - Feed and distillate solution temperatures: 60 and 20 °C.	A PMR using DCMD and UV-C radiation was applied to WWTP effluents. In general the removal efficiency by the hybrid process was in the following decreasing order, except for diclofenac: UPW > tap water > secondary effluent > primary effluent. Diclofenac was faster removed in the primary vs secondary effluents, possibly due to adsorption of the drug on the suspended matter present in the WW.	[83]
Photocatalysis	Carbamazepine 50 µM	- DW; - WW effluents.	- Carbamazepine/peroxymonosulphate (PMS) molar ratio: from 1 to 30; - Cobalt salts tested: $CoCl_2.6H_2O$ and $Co(NO_3)_2.6H_2O$.	Sulphate radical yielded a faster degradation of carbamazepine compared to $HO^•$, in both real and DI. The WW matrix had an important effect on the inhibition of degradation by both PMS/Co(II) and Fenton systems. The Cl^- ions were involved in the inhibition effect, but the organic matter could also affect the oxidation kinetic decrease.	[84]
Photocatalysis	Diatrizoate (744±28 µg L^{-1}), acetaminophen (736±36 µg L^{-1}), carbamazepine (738±31 µg L^{-1}), atenolol (757±67 µg L^{-1})	- WW effluent (pH 7.7±0.3; conductivity 1.3±0.2 mS cm^{-1}; DOC 6±2 mg L^{-1}; COD 18±6 mg L^{-1}; BOD_5 3.4±1.7 mg L^{-1}; UV_{254} 15±3 m^{-1}; Cl^- 267±35 mg L^{-1}; SO_4^{2-} 89±13 mg L^{-1}; NO_3^- 7±3 mg L^{-1}; NO_2^- 0.08±0.06 mg L^{-1}; HCO_3^- 259±64 mg L^{-1}; Na^+ 152±14 mg L^{-1}; Ca^{2+} 160±17 mg L^{-1}; Mg^{2+} 6.6±0.8 mg L^{-1}; K^+ 22±3 mg L^{-1}), France.	- Modular tube reactor; - Irradiation source: UV-A lamp (λ 365 nm, 3-40 W_{UV} m^{-2}); - Recirculation flow rate: 1.5 L min^{-1}; - Catalyst: 2 g L^{-1} TiO_2.	Organic matter, phosphate and bicarbonate ions affected negatively the process efficiency by $HO^•$ scavenging. Consequently, the kinetic constant of mineralization decreased. Degradation of target compounds ranged from 20% to 80%, decreasing for higher volumetric reduction factor.	[85]
Photocatalysis (TiO_2 and persulfate	Trimethoprim 1 mg L^{-1}	- WW effluent (pH 7.30; conductivity 2.15 mS cm^{-1}; turbidity 4.2 NTU; TOC 13.9 mg L^{-1}; IC 59.5 mg L^{-1}; Cl^- 477.4 mg L^{-1}; SO_4^{2-} 157.5 mg L^{-1}; NO_3^- 47 mg L^{-1}; Na^+ 269.5 mg L^{-1}; Ca^{2+} 81 mg L^{-1}; Mg^{2+} 54.4 mg L^{-1}; NH_4^+ 25.1 mg L^{-1}). - Natural water (pH 7.55; conductivity 1.1 mS cm^{-1}; TOC 2.6 mg L^{-1}; IC 89.4 mg L^{-1}; Cl^- 148 mg L^{-1}; SO_4^{2-} 159.4	- CPC solar pilot plant; -V 39 L; - Catalyst: 200 mg L^{-1} TiO_2; - HA: 10 mg L^{-1}; - Sodium persulphate: 0.125-0.5 mM; - pH 4-7.5;	The removal occurred by the combination of heterogeneous photocatalysis, photolysis and persulphate oxidation. Trimethoprim degradation rate decreased as the complexity of the matrix increases. The addition of sodium persulphate	[86]

	mg L^{-1}; NO$_3^-$ 3 mg L^{-1}; Na$^+$ 231.2 mg L^{-1}; Ca^{2+} 24.7 mg L^{-1}; Mg^{2+} 26 mg L^{-1}); - Well water (pH 8.1; conductivity 2.4 mS cm^{-1}; TOC 5.2 mg L^{-1}; IC 179 mg L^{-1}; Cl$^-$ 296 mg L^{-1}; SO$_4^{2-}$ 319 mg L^{-1}; NO$_3^-$ 6 mg L^{-1}; Na$^+$ 462 mg L^{-1}; Ca^{2+} 49 mg L^{-1}; Mg^{2+} 52 mg L^{-1}).		reduced the effect of scavenger species (chloride, sulphate and bicarbonate). HA competes for reactive species in the reaction mixture.

Abbreviations: BOD$_5$, biochemical oxygen demand; COD, chemical oxygen demand; CPC, compound parabolic concentrator; DCMD, direct contact membrane distillation; DI, distilled water; DO, dissolved oxygen; DOC, dissolved organic carbon; DW, drinking water; E1, estrone; EE2, 17-alpha-ethinylestradiol; GW, groundwater; HA, humic acids, Hap, hydroxyapatite; IC, inorganic carbon; MP, micropollutants; NOM, natural organic matter; NTU, nephelometric turbidity unit; PMS, peroxymonosulphate; PMR, photocatalytic membrane reactor; SS, suspended solids; SW, surface water; SWW, synthetic wastewater; TOC, total organic carbon; TS, total solids; TSS, total suspended solids; UPW, ultrapure water; VSS, volatile suspended solids; WW, wastewater; WWTP, wastewater treatment plant.

Table S5. Matrix effects occurring in studies dealing with ozone-based processes, published since 2005. Unless otherwise stated, the experimental conditions refer to the tested conditions for the evaluation of matrix effects.

AOT	Target pollutant Concentration	Matrices	Experimental conditions	Main conclusions	Reference
O_3/H_2O_2	Atrazine, sulfamethoxazole, N-nitrosodimethylamine 0.5 – 11 μM	- 3 Lake waters, Switzerland and Norway; - WW effluent (DOM 3.9 mg C L^{-1}; alkalinity 6.5 mg $CaCO_3$ L^{-1}), Switzerland.	- 500 mL batch reactor; - T 20 °C; - pH 8.0; - Spiked O_3 stock solution; - Addition of H_2O_2 (2:1, O_3/H_2O_2) prior to O_3 addition.	The O_3 dose needed was higher for WW. The addition of H_2O_2 enhanced the removal and reduced bromate formation. Generally, the waters with lower DOM concentration and/or lower $HO^•$ scavenging rates had a higher transformation. The reactivity of DOM was different in waters with the same DOC concentration. The content on CO_3^{2-}/HCO_3^- led to an inhibitory effect of O_3 decay.	[13]
O_3	Hydrochlorothiazide 1 μM	- UPW; - SW from a public reservoir (pH 7.3; TOC 4.3 mg L^{-1}; alkalinity 30 mg $CaCO_3$ L^{-1}), Spain; - WW effluent (pH 8.0; TOC 23.3 mg L^{-1}; alkalinity 250 mg $CaCO_3$ L^{-1}), Spain.	- 500 mL flask reactor; - Spiked O_3 stock solution (concentration 0 – 10 mg L^{-1}); - T 20 °C.	Ozonation led to a removal rate of the compound in the following order: WW < SW < UPW. This fact is attributed to the dissolved organic matter (DOM) in the matrices under study, which could consume part of the oxidant. A lower O_3 dose was enough to eliminate the pharmaceutical from SW, in comparison to that required for WW.	[23]
UV **O_3** **O_3/UV** **Photocatalysis** **Catalytic ozonation** **Photocatalytic ozonation**	Diclofenac, sulfamethoxazole, caffeine 10 mg L^{-1}	- UPW; - WW effluent (pH 7-8; TOC 35 mg L^{-1}; IC 23 mg L^{-1}; COD 58-84 mg L^{-1}; BOD 30-60 mg L^{-1}), Spain.	- 1L tubular glass photoreactor (450 mm height, 80 mm diameter) filled with 900 mL of solution; - pH 7.0 (UPW); - Irradiation source: HP Heraeus Hg lamp (bandwidth range 238–579 nm with three λ_{max} emitting at 254, 313 and 366) immersed in a glass well placed at the middle of the reactor, UVB radiation was cut off; - TiO_2 concentration: 1.5 g L^{-1}; - O_3: inlet concentration 10 mg L^{-1} and flow rate 30 L h^{-1}.	Diclofenac elimination rate with UVA radiation was higher in WW than that in UPW, possibly due to some substance present in the effluent acting as photosensitizing agent. The removal rates of all compounds and TOC by the other AOTs were slightly slower in WW. For all the pharmaceuticals, no significant differences were verified on their removal by single O_3 with/without the presence of HCO_3^-/CO_3^{2-}, suggesting that direct attack by O_3 is the main mechanism.	[28]
O_3	Metoprolol, naproxen, amoxicillin, phenacetin 1 μM	- GW, Spain; - SW from a public reservoir, Spain; - 3 WW effluents (pH 7.8-8.1; TOC 13.2-23.3 mg L^{-1}; COD 28.2-49.7 mg L^{-1}; conductivity 637-905 μS cm^{-1}; alkalinity 93-325 mg $CaCO_3$ L^{-1}), Spain.	- Each run was initiated by injecting a variable volume of the O_3 stock solution to achieve a dose of O_3 varying between 0.5 and 5 mg L^{-1} for the secondary effluents, and between 0.1 and 2 mg L^{-1} for the natural waters; - T 20 °C; - pH 7 by using the phosphoric acid/phosphate buffer; - Initial concentrations of p-chlorobenzoic acid of 1.0 μM.	The removal of pharmaceuticals in the WW was lower than in the SW, which was in turn lower than in GW. The amount of dissolved organic matter present in each water explains this trend (COD and TOC: GW < SW < WW effluents). The organic matter content consumed part of the oxidant in competition with the pharmaceuticals.	[87]

UV **Photocatalysis (TiO_2 and persulphate (PS))** **Photo-Fenton** **UV/PS/Fe**	Acetamiprid 100 µg L^{-1}	- DI; - Synthetic WW; - WW effluent (pH 8.6; DOC 18.5 mg L^{-1}; IC 44 mg L^{-1}; COD 71 mg L^{-1}; NO_3^- 2.1 mg L^{-1}; NO_2^- 0.02 mg L^{-1}; PO_4^{3-} 4.1 mg L^{-1}; SO_4^{2-} 58 mg L^{-1}).	- Three 30W UV-C LP lamps (254 nm); - Catalysts: TiO_2 at 50, 100, 200 mg L^{-1} and persulphate at 25, 50, 100 mg L^{-1}; - H_2O_2: 25, 50, 100 mg L^{-1}; - pH natural (2.8 for UV/H_2O_2/Fe); - Effect of organic matter: addition of HA, lignin-derivative and lauryl sulphate.	All processes at neutral pH were able to effectively remove acetamiprid, being the photo-Fenton the most efficient for all water matrices. UV/PS and UV/PS/Fe systems also showed good efficiencies. The matrix effect retarded the removal rates, due to the high alkalinity and organic matter content of both synthetic and actual effluents. HA interfered with UV photolysis at high concentration due to the absorptivity of UV radiation. In turn, they had no impact on UV/H_2O_2/Fe and UV/PS/Fe processes. AOTs using iron probably originated Fe(II) complexes with lignin, acting as filter due to the high absorptivity. The lauryl sulphate did not promoted the formation such complexes at natural pH, leading to similar removal rates for all processes.	[88]
Photocatalysis **Photo-Fenton** **O_3/H_2O_2**	Carbamazepine, diclofenac 10-1000 µg L^{-1}	- DI; - WW effluent (pH 7.45; COD 119 mg L^{-1}; BOD 250 mg L^{-1}; N_{total} 30 mg L^{-1}; P_{total} 0.38 mg L^{-1}; SS 267 mg L^{-1}).	- T 25 °C and pH 7.0, except for photo-Fenton (pH 3.0); *Photo-Fenton* - Three 4 W near-UV-A (black light) fluorescent lamps with a radiation peak at 352 nm; - Fe^{2+}: 10 mg L^{-1}; - H_2O_2: 100 mg L^{-1}; *O_3/H_2O_2* - O_3: inlet concentration 0.36 mg L^{-1} and flow rate 3.0 L h^{-1}; - H_2O_2: 20 mg L^{-1}; *Heterogeneous photocatalysis* - TiO_2: 200 mg L^{-1}.	The order of the inhibition caused by matrix components was as follows: O_3/H_2O_2 > UV/TiO_2 > UV/H_2O_2/Fe. For UV/H_2O_2/Fe, the Fenton reaction was favoured by the presence of co-existing substances, possibly providing additional iron ions, while the photo-reduction was inhibited by the complex-forming reaction and/or light scattering. For UV/TiO_2, substances present in the matrix could inhibit the removal via scavenger effects, light scattering and adsorption. In the O_3/H_2O_2 process, the matrix affected the mass transfer of O_3 from the gas to the liquid phase, in addition to the scavenger effects on both $HO^•$ and dissolved O_3.	[16]
O_3	Tetrabromobisphenol 100 mg L^{-1}	- UPW spiked with anions and HA; - River water (pH 7.49; DOC 9.10 mg L^{-1}); - Raw WW (pH 7.74; DOC 45.31 mg L^{-1}); - WW effluent (pH 7.65; DOC 17.04 mg L^{-1}).	- 100 mL conical flasks filled with 50 mL of pollutant solution; - O_3 flow rate of 36 mL min^{-1}; - inlet O_3 concentration in the gas phase was measured as 140.6 mg L^{-1}; - Effect of inorganic ions (Cl^-, NO_3^-, HCO_3^-, SO_4^{2-}) at 0.5 and 5.0 mmol L^{-1}; - Effect of HA at 5.0 and 50.0 mg L^{-1}.	Tetrabromobisphenol A was completely removed after 6 min of ozonation at pH 8.0. The anions (Cl^-, NO_3^-, HCO_3^- and SO_4^{2-}) and HA did not significantly affect its degradation. Additionally, no significant difference in the abatement of the pollutant was found employing ozonation to treat the different water matrices. The little influence of WW components in the oxidation rate is probably due to the excessive O_3 and $HO^•$ in solution.	[89]
O_3	Flumequine 20 µg L^{-1}-20 mg L^{-1}	- UPW; - River water; - WW influent; - WW effluent (characterization not provided).	- 100 mL semi-batch glass reactor filled with 50 mL of solution stirred at 450 rpm; T 25 °C; - O_3 continuously bubbled into the reactor bottom at a constant flow rate (36 mL min^{-1}) through a glass tube (0.5m) with a sintered end; - Inlet O_3 concentration in the gas phase: 140.6 mg L^{-1};	The different ions and types of water (UPW, river water, WW influent and effluent) did not influenced the reaction efficiency significantly. However, the DOM extract composed by river sediment behaved as inhibitor and two DOM extracts, namely rice straw and pig manure, promoted the oxidation of the target pollutants	[90]

			- Effect of inorganic ions (Cl^-, SO_4^{2-}, HCO_3^-, K^+, Ca^{2+}, Mg^{2+}) or extracts of DOM (HA, rice straw, river sediment, pig manure).		
O_3 **O_3/H_2O_2**	Metoprolol, naproxen, amoxicillin, phenacetin 1 µM	- UPW; - 2 WW effluents.	- 500 mL cylindrical glass reactor; - T 25 °C; - Natural pH; - O_3: 16 mg h^{-1}.	For both processes, the removal rate was lower in the WW effluents than in UPW, due to the presence of DOM in WW, which consumes part of the oxidant, competing with the target substances. The two WW had different DOM contents, giving higher degradation rates for that with less amount of DOM, for both processes. To achieve the same removal, higher oxidant doses would be required.	[91]
Photocatalytic ozonation	Diclofenac 10^{-4} and 10^{-6} M	- UPW; - WW effluent (pH 7–8; TOC 33 mg L^{-1}; IC 28 mg L^{-1}; COD 60 mg L^{-1}; BOD 33 mg L^{-1}), Spain.	- Cylindrical borosilicate glass photo-reactor (0.45 m height, 0.08 m diameter); - HP Hg lamp (UV-Vis $\lambda > 300$ nm); - T 20 °C; - pH 7.0; - Inlet O_3 gas concentration: 10 mg L^{-1}; - Gas flow rate: 30 L h^{-1}; - Catalyst: 1.5 g L^{-1} of TiO_2.	Diclofenac (initial concentration 10^{-4} M) was completely removed within 6 min and 60–75% of TOC removals were observed after 60 min, regardless of the matrix. However, for lower initial concentration of diclofenac (10^{-6} M) in WW, TOC removal largely depended on the organic–inorganic WW content.	[92]
O_3	42 APIs 1 µg L^{-1}	- 6 WW effluents (pH 6.6-7.2; TOC 5.2-13.7 mg L^{-1}; COD 29-90 mg L^{-1}; NH_4^+ 0.77-5.98 mg L^{-1}; alkalinity 154-256 mg $CaCO_3$ L^{-1}), Sweden.	- 150 mL flask reactor; - Spiked O_3 stock solution (concentration 0.5 – 12 mg L^{-1}).	A large variability was observed in the required O_3 dose to attain elimination of different APIs in the same effluent and for the same API between effluents. The removal was lower when COD and alkalinity were higher, requiring higher O_3 doses.	[93]
O_3	Ofloxacin 22 mg L^{-1}	- WW effluent (pH 7.4; DOC 8.4 mg L^{-1}; COD 28 mg L^{-1}; turbidity 7.0 NTU; conductivity 750 µS cm^{-1}; TSS 11 mg L^{-1}; Na^+ 65 mg L^{-1}; NH_4^+ 4.1 mg L^{-1}; K^+ 15 mg L^{-1}; Mg^{2+} 18 mg L^{-1}; Ca^{2+} 52 mg L^{-1}; NO_3^- 59 mg L^{-1}; PO_4^{3-} 3.3 mg L^{-1}; SO_4^{2-} 81 mg L^{-1}; Cl^- 86 mg L^{-1}), Spain. - Synthetic matrix prepared in UPW spiked with $NaHCO_3$ to equal the alkalinity and pH values of the WW effluent.	- Cylindrical reactor (51 cm height and 6.0 cm internal diameter) with a total working volume of 1.44 L, operating in continuous co-current mode; - Average retention time of 10.3 min; - Water flow rate: 142 mL min^{-1}; - Gas flow was 390 mL min^{-1} with different inlet O_3 concentrations; - Inlet O_3 dosage: 4.2 — 145 mg O_3 L^{-1}; - Samples taken once the stationary state was reached.	For similar O_3 exposures, ofloxacin was removed at a higher extent in synthetic WW, in comparison to WW effluent, showing the competition between the DOM and ofloxacin for O_3 and suggesting that O_3 and/or $HO^\bullet$ preferably attack certain moieties of DOM present in WW. A higher O_3 dose was required to achieve the complete abatement of the pharmaceutical.	[94]
O_3	Benzalkonium chloride 10 mg L^{-1}	- WW influent before biological treatment (pH 8.3; DOC 61.2 mg L^{-1}; COD 121 mg L^{-1}; turbidity 145 NTU; conductivity 1,234 µS cm^{-1}; TSS 108 mg L^{-1}; Na^+ 110 mg L^{-1}; NH_4^+ 53.8 mg L^{-1}; K^+ 26.2 mg L^{-1}; Mg^{2+} 19.3 mg L^{-1}; Ca^{2+} 41.4 mg L^{-1}; NO_3^- 0.10 mg L^{-1}; PO_4^{3-} 14.9 mg L^{-1}; SO_4^{2-} 56.0 mg L^{-1}; Cl^- 127 mg L^{-1}), Spain; - Synthetic matrix prepared in UPW spiked with $NaHCO_3$ to equal the alkalinity and pH values of the wastewater effluent.	- Cylindrical reactor with a total working volume of 1.44 L, operating in continuous co-current mode; - Average retention time of 10.3 min; - Water flow rate: 142 mL min^{-1}; - Gas flow was 390 mL min^{-1} with different inlet O_3 concentrations: - Inlet O_3 dosage: 5 — 300 mg O_3 L^{-1}; - Samples taken once the stationary state was reached.	Water matrix strongly influenced benzalkonium chloride depletion, in comparison to synthetic WW, mainly due to the high DOC content. An instantaneous ozone demand of 77 mg L^{-1} was required in non-spiked raw wastewater. The presence of NiO nanoparticles affected the ozone dose required. The consumed ozone in WW was approximately fivefold the corresponding value in synthetic WW.	[95]
O_3	Propiconazole, atrazine, 2,4 dichlorophenoxyacetic	- Reverse osmosis water; - SWW; - WW effluent.	- Ozone dose: 0, 0.2, 0.7, 1.9, 4.9, 9.9 and 14.8 mg O_3 L^{-1} in reverse osmosis water;	As the matrix complexity increased, lower removals of the studied compounds were found. Moreover, in some cases the effect was greater in	[96]

	acid, tebuconazole, climbazole, myclobutanil, irgarol, terbutryn, dicamba, mecoprop and diuron 5, 20 mg L^{-1}		- Ozone dose: 0 - 38.2 mg O_3 L^{-1} in synthetic wastewater and wastewater effluent.	SWW in comparison with WW effluent, mainly due to the higher COD values, the presence of HCO_3^-, PO_4^{3-} and Cl^-. Furthermore, dicamba and 2,4-dichlorophenoxyacetic acid, followed by atrazine, were the most recalcitrant compounds.	
O_3 Catalytic ozonation	Mesoxalic and oxalic acids 50 mg L^{-1}	- WW effluent (pH 7.7; TOC 8.1 mg L^{-1}; COD 27 mg L^{-1}; turbidity 5.3 NTU; conductivity 667 µS cm^{-1}; TSS 7.3 mg L^{-1}; Na^+ 83 mg L^{-1}; NH_4^+ 3.3 mg L^{-1}; K^+ 15 mg L^{-1}; Mg^{2+} 20 mg L^{-1}; Ca^{2+} 32 mg L^{-1}; NO_3^- 36 mg L^{-1}; PO_4^{3-} 1.2 mg L^{-1}; SO_4^{2-} 82 mg L^{-1}; Cl^- 83 mg L^{-1}), Spain.	- T 25 °C; - pH 8; - Catalyst: copper oxide supported on mesoporous silica SBA-15; - Influence of HCO_3^- (250 mg L^{-1}), PO_4^{3-} (1 mg L^{-1}), Cl^- (100 mg L^{-1}), and SO_4^{2-} (108 mg L^{-1}); - Influence of suspended solids.	The removal rate by ozonation was almost inhibited by the suspended solids and strongly dependent on the presence of inorganic anions, suggesting a scavenging effect of $HO^•$, in the following order: $HCO_3^- \approx Cl^- > PO_4^{3-} >> SO_4^{2-}$. Catalytic ozonation was more efficient to degrade organic acids, being almost unaffected by the presence of the inorganic anions or suspended solids, only PO_4^{3-} having a noticeable effect on oxalic acid depletion.	[97]
O_3 O_3/H_2O_2	Sulfamethoxazole, diclofenac 30 mg L^{-1}	- Synthetic matrix prepared in DI (pH 7; $NaHPO_4$ 1.44 g L^{-1}; NaH_2PO_4 0.24 g L^{-1}; NaOH 0.5 M; COD 88.5±4.0 mg O_2 L^{-1}). - WW effluent (pH 7.58; COD 188.2±13.2 mg L^{-1}).	- 0.5 L magnetically stirred reactor operating in semi-continuous mode; - Inlet O_3 concentration: 20 g Nm^{-3}; - H_2O_2 concentration: 5 mM; - Gas flow rate: 0.2 L min^{-1}.	Significant differences were not found on the removal of sulfamethoxazole and diclofenac in both synthetic and WW matrices, which were totally removed in 45 and 60 min, respectively. On the other hand, the removal of COD was much lower, with higher ozone and H_2O_2 consumption, when WW was used, which might be explained by the presence of ions, such as CO_3^{2-}, HCO_3^-, SO_4^{2-}, PO_4^{3-}, among others.	[98]
O_3 O_3/H_2O_2	33 pharmaceuticals ng L^{-1} levels	- 2 WW effluents: urban WW composed by domestic and industrial WW (pH 7.54-8.01; TOC 5.7-15.7 mg L^{-1}; COD 35-72 mg L^{-1}; BOD_5 3.0-18 mg L^{-1}; conductivity 407-614 µS cm^{-1}; TSS ≈0-12.4 mg L^{-1}; alkalinity 345-539 mg $CaCO_3$ L^{-1}; Cl^- 61-81 mg L^{-1}; SO_4^{2-} 91-133 mg L^-) and domestic WW (pH 7.52-8.38; TOC 8.4-17.5 mg L^{-1}; COD 44-182 mg L^{-1}; BOD_5 4.7-24 mg L^{-1}; conductivity368-631 µS cm^{-1}; TSS 0.55-23.9 mg L^{-1}; alkalinity 305-580 mg $CaCO_3$ L^{-1}; Cl^- 52-63 mg L^{-1}; SO_4^{2-} 81-114 mg L^-), Madrid, Spain.	-5-L glass jacketed reactor; - T 25 °C; - pH 8.0; - Gas flow rate: 360 L h^{-1}; - O_3 concentration: 46 g N m^{-3}.	The degradation kinetics in urban and domestic WW was significantly different and TOC elimination was markedly higher for urban WW.	[99]
Catalytic ozonation	Diclofenac, sulfamethoxazole, EE2 10 mg L^{-1}	- WW effluent pre-treated to partially remove its CO_3^{2-} and HCO_3^- content by stripping (pH 7.52; TOC 8 mg L^{-1}; COD 64 mg L^{-1}; BOD_5 15 mg L^{-1}; turbidity 15.9 NTU; conductivity 710 µS cm^{-1}; TSS 28 mg L^{-1}; N_{total} 22.1 mg L^{-1}; NH_4^+ 18.3 mg L^{-1}; PO_4^{3-} 5.0 mg L^-), Spain.	- Reactor system: one gas–liquid reactor (300 mm height, 50 mm diameter) with a porous plate at its bottom to bubble an O_3–O_2 mixture and a fixed bed reactor where 5g of catalyst were loaded; - Catalysts: commercial γ-Al_2O_3 and synthesized Co_3O_4/Al_2O_3;	Regardless of the water matrix and the presence/absence of any catalyst, the elimination of the pharmaceuticals occurred through fast direct reactions with O_3 in less than 10 min. Catalytic ozonation, particularly in the presence of the synthesized Co_3O_4/Al_2O_3, improved the COD and TOC removals obtained when single ozonation was applied. The ozonation developed through fast initial COD removal followed by a second slower	[100]

				stage, which could be greatly improved by the Co_3O_4/Al_2O_3 catalyst.	
Photocatalytic ozonation	Diclofenac, amoxicillin 0.1 mM	- UPW; - WW effluent (characterization not provided), Portugal.	- O_3: 50 g Nm^{-3} and 150 Ncm^3 min^{-1}; - MP Hg vapour lamp (UV-Vis $\lambda > 300$ nm); - Catalyst: 0.5 g L^{-1} of TiO_2.	The removal of the investigated compounds was similar in both matrices. The oxamic acid formed in DI by photocatalytic ozonation was further degraded, whereas it was refractory to the photocatalytic ozonation in the case of spiked WW effluents, where the concentration of this carboxylic acid increased during 45 min and then remained constant.	[101]
O_3 **Catalytic ozonation**	Formic, acetic, oxalic and maleic acids 7 mg L^{-1}	- WW effluent (pH 7.24; TOC 5.12 mg L^{-1}; COD 14.3 mg L^{-1}; turbidity 0.4 NTU; conductivity 800 µS cm^{-1}; TSS 30 mg L^{-1}; Na^+ 67.5 mg L^{-1}; NH_4^+ 0.34 mg L^{-1}; K^+ 13.9 mg L^{-1}; Mg^{2+} 20.1 mg L^{-1}; Ca^{2+} 52.8 mg L^{-1}; NO_3^- 36.8 mg L^{-1}; NO_2^- 0.49 mg L^{-1};PO_4^{3-} 3.31 mg L^{-1}; SO_4^{2-} 68.8 mg L^{-1}; Cl^- 88.2 mg L^{-1}; HCO_3^- 189 mg L^{-1}), Spain; - Synthetic matrix prepared in UPW spiked with $NaHCO_3$ to equal the alkalinity and pH values of the WW effluent.	- Cylindrical reactor (51 cm height and 6.0 cm internal diameter) with a total working volume of 1.44 L, operating in continuous co-current mode; - Average retention time: 10.3 min; - Water flow rate: 142 mL min^{-1}; - Gas flow was 390 mL min^{-1} with different inlet O_3 concentrations; - Copper: 1-250 µg L^{-1} (synthetic WW) and 10-500 µg L^{-1} (WW effluent); - Samples taken once the stationary state was reached.	Catalytic ozonation was strongly influenced by the water matrix, since the complexation with organic matter reduces the availability of metal as catalyst. In WW, a five-fold copper concentration is required to achieve similar removal of oxalic acid to that obtained in the synthetic WW.	[102]
O_3 **Photocatalysis** **Photocatalytic ozonation**	Acetaminophen, norfloxacin, metoprolol, cafeine, antipyrine, sulfamethoxazole, ketorolac, hydroxyl-biphenyl, diclofenac 50 µg L^{-1}	- UPW; - WW effluent (pH 8-8.5; TOC 25-30 mg L^{-1}; IC 35-40 mg L^{-1}; COD 40 mg L^{-1}), Spain.	- 1 L cylindrical borosilicate glass reactor; - 15-W black-light lamps (350–410 nm); - Catalyst: 0.25 g L^{-1} of TiO_2 or 5 g L^{-1} TiO_2 supported on activated carbon; - O_3: inlet concentration 15 mg L^{-1} and flow rate 30 L h^{-1}.	The efficiency of the treatments was lower using WW as matrix in comparison to ultra-pure water, due to the effect of other organic/inorganic components occurring in the secondary effluents.	[103]
O_3 **UV** **UV/H_2O_2** **O_3/H_2O_2 as pre-treatment for nanofiltration**	Amoxicillin, hydrochlorothiazide, metoprolol, naproxen, phenacetin 1 µM	- GW, Spain; - Surface water from a public reservoir, Spain; WW effluent (pH 7.6; TOC 15 mg L^{-1}; conductivity 650 µS cm^{-1}; alkalinity 250 mg $CaCO_3$ L^{-1}), Spain.	- 25 mL flask reactors; - T 20 °C; pH natural (7); - Spiked O_3 stock solution or 10^{-3} M hypochlorous acid solution; - Irradiation source: LP Heraeus Hg lamp TN 15/35 with a nominal output of 15 W (λ_{max} 254 nm); *Membrane filtration* - Cross-flow membrane filtration unit; Transmembrane pressure: 5 bar (ultrafiltration) and 20 bar (nanofiltration).	Removal rates by chemical oxidation of water pre-treated by membrane filtration showed the following trend among each water matrix: GW > reservoir > WW. The different amount of DOM in each water matrix might consume partially the oxidant and compete with the target substances. In the case of ozonation of WW, higher initial O_3 dose was required to achieve similar removal efficiency of those obtained in natural waters.	[104]
O_3 **UV/H_2O_2**	Organophosphate esters 50 µg L^{-1}	- UPW; - HA solution; - WW effluent (pH 8.2; TOC 7.8 mg L^{-1}; COD 28.4 mg L^{-1}; turbidity 1.99 NTU; alkalinity 325 mg $CaCO_3$ L^{-1}; NH_4^+ 13.9 mg L^{-1}; Mg^{2+} 52.1 mg L^{-1}; Ca^{2+} 115.4 mg L^{-1}; NO_3^- 24.9 mg L^{-1}; NO_2^- 7.35 mg L^{-1}; SO_4^{2-} 203.3 mg L^{-1}; Cl^- 624.2 mg L^{-1}), Canada.	- 2.0 L jacketed glass reactor; - natural pH; O_3 - T 20 °C; - O_3: 60 L h^{-1} and 10 mg L^{-1}; UV/H_2O_2 - T 25 °C;	The aromatic and aliphatic pollutants were rapidly oxidized by ozone and UV/H_2O_2, while the chlorinated and the ramified aliphatic compounds were more recalcitrant. For ozonation, the following decreasing order of removal was reported: HA solution > UPW > WW effluents. The acidic pH of UPW led to selective ozonation of organic compounds with electron-rich	[105]

			- 3 LP UV lamps (8 W, 26% UVC efficiency) (λ_{max} 254 nm); - H_2O_2: 20 mg L^{-1}.	functional groups. The reactions between O_3 and the electron-rich moieties of HA explain the faster degradation rates of the reactive organophosphate esters due to the production of $HO^{\bullet}$. Direct and indirect oxidation occurred in the municipal secondary effluent (pH 8-8.2). The EfOM could react with molecular O_3. Some ions (e.g., Cl^-, SO_4^{2-}, NO_3^{2-}, HCO_3^-) and EfOM were ascribed as radical scavengers. The reactivity of the target pollutants exhibited a similar trend in UV/H_2O_2 to that in ozonation. The elimination efficiencies in the effluent were generally similar to those in HA solution.	
O_3 **UV** **UV/H_2O_2** **UV/O_3,** **O_3/H_2O_2** **O_3/UV/H_2O_2**	E1 3 µg L^{-1} – 5 mg L^{-1}	- UPW; - WW effluent (pH 7.4; TOC 9.61 mg L^{-1}; COD 36 mg L^{-1}; turbidity 10 NTU; TSS 23 mg L^{-1}; TDS 373 mg L^{-1}; Na^+ 83.3 mg L^{-1}; NH_4^+ 2.3 mg L^{-1}; K^+ 10.4 mg L^{-1}; Mg^{2+} 18.5 mg L^{-1}; Ca^{2+} 83.9 mg L^{-1}; NO_3^- 18.1 mg L^{-1}), Canada.	- Annular reactor (750 mL); - 13 W LP UV lamp (λ_{max} 253.7 nm); - O_3: 0.33 – 1.31 mg L^{-1}; - H_2O_2: 20, 40 and 60 mg L^{-1}.	The best performing treatment for E1 removal was ozonation. The removal rate decreased slightly with the background TOC in water, however, in the WW effluent with low COD values, E1 removal was only reduced by 5%.	[106]
Catalytic ozonation	Benzotriazole 10 mg L^{-1}	- WW effluent (pH 6.5; conductivity 750 µS cm^{-1}; COD 20 mg L^{-1}, TP 15.4 mg L^{-1}; TN 15.4 mg L^{-1}; TDS 540 mg L^{-1}; Cl^- 75 mg L^{-1}; NO_3^- 21.6 mg L^{-1}; NO_2^- 2.3 mg L^{-1}; PO_4^{3-} 9.1 mg L^{-1}; NH_4^+ 10.3 mg L^{-1}), Iran.	- Semi-continuous reactor; - V 1.2 L; - Catalyst: 0.5 g L^{-1} magnetic alumina nanocomposite; - Oxygen gas flow rate: 0.3 L min^{-1}.	The catalyst addition enhanced greatly the removal rate of target compound. Experiments using secondary municipal wastewater effluent indicated that no significant decrease in the performance of the catalyst occurred.	[107]

Abbreviations: API, active pharmaceutical ingredient; AOT, advanced oxidation technologies; BOD_5, biochemical oxygen demand; COD, chemical oxygen demand; DI, distilled water; DOC, dissolved organic carbon; DOM, dissolved organic matter; E1, estrone; EE2, 17-alpha-ethinylestradiol; GW, groundwater; HA, humic acids, HP, high pressure; IC, inorganic carbon; LP, low pressure; MP, micropollutants; NTU, nephelometric turbidity unit; PS, persulphate; SS, suspended solids; SW, surface water; SWW, synthetic wastewater; TOC, total organic carbon; TDS, total dissolved solids; TSS, total suspended solids; UPW, ultrapure water; WW, wastewater.